

Explicit solutions for replicator-mutator equation: extinction vs. acceleration

Matthieu Alfaro

Université Montpellier 2

CIRM, june 2014

Joint work with Rémi Carles (Univ. Montpellier 2).

(Nearly) all about:

$$\partial_t u = \partial_{xx} u + (x - \bar{u}(t))u, \quad t > 0, x \in \mathbb{R},$$

where the nonlocal term is given by

$$\bar{u}(t) := \int_{\mathbb{R}} xu(t, x) dx,$$

with initial data

$$u_0 \geq 0, \quad \int_{\mathbb{R}} u_0 = 1.$$

Contents

- 1 Introduction: the replicator-mutator equation
- 2 Reduction to the heat equation
- 3 Various scenarii depending on initial data
- 4 Conclusion

Contents

- 1 Introduction: the replicator-mutator equation
- 2 Reduction to the heat equation
- 3 Various scenarii depending on initial data
- 4 Conclusion

Deleterious vs. advantageous mutations

A central issue in evolutionary genetics is to predict whether a population accumulates deleterious or advantageous mutations.

For asexual (clonal) populations:

Muller's ratchet: the population will accumulate deleterious mutations and, therefore, its fitness will decay.

≠

Recent experiments on viruses: beneficial mutations are more abundant than previously suspected.

Construct a mathematical model for such beneficial mutations.

The replicator-mutator equation

Model proposed by Tsimring, Levine, and Kessler 1996, for the evolution of RNA virus populations on a fitness space:

$$\partial_t u = \underbrace{\partial_{xx} u}_{\text{mutations}} + \underbrace{\left(x - \int_{\mathbb{R}} xu(t, x) dx \right)}_{\text{replication}} u.$$

- ▶ $x \in \mathbb{R}$: a one dimensional **fitness** space.
- ▶ $u(t, x)$: density of a population at time t and per unit of fitness.
- ▶ $\bar{u}(t) = \int_{\mathbb{R}} xu(t, x) dx$: mean fitness at time t .

Equation for “arms run”.

Formal conservation of mass...

We assume

$$u_0 \geq 0, \quad \int_{\mathbb{R}} u_0(x) dx = 1.$$

Define $m(t) := \int_{\mathbb{R}} u(t, x) dx$. Integrating the equation,

$$\frac{d}{dt} m(t) = (1 - m(t)) \bar{u}(t), \quad m(0) = 1,$$

so that $m(t) = 1$ as long as $\bar{u}(t)$ is meaningful.

Actually, conservation of mass may completely fail: solution may become extinct in finite time...

Contents

- 1 Introduction: the replicator-mutator equation
- 2 Reduction to the heat equation**
- 3 Various scenarii depending on initial data
- 4 Conclusion

Absorbing an external time dependent factor $a(t)$

$$\partial_t u = \partial_{xx} u + xu - a(t)u$$

and

$$\partial_t v = \partial_{xx} v + xv$$

are related through

$$v(t, x) = u(t, x) \exp \left(\int_0^t a(s) ds \right).$$

Absorbing the momentum factor $\bar{u}(t)$

$$\partial_t u = \partial_{xx} u + xu - \bar{u}(t)u$$

and

$$\partial_t v = \partial_{xx} v + xv$$

are **formally** related through

$$v(t, x) = u(t, x) \exp \left(\int_0^t \bar{u}(s) ds \right),$$

which can be inverted...

By multiplying by x and integrating over $x \in \mathbb{R}$

$$\bar{v}(t) = \bar{u}(t) \exp \left(\int_0^t \bar{u}(s) ds \right) = \frac{d}{dt} \exp \left(\int_0^t \bar{u}(s) ds \right).$$

By integrating in time

$$\int_0^t \bar{v}(s) ds = \exp \left(\int_0^t \bar{u}(s) ds \right) - 1,$$

so that, as long as $\int_0^t \bar{v}(s) ds > -1$,

$$u(t, x) = \frac{v(t, x)}{1 + \int_0^t \bar{v}(s) ds}.$$

► Computations are licit provided that \bar{u} (and therefore \bar{v}) is finite.

Absorbing the linear factor x

$$\partial_t v = \partial_{xx} v + xv$$

and

$$\partial_t w = \partial_{xx} w$$

are related through

$$v(t, x) = w\left(t, x + t^2\right) \exp\left(tx + \frac{t^3}{3}\right).$$

► Known as **Avron–Herbst formula** for the Schrödinger equation modelling evolution of particles under effect of an electric field x :

$$i\partial_t v = \partial_{xx} v + xv.$$

Not so nice explicit formulas...

Combining the above

$$u(t, x) = \frac{e^{tx+t^3/3} w(t, x+t^2)}{1 + \int_0^t \int_{\mathbb{R}} x e^{sx+s^3/3} w(s, x+s^2) dx ds},$$

so that

$$u(t, x) = \frac{e^{tx+t^3/3} \int_{\mathbb{R}} \frac{1}{\sqrt{4\pi t}} e^{-(x+t^2-y)^2/4t} u_0(y) dy}{1 + \int_0^t \int_{\mathbb{R}} x e^{sx+s^3/3} \int_{\mathbb{R}} \frac{1}{\sqrt{4\pi s}} e^{-(x+s^2-y)^2/4s} u_0(y) dy dx ds}.$$

Nicer explicit formulas

Fubini and elementary algebra yield

$$u(t, x) = \frac{e^{tx} \int_{\mathbb{R}} \frac{1}{\sqrt{4\pi t}} e^{-(x+t^2-y)^2/(4t)} u_0(y) dy}{\int_{\mathbb{R}} e^{ty} u_0(y) dy},$$

and

$$\bar{u}(t) = t^2 + \frac{\int_{\mathbb{R}} e^{ty} y u_0(y) dy}{\int_{\mathbb{R}} e^{ty} u_0(y) dy}.$$

Contents

- 1 Introduction: the replicator-mutator equation
- 2 Reduction to the heat equation
- 3 Various scenarii depending on initial data**
- 4 Conclusion

Global existence vs. extinction

$$T = \sup \left\{ t \geq 0, \int_0^\infty e^{ty} u_0(y) dy < \infty \right\}.$$

- ▶ If $T = \infty$, then both $u(t, x)$ and $\bar{u}(t)$ are global in time.
- ▶ If $0 < T < \infty$, then extinction in finite time occurs, that is

$$u(t, x) = 0, \quad \forall t > T, \quad \forall x \in \mathbb{R}.$$

- ▶ If $T = 0$, then $u(t, x)$ is defined for no $t > 0$.

The right tail of initial data plays the key role.

Gaussian data: acceleration

If $u_0(x) = \sqrt{\frac{a}{2\pi}} e^{-a(x-m)^2/2}$, then

$$u(t, x) = \sqrt{\frac{a(t)}{2\pi}} e^{-a(t)(x-m(t))^2/2},$$

where

$$a(t) := \frac{a}{1+2at} \sim \frac{1}{2t}, \quad m(t) := m + t^2 + \frac{t}{a} \sim t^2.$$

Starting from a Gaussian profile, the solution remains a Gaussian function, is accelerating and flattening.

► This self similar family of solutions was already noticed by Biktashev (J. Math. Biol. 2014).

Compactly supported data: *universal* acceleration

If u_0 is compactly supported, then

$$\sup_{x \in \mathbb{R}} \left| u(t, x) - \underbrace{\frac{1}{\sqrt{4\pi t}} e^{-(x-t^2)^2/4t}}_{\text{elementary solution, } u_0(y)=\delta_0(y)} \right| \leq \frac{C}{t}.$$

Deviation from the elementary solution is uniformly estimated w.r.t. x .

Data with *light* tails: extinction in finite time

If $u_0(y) = \alpha e^{-\alpha y} \mathbf{1}_{(0, \infty)}(y)$, then

$$\bar{u}(t) = t^2 + \frac{1}{\alpha - t} \xrightarrow{t \rightarrow \alpha} \infty,$$

and

$$u(t, x) = \frac{1}{\sqrt{2\pi}} (\alpha - t) e^{-(\alpha - t)x} e^{-\alpha t^2 + \alpha^2 t} \int_{\frac{-(x + t^2 - 2\alpha t)}{\sqrt{2t}}}^{\infty} e^{-z^2/2} dz$$

$\xrightarrow{t \rightarrow \alpha} 0$, uniformly in $x \in \mathbb{R}$.

Extinction of $u(t, x)$, blow-up of $\bar{u}(t)$ at finite time $t = \alpha$.

Data with *very light* tails: immediate extinction

If u_0 decays only algebraically, then

$u(t, x)$ is defined for no $t > 0$.

Actually, the above reduction requires to be able to consider an open time interval, in order for the integration procedure to make sense. This approach becomes meaningless if we have $\bar{u}(t) = \infty$ for all $t > 0$.

Contents

- 1 Introduction: the replicator-mutator equation
- 2 Reduction to the heat equation
- 3 Various scenarii depending on initial data
- 4 Conclusion

Summary

Replicator-mutator equation:

$$\partial_t u = \partial_{xx} u + \left(x - \int_{\mathbb{R}} xu(t, x) dx \right) u,$$

with initial data $u_0 \geq 0$, $\int_{\mathbb{R}} u_0 = 1$.

- Heavy right tails (Gaussian like...) \Rightarrow global existence.
 - ▶ Accelerating self similar Gaussian solutions.
 - ▶ Convergence to the fundamental solution, which accelerates, for compactly supported data.
- Light right tails (exponential...) \Rightarrow extinction in finite time.
- Very light right tails (algebraic...) \Rightarrow immediate extinction.

How to treat the “large fitness region” ...

For biological applications, because of

- ▶ extinction in finite time
- ▶ acceleration $x = t^2$
- ▶ the change of sign of traveling pulse (that can be computed by using Fourier transform and that involve the Airy function),

the unlimited growth rate of $u(t, x)$ at large x in the replicator mutator equation is not admissible.

Two ways of dealing such a problem:

- ▶ consider a **cut-off version of the equation** at large x : Rouzine, Wakekey, and Coffin 2003, Sniegowski and Gerrish 2010...
- ▶ provide a **proper stochastic treatment** for large fitness region: Rouzine, Brunet, and Wilke 2008...

Thanks for your attention.

Dynamics induced by long-range connections in the visual cortex

Romain Veltz*, Pascal Chossat* **

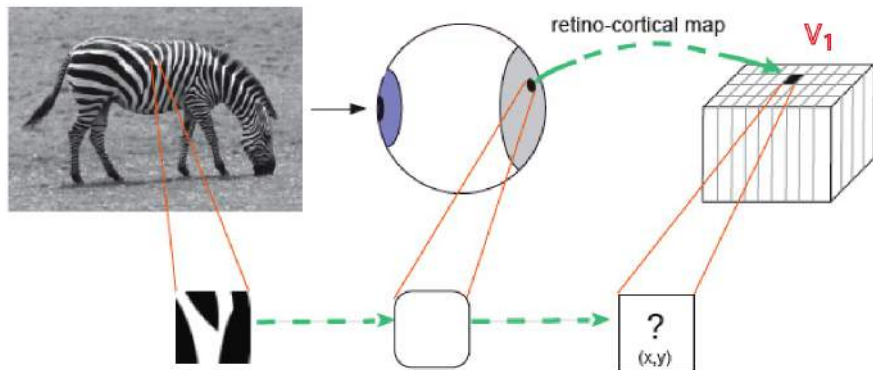
* NeuroMathComp project, INRIA, Sophia Antipolis, France

** Laboratory J-A Dieudonné, CNRS-University of Nice

ReaDiLab Conference
CIRM, Luminy June 03-05, 2014

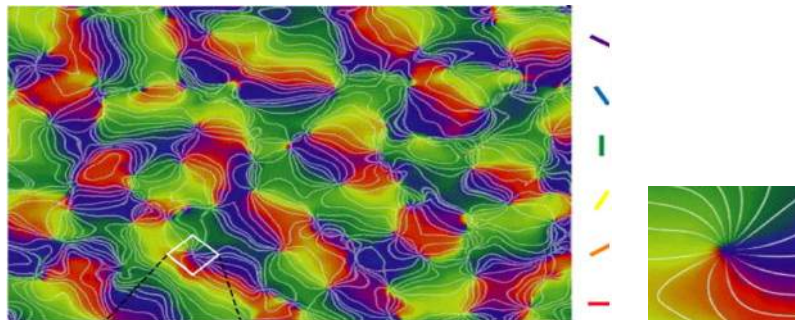
Orientation detection in the area V1 of the visual cortex

The retinocortical map



Orientation detection in the area V1 of the visual cortex

The preferred orientation map: experimental observations



PO map: $\Theta : V1 \rightarrow S^1/\mathbb{Z}_2 \simeq (-\pi/2, \pi/2]$

Patches of iso-orientation.

Singular points are called **pinwheels**.

Domains surrounding pinwheels define **hypercolumns** which tile V1.

Orientation detection in the area V1 of the visual cortex

The model equation

Wilson-Cowan equation for average membrane potential $V(\mathbf{x}, t)$:

$$(1) \quad \frac{\partial V}{\partial t}(\mathbf{x}, t) = -\kappa V(\mathbf{x}, t) + \int_{\Omega} J(\mathbf{x}, \mathbf{x}') S(V(\mathbf{x}', t)) d\mathbf{x}' + I_{thal}(\mathbf{x})$$

- $\kappa > 0$, S is a sigmoidal function,
 $I_{thal} = I_0 + \epsilon_{thal} f(\Theta(\mathbf{x}) - \Theta_{aff}(\mathbf{x}), \mathbf{x})$ is the input from thalamus.
- The *connectivity function* J must reflect the patchy distribution of neurons **with same orientation preference in V1**.
- Ω is approximated by a rectangle $L_1 \times L_2$ with periodic boundary conditions.

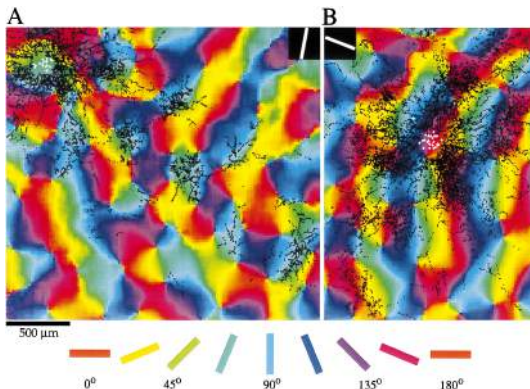
We assume hypercolumns form **a periodic tiling of Ω** :

$$\Omega = \{x_1 \mathbf{e}_1 + x_2 \mathbf{e}_2 \mid -L_j/2 \leq x_j \leq L_j/2, \|\mathbf{e}_j\| = L_j/N_j\} \text{ and}$$

$$\Theta(\mathbf{x} + n_j \mathbf{e}_j) = \Theta(\mathbf{x}), \quad \mathbf{x} \in \Omega, \quad n_j = 0, \dots, N_j - 1.$$

Orientation detection in the area V1 of the visual cortex

The connectivity function $J = J_{loc} + \epsilon J_{LR}$, $\epsilon \ll 1$



Local connections (within the hypercolumns) are isotropic.

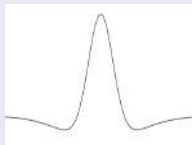
Long range connections (between hypercolumns) preferentially connect neurons with same preferred orientation and in certain species the connection is roughly aligned with the preferred orientation (anisotropy).

Orientation detection in the area V1 of the visual cortex

The connectivity function (next)

Local connections: selection of a critical wave number

$J_{loc}(\mathbf{x}, \mathbf{x}') = h(\|\mathbf{x} - \mathbf{x}'\|^2)$
with h "Mexican hat
function".



$J_{loc}(T\mathbf{x}, T\mathbf{x}') = J_{loc}(\mathbf{x}, \mathbf{x}')$ for any $T \in E(2, \mathbf{R})$.

Long-range connections

$J_{LR}(\mathbf{x}, \mathbf{x}') = G(\Theta(\mathbf{x}) - \Theta(\mathbf{x}'))J_0(\chi, R_{-2\Theta(\mathbf{x})}(\mathbf{x} - \mathbf{x}'))$ where G is a Gaussian function, R_θ is the rotation of angle θ , $0 \leq \chi \leq 1$

$$J_0(\chi, \mathbf{x}) = e^{-[(1-\chi)^2 x_1^2 + x_2^2]/2\sigma_{LR}^2} \quad (\text{from Bressloff 2003}).$$

Remarks: 1. χ measures anisotropy. In treeshrew $\chi \neq 0$.
2. In Bressloff 2003, $G(\Theta(\mathbf{x} - \mathbf{x}'))$ instead of $G(\Theta(\mathbf{x}) - \Theta(\mathbf{x}'))$.

Analysis of the spontaneous activity: $I_{thal} = 0$

The strategy

- 1 Choose a periodic lattice (hence Ω). It can be rhombic, square or hexagonal. Then build a PO map Θ on this lattice.
- 2 Set $\epsilon = 0$ and compute the bifurcated patterns $V(\mathbf{x})$ in Ω :
bifurcation with $D_n \times \mathbb{T}$ symmetry, $\mathbb{T} \simeq \mathbb{R}^2/\mathbb{Z}^2$ ($n = 2, 4$ or 6).
- 3 Choose a D_n -symmetric solution V and study its perturbation when $\epsilon \neq 0$.

Fundamental remark: V is not isolated but part of a torus group orbit $\mathbb{T}V$ (group action $T \cdot V(\mathbf{x}) = V(T^{-1}\mathbf{x})$).

If $\mathbb{T}V$ is *normally hyperbolic*, perturbations with small ϵ transform it in an **invariant torus manifold** \mathcal{T}_ϵ for eq. (1).

Hence problem reduces to look for the induced dynamics in \mathcal{T}_ϵ .

Note: \mathcal{T}_ϵ invariant under subgroup Γ_Θ of symmetries of J_{LR} .

- 4 Numerical simulations of the dynamics on \mathcal{T}_ϵ .

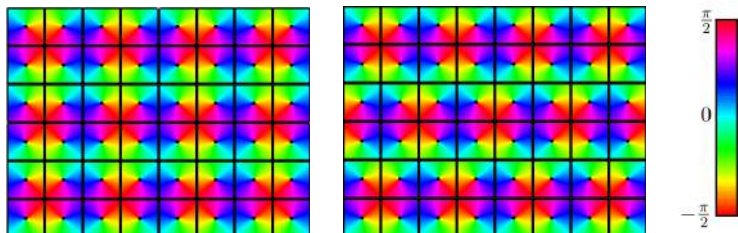
An example: the square lattice

The PO map

The PO map Θ defines a tiling of Ω (or \mathbb{R}^2), characterized by its wallpaper group (invariance group of Θ).

In the square lattice case, among all possibilities only two are biologically plausible: *pmm* (left) or *cm* (right) (IUC notation).

Pinwheels are the black dots.



In both cases the wall-paper group is isomorphic to D_2 (sym. of rectangle). However Γ_Θ is different as we see next.

An example: the square lattice

The symmetry group Γ_Θ

Define R_ϕ the rotation by $\phi = \pi/2$ around a pinwheel. Then

$$\Theta(R_\phi \mathbf{x}) = \Theta(\mathbf{x}) \pm \pi/4.$$

Lemma. $J_{LR}(R_\phi \mathbf{x}, R_\phi \mathbf{x}') = J_{LR}(\mathbf{x}, \mathbf{x}')$

Proof: recall that

$$J_{LR}(\mathbf{x}, \mathbf{x}') = G(\Theta(\mathbf{x}) - \Theta(\mathbf{x}')) J_0(\chi, R_{-2\Theta(\mathbf{x})}(\mathbf{x} - \mathbf{x}')).$$

But $J_0(\chi, R_{-2\Theta(R_\phi \mathbf{x})} R_\phi(\mathbf{x} - \mathbf{x}')) = J_0(\chi, R_{2\phi(1\pm 1)} R_{-2\Theta(\mathbf{x})}(\mathbf{x} - \mathbf{x}')) = J_0(\chi, \pm R_{-2\Theta(\mathbf{x})}(\mathbf{x} - \mathbf{x}')) = J_0(\chi, R_{-2\Theta(\mathbf{x})}(\mathbf{x} - \mathbf{x}'))$.

Corollary. Equation (1) is R_ϕ -invariant, hence $\Gamma_\Theta \supset C_4$

Remark: in general Γ_Θ does not contain reflections.

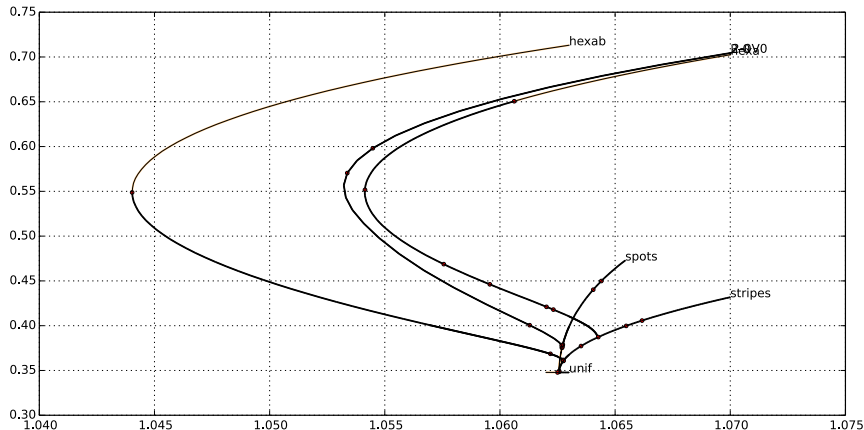
An example: the square lattice

The solution with $\epsilon = 0$

- Classical Turing-like bifurcation analysis of $0 = -V + J_0 \star S(V)$ with bifurcation parameter=slope of S .
- There exists a branch with D_4 symmetry (squares), with leading part $V_0(x, y) = \sqrt{\lambda}a(\cos x + \cos y)$.
- Torus $\mathbb{T}V_0 \simeq \mathcal{T}_0 = \{(\cos(x + \vartheta), \cos(y + \varphi))\}$, $\vartheta, \varphi \in S^1$.
- Action of R_ϕ on \mathcal{T} : $R_\phi(\vartheta, \varphi) = (\varphi, -\vartheta)$
4 fixed points $(k\pi, l\pi)$ ($k, l = 0, 1$) \Rightarrow 4 equilibria with 4-fold (C_4) symmetry.
- With suitable choice of parameters the squares are stable, *i.e.* the group orbit $\mathbb{T}V_0$ is attracting (hence normally hyperbolic).
- With $\epsilon \neq 0$ but small enough, perturbed torus $\mathcal{T}_\epsilon \simeq \mathcal{T}_0$ inherits the same action of Γ_Θ , hence also 4 equilibria with C_4 symmetry.

An example: the square lattice

Stability diagram with $\epsilon = 0$



Stable branches in braun color. Note that the stability domain of spots (squares) is very near bifurcation (hence "weakly" hyperbolic).

An example: the square lattice

Qualitative analysis of dynamics on \mathcal{T}_ϵ

Poincaré-Hopf theorem. Let \mathcal{M} be a compact surface, flow-invariant for a vector field F , and ξ_1, \dots, ξ_n the equilibria on \mathcal{M} , then

$$\sum_{j=1}^n \text{sign det } dF(\xi_j) = \text{Euler characteristic of } \mathcal{M}.$$

Consequences.

- For $\mathcal{M} = \mathcal{T}_\epsilon$ the Euler characteristic is 0. We already know there are 4 foci (due to C_4 symmetry), hence with $\text{sign det } dF(\xi_j) = +1$.
- Therefore the simplest situation is that there exist **4 additional equilibria of saddle type**, hence with $\text{sign det } dF(\xi_j) = -1$.
- The dynamics is constrained by these equilibria and it can exhibit periodic orbits (next slide).

An example: the square lattice

Qualitative analysis of dynamics on \mathcal{T}_ϵ : typical phase portrait

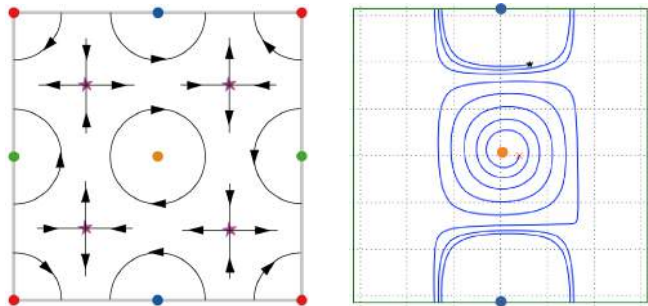


Figure: **Left:** Sketch of the dynamics. **Right:** a computed trajectory. Opposite sides are identified by periodicity.

Remark: additional reflection symmetry would strongly modify the diagram.

Short bibliography

- ① P. C. Bressloff and J. D. Cowan. *The functional geometry of local and horizontal connections in a model of v1*. Journal of Physiology, Paris, 97:221–236, 2003.
- ② P.C. Bressloff. *Spatially periodic modulation of cortical patterns by long-range horizontal connections*. Physica D: Nonlinear Phenomena, 185(3-4):131–157, 2003.
- ③ P.C. Bressloff, J.D. Cowan, M. Golubitsky, P.J. Thomas, and M.C. Wiener. *Geometric visual hallucinations, euclidean symmetry and the functional architecture of striate cortex*. Phil. Trans. R. Soc. Lond. B, 306(1407):299–330, March 2001.
- ④ R. Veltz. PhD thesis, INRIA Sophia Antipolis, dec. 2011.

Sharp interface limit for mass conserving Allen-Cahn equation with stochastic term

Tadahisa Funaki

University of Tokyo

June 4, 2014

Mathematics and its applications to complex phenomena arising in biology, chemistry and medicine, CIRM, Luminy
Jointly with Satoshi Yokoyama

Known results on sharp interface limit for equations with noises

- Allen-Cahn +noise:
 - Kawasaki-Ohta (Physics)
 - F. $d = 1$ (space-time white noise),
 $d = 2$ (temporal noise, convex curve)
 - Weber: $d \geq 2$, general case (additive noise)
- Cahn-Hilliard +noise:
 - $d=1$: Antonopoulou-Blmker-Karali (2012),
rather heuristic
 - $d=1$: Bertini-Brassesco-Buta (2014), fractional BM
- Mass conserving Allen-Cahn eq
Another conservative system

Plan of the talk

- 1 Mass conserving Allen-Cahn eq with stochastic term
- 2 Main result
- 3 Asymptotic expansion
- 4 Limit Stochastic PDE — 2D, convex curve

References:

- Chen-Hilhorst-Logak , Mass conserving Allen-Cahn equation and volume preserving mean curvature flow, Interfaces Free Bound., 12 (2010)
- F., Singular limit for stochastic reaction-diffusion equation and generation of random interfaces, Acta Math. Sin., 15 (1999).

1. Mass conserving Allen-Cahn equation with stochastic term

$u = u^\varepsilon(t, x) = u^\varepsilon(t, x; \omega)$: sol of the Stochastic PDE (1) in a smooth bounded domain D in \mathbb{R}^n :

$$(1) \quad \begin{cases} \partial_t u^\varepsilon = \Delta u^\varepsilon + \varepsilon^{-2} \left(f(u^\varepsilon) - \int_D f(u^\varepsilon) \right) + \alpha \dot{w}^\varepsilon(t), & x \in D \\ \partial_\nu u^\varepsilon = 0, & x \in \partial D \\ u^\varepsilon(\cdot, 0) = g^\varepsilon(\cdot), \end{cases}$$

where $\alpha > 0$, ν is the inward normal vector on ∂D ,

$$\int_D f(u^\varepsilon) = \frac{1}{|D|} \int_D f(u^\varepsilon(t, x)) dx,$$

- $\dot{w}^\varepsilon(t)$ is a time derivative of $w^\varepsilon(t) \equiv w^\varepsilon(t; \omega) \in C([0, \infty))$ a.s. defined on a certain probability space (Ω, \mathcal{F}, P) such that $w^\varepsilon(t)$ converges to 1D Brownian motion $w(t)$ in a suitable sense.
- The reaction term $f \in C^\infty(\mathbb{R})$ is bistable s.t.

$$f(\pm 1) = 0, f'(\pm 1) < 0, \int_{-1}^1 f(u) du = 0.$$

- Mass conservation law is destroyed by noise:

$$\int_D u^\varepsilon(t) = \int_D u^\varepsilon(0) + \alpha w^\varepsilon(t)$$

- **Goal:** To study the limit $\lim_{\varepsilon \downarrow 0} u^\varepsilon(t, x)$.

2. Main result

- Evolution of limit hypersurfaces $\gamma_t \subset D$:

$$(2) \quad V = \kappa - \int_{\gamma_t} \kappa + \frac{\alpha|D|}{2|\gamma_t|} \circ \dot{w}(t), \quad t \in [0, \sigma],$$

up to a certain stopping time $\sigma > 0$ (a.s.), where $V =$ inward normal velocity of γ_t , $\kappa =$ mean curvature of γ_t (multiplied by $n - 1$), $\dot{w}(t) =$ white noise process, \circ means Stratonovich stochastic integral.

- Evolution of approximating hypersurfaces $\gamma_t^\varepsilon \subset D$:

$$(3) \quad V^\varepsilon = \kappa - \int_{\gamma_t^\varepsilon} \kappa + \frac{\alpha|D|}{2|\gamma_t^\varepsilon|} \dot{w}^\varepsilon(t), \quad t \in [0, \sigma^\varepsilon],$$

- We assume $\gamma_t^\varepsilon \rightarrow \gamma_t$ in a proper sense.

Theorem 1

Assume that γ_0 has the form $\gamma_0 = \partial D_0$ with some $D_0 \Subset D$ and satisfies the same condition as in [CHL]. Suppose that a smooth local solution $\Gamma = \cup_{0 \leq t \leq \sigma} (\gamma_t \times \{t\})$ of (2) such that $\gamma_t \Subset D$ for all $t \in [0, \sigma]$ uniquely exists. Then, there exist a family of continuous functions $\{g^\varepsilon(\cdot)\}_{\varepsilon \in (0,1)}$ satisfying

$$(4) \quad \lim_{\varepsilon \rightarrow 0} g^\varepsilon(x) = \begin{cases} 1, & x \in D \setminus \bar{D}_0 \\ -1, & x \in D_0, \end{cases}$$

and stopping times σ^ε such that $(u^\varepsilon(t \wedge \sigma^\varepsilon, \cdot), \sigma^\varepsilon)$ converges weakly to $(\chi_{\gamma_{t \wedge \sigma}}(\cdot), \sigma)$ on $C([0, T], L^2(D)) \times [0, \infty)$ and $\sigma > 0$ a.s.

We need to assume the diverging speeds of $|\frac{d^k}{dt^k} w^\varepsilon(t)|$ are sufficiently slow.

3. Asymptotic expansion

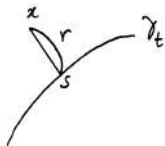
- Eq (1) is rewritten as

$$(5) \quad 0 = f(u^\varepsilon) + \varepsilon^2(-\partial_t u^\varepsilon + \Delta u^\varepsilon + \alpha \dot{w}^\varepsilon(t)) - \varepsilon \lambda_\varepsilon(t),$$

where

$$\begin{aligned} \lambda_\varepsilon(t) &:= \varepsilon^{-1} \int_D f(u^\varepsilon) \\ &= \lambda_0(t) + \varepsilon \lambda_1(t) + O(\varepsilon^2). \end{aligned}$$

- Near γ_t , we introduce a coordinate $x = (r, s)$ and stretched variable $\rho = r/\varepsilon$:



- Under the change of variables: $x \in D \mapsto (\rho, s) \in \mathbb{R} \times U$,

$$\partial_t u = \varepsilon^{-1} V \partial_\rho u + O(\varepsilon),$$

$$\Delta u = \varepsilon^{-2} \partial_\rho^2 u + \varepsilon^{-1} \Delta d \partial_\rho u + O(\varepsilon),$$

near γ_t . (We heuristically ignore the terms of $O(1)$.)

- We expand $u = m + \varepsilon u_0 + \varepsilon^2 u_1 + O(\varepsilon^3)$ near γ_t . Then,

$$f(u) = f(m) + \varepsilon f'(m) u_0 + \varepsilon^2 f'(m) u_1 + \frac{1}{2} f''(m) \varepsilon^2 u_0^2 + O(\varepsilon^3),$$

so that from (5)

$$\begin{aligned} 0 = & f(m) + \varepsilon f'(m) u_0 + \varepsilon^2 f'(m) u_1 + \frac{1}{2} f''(m) \varepsilon^2 u_0^2 \\ & + \varepsilon^2 \left(-\varepsilon^{-1} V \partial_\rho u + \varepsilon^{-2} \partial_\rho^2 u + \varepsilon^{-1} \Delta d \partial_\rho u + \alpha \dot{w}^\varepsilon(t) \right) - \varepsilon \lambda_\varepsilon(t) + O(\varepsilon^3). \end{aligned}$$

- Since $f(m) + m'' = 0$, we have

$$\begin{aligned} 0 = & \varepsilon \left(f'(m) u_0 + \partial_\rho^2 u_0 - V m' + \Delta d m' - \lambda_0 \right) \\ & + \varepsilon^2 \left(f'(m) u_1 + \frac{1}{2} f''(m) u_0^2 - V \partial_\rho u_0 + \partial_\rho^2 u_1 + \Delta d \partial_\rho u_0 + \alpha \dot{w}^\varepsilon(t) - \lambda_1 \right) \\ & + O(\varepsilon^3). \end{aligned}$$

- To vanish the terms of $O(\varepsilon)$ and $O(\varepsilon^2)$,

$$(6) \quad \begin{aligned} \mathcal{L}u_0 &= -Vm' + \Delta d m' - \lambda_0, \\ \mathcal{L}u_1 &= \partial_\rho u_0(\Delta d - V) + \frac{1}{2}f''(m)u_0^2 + \alpha \dot{w}^\varepsilon(t) - \lambda_1, \end{aligned}$$

where $\mathcal{L}u = -(\partial_\rho^2 u + f'(m)u)$.

- By the solvability condition for the first, we obtain

$$\int_{\mathbb{R}} (-Vm' + \Delta d m' - \lambda_0(t))m' d\rho = 0.$$

This shows

$$(7) \quad V = \Delta d - \lambda_0(t)\sigma,$$

where $\sigma = 2(\int (m')^2 d\rho)^{-1}$ is the surface tension.

- The next task is to search for $\lambda_0(t)$. Similarly as above and from (6),

$$\begin{aligned} & \Delta u + \varepsilon^{-2}f(u) - \varepsilon^{-1}\lambda_\varepsilon(t) \\ &= \varepsilon^{-1}(-\mathcal{L}u_0 + \Delta d m' - \lambda_0) + (-\mathcal{L}u_1 + \frac{1}{2}f''(m)u_0^2 + \Delta d \partial_\rho u_0 - \lambda_1) + O(\varepsilon) \\ &= \varepsilon^{-1}Vm' + (\partial_\rho u_0 V - \alpha \dot{w}^\varepsilon(t)) + O(\varepsilon). \end{aligned}$$

- Since this integrated over D vanishes, denoting the Jacobian by $\varepsilon J_\varepsilon$,

$$0 = \int_{\{\rho; |\rho| \leq \frac{d}{\varepsilon}\}} \int_U \left(\varepsilon^{-1}Vm' + (\partial_\rho u_0 V - \alpha \dot{w}^\varepsilon(t)) + O(\varepsilon) \right) \varepsilon J_\varepsilon(\rho, s, t) d\rho ds.$$

- Noting that $J_\varepsilon(\rho, s, t) = 1 + O(\varepsilon)$, the right hand side is rewritten into

$$\begin{aligned} &= 2 \int_U V ds + \int_{\{\rho; |\rho| \leq \frac{d}{\varepsilon}\}} \int_U \varepsilon \partial_\rho u_0 V d\rho ds - \alpha \dot{w}^\varepsilon(t) \int_{\{\rho; |\rho| \leq \frac{d}{\varepsilon}\}} \int_U \varepsilon d\rho ds + O(\varepsilon) \\ &= 2 \int_U (\Delta d - \lambda_0(t)\sigma) ds + \varepsilon \int_{\{\rho; |\rho| \leq \frac{d}{\varepsilon}\}} \int_U \partial_\rho u_0 (\Delta d - \lambda_0(t)\sigma) d\rho ds - \alpha \dot{w}^\varepsilon(t) |D| + O(\varepsilon), \end{aligned}$$

where we have used (7) and $\int_{\{\rho; |\rho| \leq \frac{d}{\varepsilon}\}} \int_U \varepsilon d\rho ds = |D|$.

- Noting that $\partial_\rho u_0$ is of order $O(e^{-\sqrt{2}|\rho|})$ as $|\rho| \rightarrow \infty$, the middle term is $O(\varepsilon)$. Thus we have

$$0 = 2 \int_U \Delta d(s, t) ds - 2\lambda_0(t)\sigma|U| - \alpha \dot{w}^\varepsilon(t)|D| + O(\varepsilon).$$

This shows

$$\lambda_0(t) = \frac{1}{\sigma|U|} \int_U \Delta d(s, t) ds - \frac{\alpha|D|}{2\sigma|U|} \dot{w}^\varepsilon(t) + O(\varepsilon).$$

- Combining this with (7), we finally obtain the equation:

$$V = \Delta d - \frac{1}{|U|} \int_U \Delta d(s, t) ds + \frac{\alpha|D|}{2|U|} \dot{w}^\varepsilon(t) + O(\varepsilon).$$

Since $\Delta d(s, t) = \kappa(s, t) + O(\varepsilon)$, $s \in U$, in the limit as ε tends to 0, we formally obtain

$$V(s, t) = \kappa(s, t) - \frac{1}{|\gamma_t|} \int_{\gamma_t} \kappa(s, t) ds + \frac{\alpha|D|}{2|\gamma_t|} \circ \dot{w}(t)$$

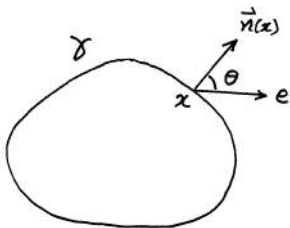
In the real proof:

- We expand u^ε around γ_t^ε (not γ_t).
- In order to derive error estimates, we need to expand u^ε up to k th order terms with $k > K := \max\{4, n\}$.
- In the 0 th order term, only $\dot{w}^\varepsilon(t)$ appears.
- However, in the k th order terms with $k \geq 1$, diverging terms like higher order derivatives of $w^\varepsilon(t)$ and their products appear. Fortunately, these terms multiplied by ε^k converges to 0, if the diverging speed of derivatives of $w^\varepsilon(t)$ is sufficiently slow:

$$\left| \frac{d^k}{dt^k} w^\varepsilon(t) \right| \leq C |\log \varepsilon|^{k/2}, \quad t \in [0, T], \quad k = 1, 2, \dots, K.$$

4. Limit SPDE (2) — 2D, convex curve

- γ : strictly convex closed plane curve
- Gauss map: $\theta \in S := [0, 2\pi) \mapsto x = x(\theta) \in \gamma$ if the angle between one fixed direction $\mathbf{e} := (1, 0)$ in the plane \mathbb{R}^2 and the outward normal $\vec{n}(x)$ at x to γ is θ .
- Denote by $\kappa = \kappa(\theta) > 0$ the curvature of γ at $x = x(\theta)$.



- Under these notation, the dynamics (2) is rewritten into the stochastic integro-differential equation for $\kappa = \kappa(t, \theta)$:

$$(8) \quad \partial_t \kappa = \kappa^2 \partial_\theta^2 \kappa + \kappa^3 - \kappa^2 \cdot \bar{\kappa} - \frac{c\kappa^2}{|\gamma_t|} \circ \dot{W}_t,$$

where $\bar{\kappa}$ denotes the average of κ over the curve γ_t and $|\gamma_t|$ stands for the length of γ_t .

- Similarly, the dynamics (3) is rewritten into the equation for $\kappa = \kappa^\varepsilon$:

$$(9) \quad \partial_t \kappa = \kappa^2 \partial_\theta^2 \kappa + \kappa^3 - \kappa^2 \cdot \bar{\kappa} - \frac{c\kappa^2}{|\gamma_t^\varepsilon|} \dot{W}_t^\varepsilon,$$

where $\bar{\kappa}$ denotes the average of κ over the curve γ_t^ε .

- Since $x(\theta) \in \mathbb{R}^2 \cong \mathbb{C}$ is written as

$$x(\theta) = x(0) - \sqrt{-1} \int_0^\theta \frac{e^{\sqrt{-1}\theta'}}{\kappa(\theta')} d\theta',$$

we see that $|x'(\theta)| = 1/\kappa(\theta)$.

- Therefore, $\bar{\kappa}$ and $|\gamma|$ are given by

$$\bar{\kappa} := \frac{1}{|\gamma|} \int_S \kappa(\theta) |x'(\theta)| d\theta = \frac{2\pi}{|\gamma|},$$

$$|\gamma| := \int_S |x'(\theta)| d\theta = \int_S \frac{d\theta}{\kappa(\theta)},$$

respectively, which are functionals of $\kappa = \{\kappa(\theta); \theta \in S\}$.

$$\sigma_N^\varepsilon := \inf\{t > 0; \kappa^\varepsilon(t, \theta), \kappa^\varepsilon(t, \theta)^{-1}, |\kappa^\varepsilon(t, \theta)'| \geq N$$

for some θ or $\text{dist}(\gamma_t^\varepsilon, \partial D) \leq 1/N\}$

Theorem 2

For each $m \in \mathbb{N}$ and $T > 0$, let P^ε be the distribution of the solution $\kappa^\varepsilon(t \wedge \sigma_N^\varepsilon, \cdot)$ of SPDE (9) corresponding to (3) on $C([0, T], C^m(S))$. Then, $\{P^\varepsilon\}_{0 < \varepsilon < 1}$ is tight.

- The pathwise uniqueness combined with the existence of the solution in law sense implies the existence of a strong solution of (8).
- Therefore γ_t^ε converges to γ_t up to time $\sigma \leq T$ in $C([0, T], C^m)$ sense.
- In the present setting, the assumption “ $\gamma_t^\varepsilon \rightarrow \gamma_t$ ” for Theorem 1 holds.

5. Summary of the talk

- We discussed the sharp interface limit for mass conserving Allen-Cahn equation with stochastic term by extending the method of the asymptotic expansion employed by Chen-Hilhorst-Logak.
- Then, diverging term like $(\dot{w}^\varepsilon(t))^2$, $(\dot{w}^\varepsilon(t))^3$ etc. appear. Usually, we cannot control such terms, but fortunately they appear only in the higher order terms in the expansion.
- Therefore, if the diverging speed of derivatives of $w^\varepsilon(t)$ is sufficiently slow, we can control them.

Thank you for your attention!

Spreading speeds in diffusive prey-predator systems

Thomas GILETTI

University of Lorraine

joint work with A. Ducrot and H. Matano

ReaDiLab Conference

CIRM - June 2014

Our system and assumptions

The spreading dynamics

Our system and assumptions

The spreading dynamics

A prey-predator reaction-diffusion system

- ▶ A two-component reaction-diffusion system:

$$\begin{cases} \partial_t u = d\Delta u + uF(u, v) \\ \partial_t v = \Delta v + vG(u, v) \end{cases} \quad x \in \mathbb{R}^N, t > 0,$$

together with nontrivial & nonnegative initial data

$$0 \leq u_0(x) \leq 1, \quad 0 \leq v_0(x).$$

- ▶ $F(u, v)$ is the growth rate of the prey u ,
 $G(u, v)$ is the growth rate of the predator v .
 - ▶ Both growth rates will be positive in some range.

A prey-predator reaction-diffusion system

- ▶ The predation effect:

$$\partial_v F(u, v) < 0, \quad \partial_u G(u, v) \geq 0.$$

- ▶ A KPP type assumption:

$$\partial_u F(u, v) \leq 0, \quad \partial_v G(u, v) \leq 0.$$

- ▶ Survival of the prey when there is no predator:

$$\forall u \in [0, 1), \quad F(u, 0) > F(1, 0) = 0, \quad \text{but} \quad F(0, +\infty) < 0.$$

- ▶ The predator requires the prey to survive and grow:

$$G(0, 0) < 0 < G(1, 0).$$

The propagation dynamics

- ▶ Under our assumptions, both the prey and the predator have the ability to invade the domain.

- ▶ **Question:**

Assuming that both populations are compactly supported at time $t = 0$, how fast do they spread through the domain?

- ▶ **The difficulty:** The system as a whole does not satisfy the comparison principle!
- ▶ However, we will see that both species spread, but also that their respective speeds may differ.

Our system and assumptions

The spreading dynamics

Single equation dynamics

- ▶ Assume that $v \equiv 0$ (no predators).
 $\Rightarrow u$ satisfies the classical KPP equation

$$\partial_t u = d\Delta u + uF(u, 0).$$

- ▶ Then the prey u spreads with speed c^* [Aronson-Weinberger]:

$$\forall c > c^*, \limsup_{t \rightarrow \infty} \sup_{\|x\| \geq ct} u(t, x) = 0,$$

$$\forall c < c^*, \limsup_{t \rightarrow \infty} \sup_{\|x\| \leq ct} |1 - u(t, x)| = 0,$$

where $c^* = 2\sqrt{dF(0,0)}$ speed of the linearized problem.

Single equation dynamics

- ▶ Assume that $u \equiv 1$ (many preys).
- ▶ Then the predator v spreads with speed c^{**} [AW]:

$$\forall c > c^{**}, \limsup_{t \rightarrow \infty} \sup_{\|x\| \geq ct} v(t, x) = 0,$$

$$\forall c < c^{**}, \liminf_{t \rightarrow \infty} \inf_{\|x\| \leq ct} |v(t, x)| > 0,$$

where $c^{**} = 2\sqrt{G(1, 0)}$.

- ▶ It is not assumed that there exists a positive stable state.
- ▶ Comparing c^* and c^{**} , which species is faster?

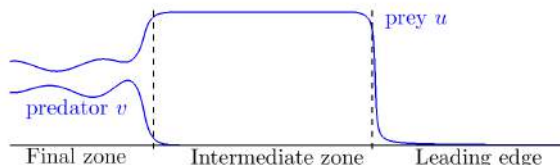
Our results: the slow predator case

- **Theorem 1:** Assume that $c^{**} < c^*$, then:

$$\forall c > c^*, \limsup_{t \rightarrow \infty} \sup_{\|x\| \geq ct} |u| + |v| = 0,$$

$$\forall c^{**} < c_1 < c_2 < c^*, \limsup_{t \rightarrow \infty} \sup_{c_1 t \leq \|x\| \leq c_2 t} |1 - u| + |v| = 0,$$

$$\forall c < c^{**}, \liminf_{t \rightarrow \infty} \inf_{\|x\| \leq ct} \min\{1 - u, u, v\} > 0.$$



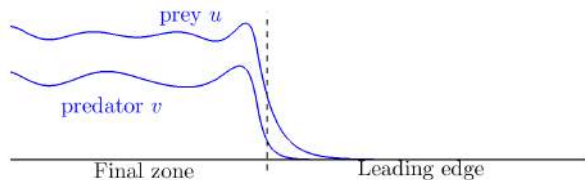
Prey spreads with speed c^ and predator with speed c^{**} .*

Our results: the fast predator case

- **Theorem 2:** Assume that $c^{**} \geq c^*$, then:

$$\forall c > c^*, \limsup_{t \rightarrow \infty} \sup_{\|x\| \geq ct} |u| + |v| = 0,$$

$$\forall c < c^*, \liminf_{t \rightarrow \infty} \inf_{\|x\| \leq ct} \min\{1 - u, u, v\} > 0,$$



Both the prey and predator spread with speed c^ .*

The proof: leading edge and intermediate zone

- ▶ **The leading edge** can be dealt with by simple comparison arguments.
- ▶ **The intermediate zone** is more intricate: (here $c^* > c^{**}$)
 - ▶ it relies on the KPP assumption, for small densities of preys to propagate away of the predator's reach;
 - ▶ this intermediate zone appears as long as

$$2\sqrt{dF(0,0)} > 2\sqrt{\|G(1,\cdot)\|_\infty}.$$

Otherwise, there may be some threshold effect with respect to initial data.

The proof: final zone

- ▶ **Weak dissipativity property:** $\forall \kappa > 0, \exists M(\kappa) > 0$ s.t.

$$(u_0, v_0) \leq \kappa \Rightarrow \forall t, (u(t, \cdot), v(t, \cdot)) \leq M(\kappa).$$

- ▶ It is satisfied if $G(0, 0) < 0$ and $F(0, +\infty) < 0$.
- ▶ **The final zone:**
 - ▶ $(u = 1, v = 0)$ is linearly unstable w.r.t. the ODE system;
 - ▶ Step 1: by contradiction, there exists $\varepsilon > 0$ so that v may not stay smaller than ε indefinitely in a moving frame with speed $c < \min\{c^*, c^{**}\}$;
 - ▶ Step 2: by a strong maximum principle argument, if there exists a sequence $v(t_n, x_n) \rightarrow 0$ in the final zone, one can construct a solution contradicting step 1.

Inside the final zone

- ▶ We only know that

$$0 < u < 1, 0 < v$$

uniformly in the final zone.

- ▶ What is the shape of the solution?
- ▶ **Conjecture:** the solution always converges to the same entire solution.
 - ▶ Holds true if $d = 1$, the ODE system admits a stable stationary state and a strong Lyapunov function.
- ▶ What about $d \neq 1$, stable cycles and patterns?

Thank you for your attention.

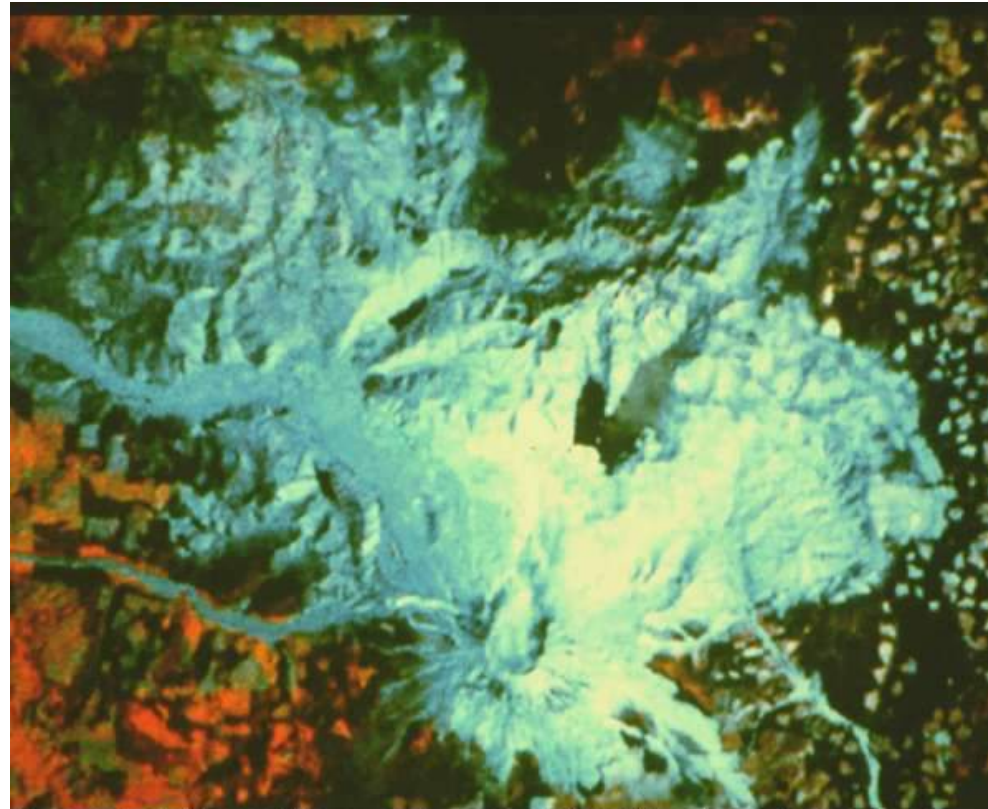
June.3 - 5, 2014,CIRM

Mathematics and its applications to complex phenomena
arising in biology, chemistry and medicine

Revisit to Traveling Waves for the Lotka-Volterra Predator-Prey Models - Analysis of Invasion Processes -

Yuzo Hosono
Kyoto Sangyo University

1. Example: Eruption of Mount St. Helen (1980): Invasion into the open space.



The massive size of the 230 square mile blast zone as seen from space is revealed in this 1980 false color composite image from the Landsat MSS satellite.
[Landsat, MSS Composite, 1980]

From <http://www.fs.usda.gov/main/mountsthelens/learning>

Succession



It is not unusual to see large herds of bull elk running together on the debris avalanche or in the blast zone north of the volcano. Elk viewing is a very popular activity among Monument visitors. [C. Tonn, USDA Forest Service]



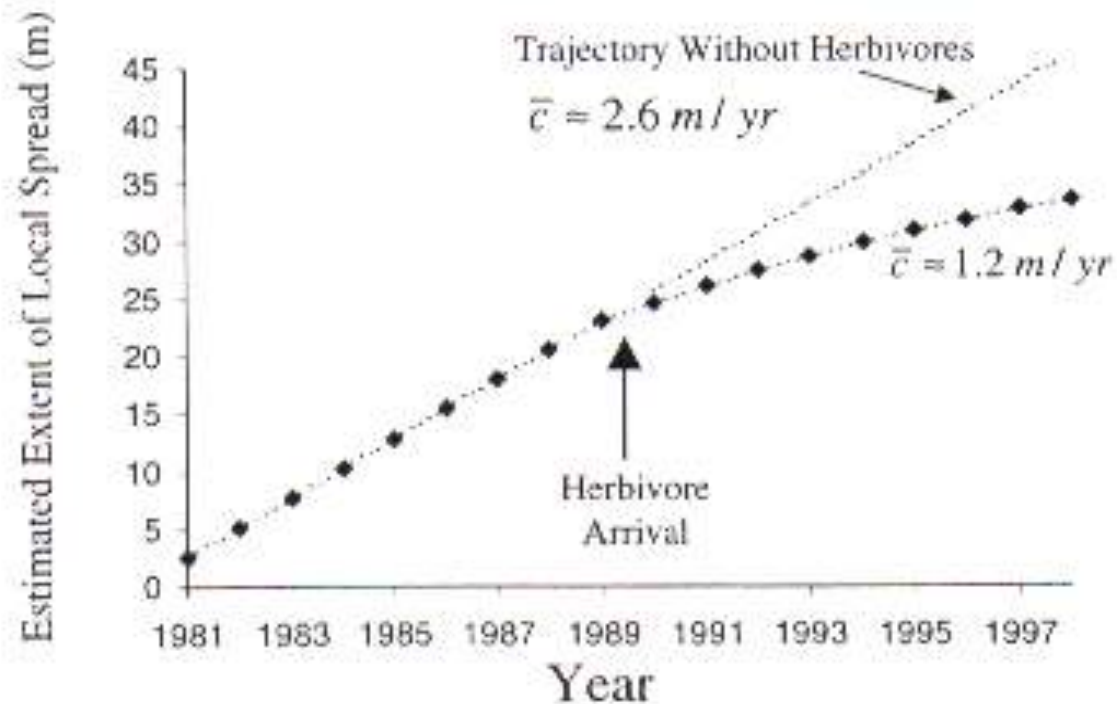
Prairie lupine (*Lupinus lepidus*) have been an important early colonizing plant on the Pumice Plain (pyroclastic flow) north of the crater.
[James Cook, University of Wisconsin-Stevens Point, 1999]



More and more insects are colonizing the blast zone as developing plant life provides a source of food and shelter. Grasshoppers forage among the lupines on the pumice plain. Such insects provide a food source for small mammals and insectivorous birds. As food and shelter becomes increasingly available animals are colonizing the blast zone in ever increasing numbers. [J. Gale, USDA Forest Service, 1994]

The ecological question:

Can the predation slow down the invasion of a prey ?



- Fagan, W.F. and Bishop, J.G., Trophic interactions during primary succession: herbivores slow a plant reinvasion at Mount St. Helens, Am. Nat. 155 (2000), 238-251.

2. The model equation and the preliminaries.

The Lotka-Volterra Predator-Prey model

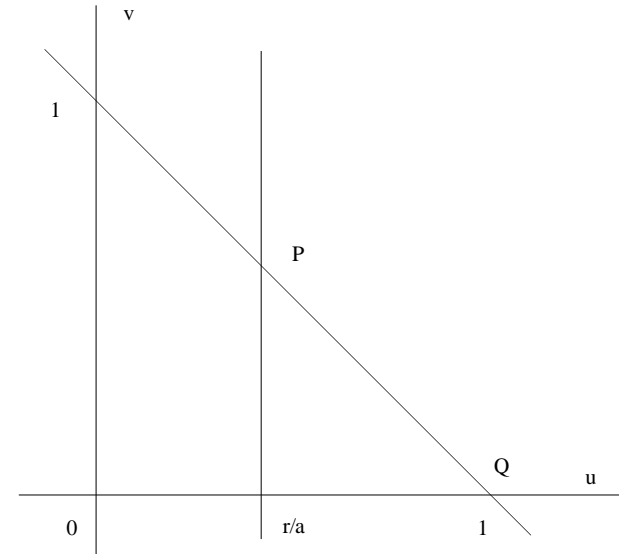
$$(PP) \quad \begin{cases} u_t = d_1 u_{xx} + r(1 - u - v)u \\ v_t = d_2 v_{xx} + (-1 + au - bv)v \end{cases}$$

Assumption: $a > 1, b \geq 0$

$$\begin{aligned} \Rightarrow (u, v) = (0, 0) = O: & \text{ unstable (saddle)} \\ (u, v) = (1, 0) = Q: & \text{ unstable (saddle)} \\ (u, v) = (u^*, v^*) = P: & \text{ stable} \\ & \text{where } u^* = (b+1)/(a+b), v^* = (a-1)/(a+b) \end{aligned}$$

$$(BC1) \quad (u(-\infty, t), v(-\infty, t)) = (u^*, v^*), \quad (u(\infty, t), v(\infty, t)) = (1, 0).$$

$$(BC2) \quad (u(-\infty, t), v(-\infty, t)) = (u^*, v^*), \quad (u(\infty, t), v(\infty, t)) = (0, 0).$$



See,

- Owen M.R. and Lewis M.A., How predation can slow, stop or reverse a prey invasion, *Bulletin Math. Biology*, 63 (2001), 655-684.
- Fagan, W.F., Lewis M.A., Neubert M.G. and van den Driessche, P., Invasion theory and biological control, *Ecological Letters*, 5 (2002), 148-157.

Traveling wave solutions :

a couple of nonnegative functions satisfying

$$(U(z), V(z)) \in C^2(\mathbb{R}) \times C^2(\mathbb{R})$$

$$(T) \quad \begin{cases} d_1 U'' + cU' + rf(U, V) = 0 \\ d_2 V'' + cV' + g(U, V) = 0, \end{cases} \quad z = x - ct,$$

or (BC1) $(U(-\infty), V(-\infty)) = (u^*, v^*), (U(\infty), V(\infty)) = (1, 0).$

(BC2) $(U(-\infty), V(-\infty)) = (u^*, v^*), (U(\infty), V(\infty)) = (0, 0).$

where ' denotes d/dz .

According to Dunbar, we call that

traveling waves satisfying (BC1) is type I waves,
traveling waves satisfying (BC2) is type II waves.

c : constant to be determined

The known results ($b = 0$)

Theorem 1 (Dunbar, S (1983))

Assume that $d_1 = 0$, $d_2 = 1$.

If $0 < c < 2\sqrt{a-1}$, traveling waves of type I do not exist, and traveling waves of type II exist.

If $c \geq 2\sqrt{a-1}$, traveling waves of type II do not exist, and traveling waves of type I exist.

Theorem 2 (Dunbar, S (1984))

Assume that $0 < d_1 \leq 1$, $d_2 = 1$.

If $c \geq 2\sqrt{a-1}$, traveling waves of type I exist.

Theorem 3 (Ma, S (2001))

Assume that $d_1 > 0$, $d_2 > 0$.

For any $c > 2\sqrt{d_1 r}$, the monotone traveling waves of type II exist.

3. The heuristic and numerical argument on the invasion processes

$$d_1 = d, d_2 = 1.$$

When $v = 0$, there exists a traveling prey wave with the minimal wave speed

$$c_2^* = 2\sqrt{rd}$$

$0 \leq u \leq 1$ implies that the fastest speed of v is

$$c_1^* = 2\sqrt{a-1}$$

If $c_1^* < c_2^*$, the prey u -wave with the speed c_2^* goes ahead and the predator wave with the speed c_1^* follows the prey.

If $c_1^* > c_2^*$, the predator can catch the prey at the invasion front and they invade with the same speed.

The numerical example:

$$c_1^* = 2\sqrt{a-1} = \sqrt{2} \quad (a = 2) < c_2^* = 2\sqrt{rd} = 2$$

$$c_1^* = 2\sqrt{a-1} = \sqrt{6} \quad (a = 5/2) > c_2^* = 2\sqrt{rd} = 2$$

$$c_1^* = 2\sqrt{a-1} = \sqrt{2} < c_2^* = 2\sqrt{rd} = 2$$

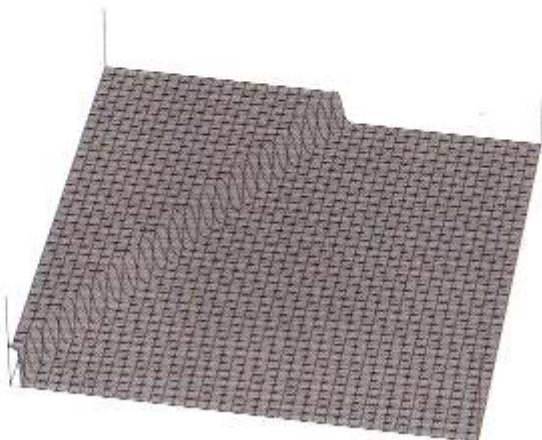
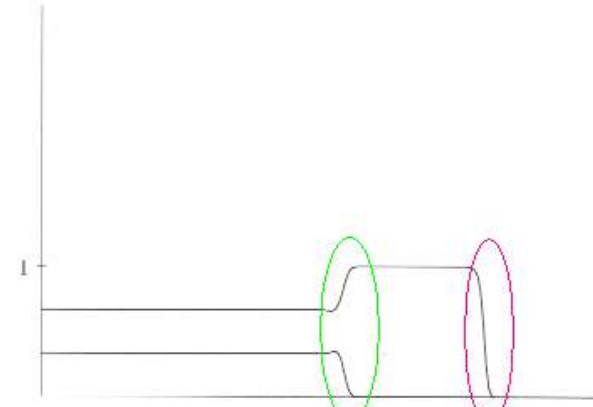
l=500, T=200

l=500, T=200

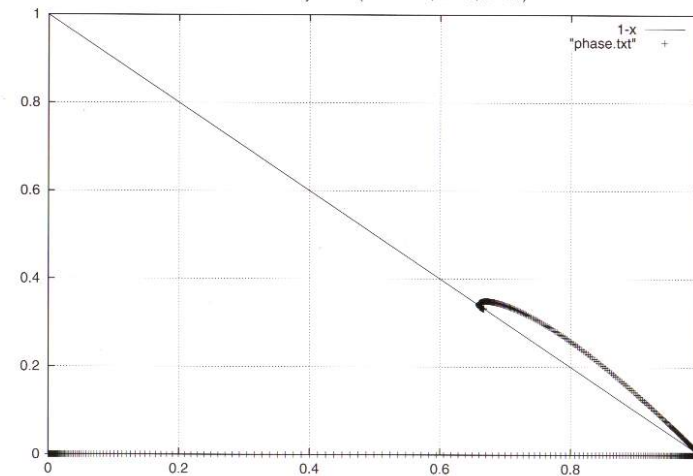
a1=1, a2=1.5
 b1=1, b2=0
 r1=1, r2=1.0
 d1=1, d2=1
 h=0.1, k=0.01
 bairitsu=1



a1=1, a2=1.5
 b1=1, b2=0
 r1=1, r2=1.0
 d1=1, d2=1
 h=0.1, k=0.01
 bairitsu=1



Predator-Prey Model (d1=d2=1.0, r2=1.0, a2=1.5)

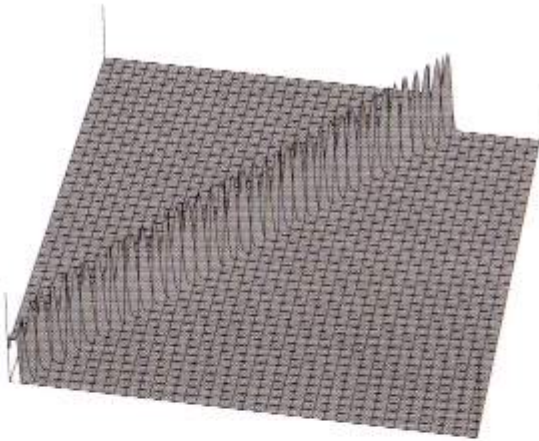


$$c_1^* = 2\sqrt{a-1} = \sqrt{6} > c_2^* = 2\sqrt{rd} = 2$$

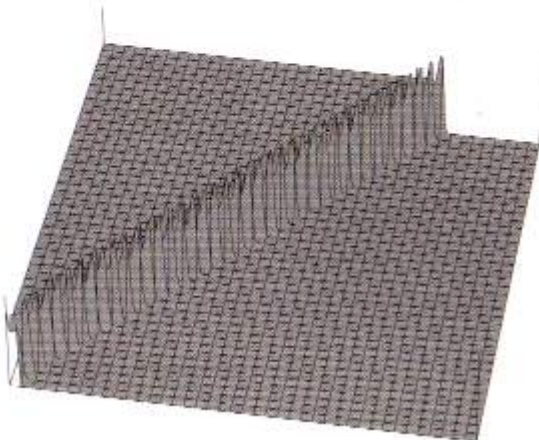
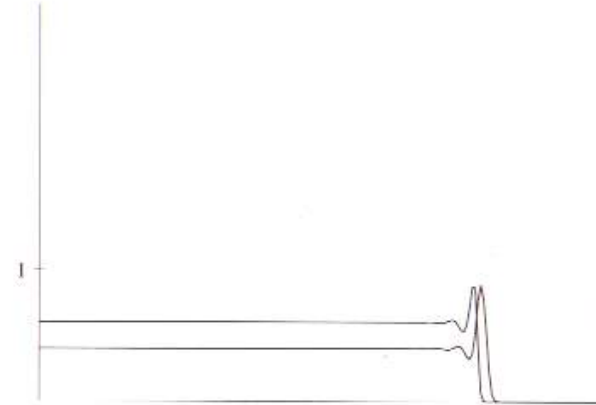
l=500, T=200

l=500, T=200

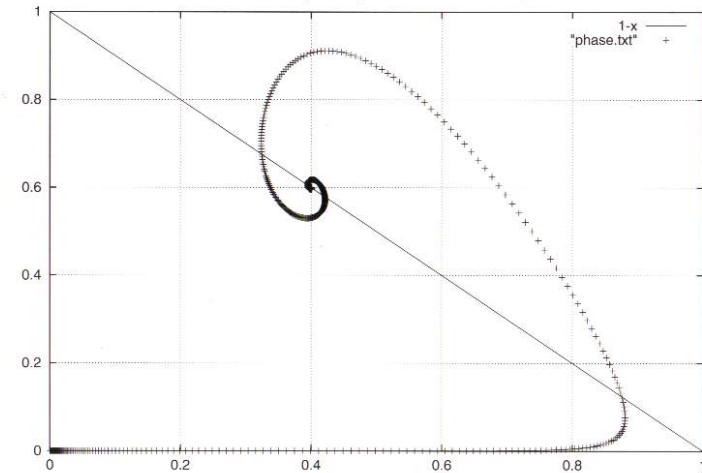
a1=1, a2=2.5
 b1=1, b2=0
 r1=1, r2=1.0
 d1=1, d2=1
 h=0.1, k=0.01
 bairitsu=1



a1=1, a2=2.5
 b1=1, b2=0
 r1=1, r2=1.0
 d1=1, d2=1
 h=0.1, k=0.01
 bairitsu=1



Predator-Prey Model (d1=d2=1.0, r2=1.0, a2=2.5)



Mathematical Questions :

[1] For $d_1/d_2 > 1$, do there exist type I waves and type II waves ?

[2] Do there exist type II waves which are not monotone ?

[3] For $d_2 = 0$, do there exist type I waves and type II waves ?

Remark 1 :

The linearization at the critical points O and Q implies that

[1] Type II waves exist only for $c \geq c_2^* = 2\sqrt{rd_1}$,

[2] Type I waves exist only for $c \geq c_1^* = 2\sqrt{d_2(a-1)}$.

[1] implies that a predator cannot slow down the invasion of a prey.

For the standard predator-prey model, this is true.

4. The degenerate case $d_2 = 0$.

Theorem 4 (Y.H.) Assume that $b \geq 0$.

For any $c > 0$, there exists no type II traveling wave, and there exist type I traveling waves.

(Proof) The existence of type I waves is proved by the shooting argument based on the Wazewski theorem for

$$(D) \quad \begin{cases} U' = V, \\ V' = -r(1 - U - V)U, \\ W' = -\frac{1}{c}(-1 + aU - bV)V, \end{cases}$$

with the boundary conditions

$$(BC1) \quad (U(-\infty), V(-\infty), W(-\infty)) = (u^*, 0, v^*), \quad (U(\infty), V(\infty), W(\infty)) = (1, 0, 0).$$

The nonexistence of type II waves is derived from the property of the critical point $O = (0, 0, 0)$.

5. Type II waves for the case: $d_1 = \varepsilon^2$, $c = \sigma\varepsilon$, $d_2 = 1$.

The formal singular perturbation analysis.

The traveling wave equations of (PP) are

$$(TPP) \quad \begin{cases} \varepsilon^2 U'' + \varepsilon \sigma U' + r(1 - U - V)U = 0 \\ V'' + \varepsilon \sigma V' + (-1 + aU - bV)V = 0 \end{cases}$$

$$\text{Put } \varepsilon = 0. \quad \begin{cases} r(1 - U - V)U = 0 \\ V'' + (-1 + aU - bV)V = 0 \end{cases}$$

Define

$$U = h_\beta(V) \equiv \begin{cases} 0 & (0 < V < \beta) \\ 1 - V & (\beta < V < v^*) \end{cases}$$

Outer Problem :

$$(R) \quad \begin{aligned} V'' + g(h_\beta(V), V) &= 0, \\ V(-\infty) &= v^*, V(\infty) = 0, V(0) = \beta. \end{aligned}$$

Lemma 1 (R) has a unique C^1 solution only for $\beta = \beta^* \in (0, v^*)$,
where β^* is a unique zero of

$$J(\beta) = \int_0^{v^*} g(h_\beta(s), s) ds.$$

Inner Problem : stretched variable $\xi = z/\varepsilon$.

$$(I) \quad \begin{aligned} \ddot{U} + \sigma \dot{U} + r(1 - \beta^* - U)U &= 0, \\ U(-\infty) &= 1 - \beta^*, U(\infty) = 0. \end{aligned}$$

Lemma 2 (I) has a unique monotone solution for each

$$\sigma \geq \sigma^* \equiv 2\sqrt{r(1 - \beta^*)},$$

except for modulo translation.

Remark 2 : This formal singular perturbation analysis may suggest

[1] type II waves exist for any $c \geq \varepsilon \sigma^*$ with $\sigma^* \equiv 2\sqrt{r(1-\beta^*)}$.

However, this is not true since type II waves exist only for

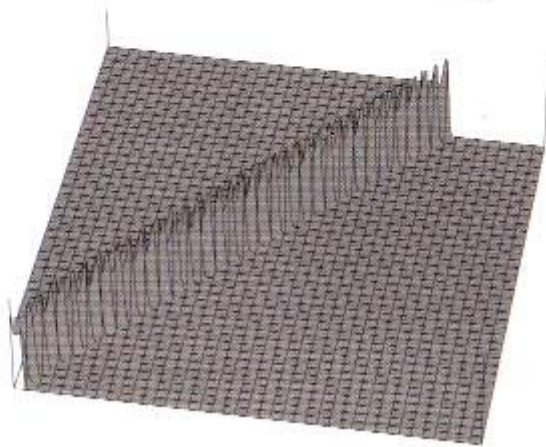
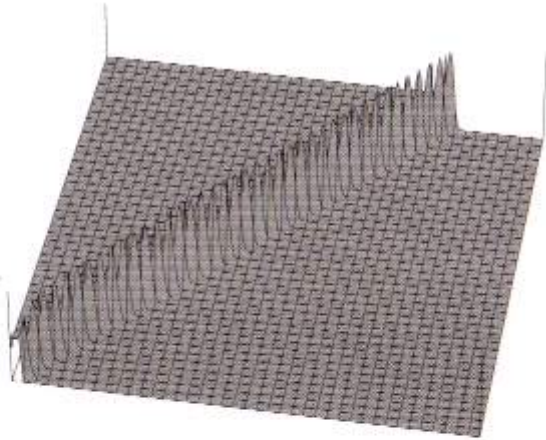
$$c = \varepsilon \sigma \geq c_2^* \equiv 2\sqrt{r}.$$

[2] The profile of a prey is not monotone because the internal layer $U(\zeta)$ decreases monotonely w.r.t. ζ from $1 - \beta^*$ to 0 where $1 - \beta^* > u^*$.

The uniqueness of traveling waves may not valid. (See, Ma's result.)

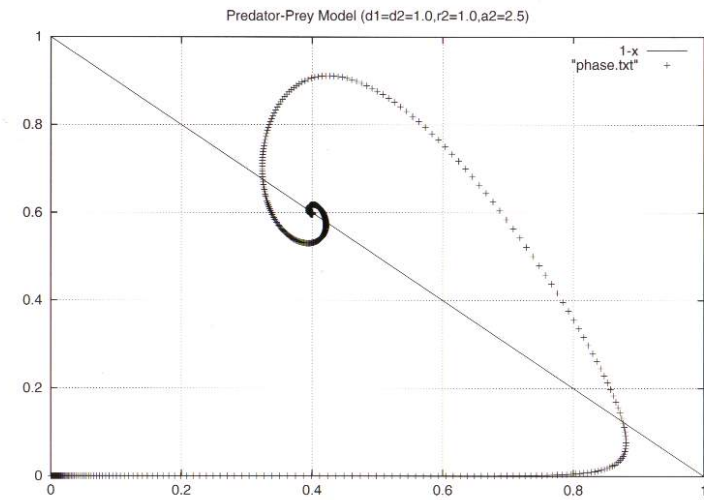
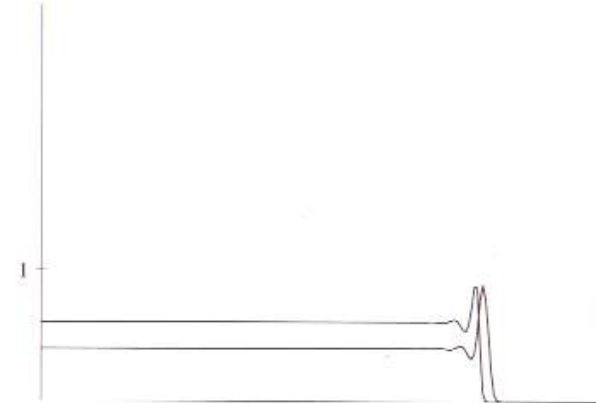
$l=500, T=200$

$a_1=1, a_2=2.5$
 $b_1=1, b_2=0$
 $r_1=1, r_2=1.0$
 $d_1=1, d_2=1$
 $h=0.1, k=0.01$
 $bairitsu=1$

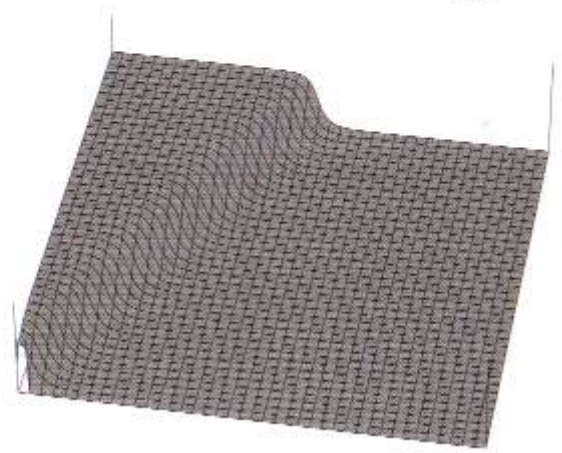
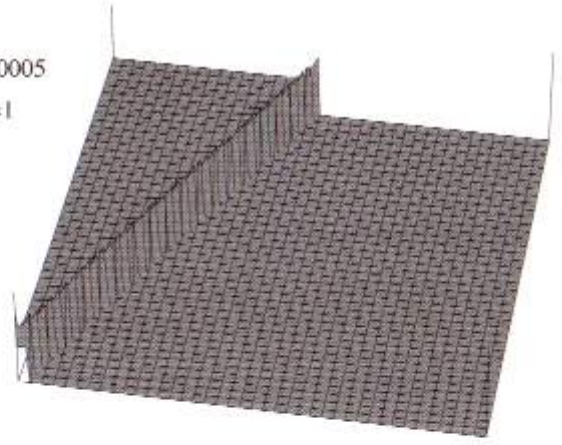


$l=500, T=200$

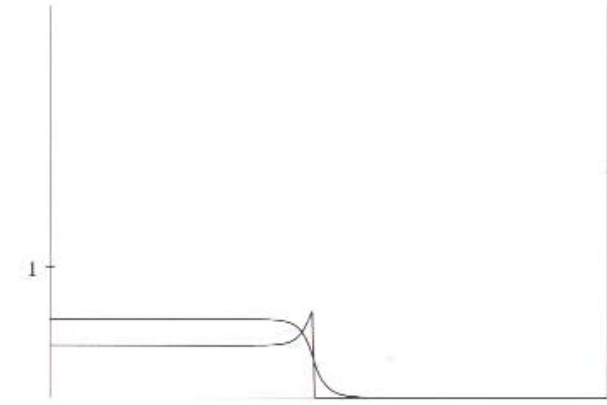
$a_1=1, a_2=2.5$
 $b_1=1, b_2=0$
 $r_1=1, r_2=1.0$
 $d_1=1, d_2=1$
 $h=0.1, k=0.01$
 $bairitsu=1$



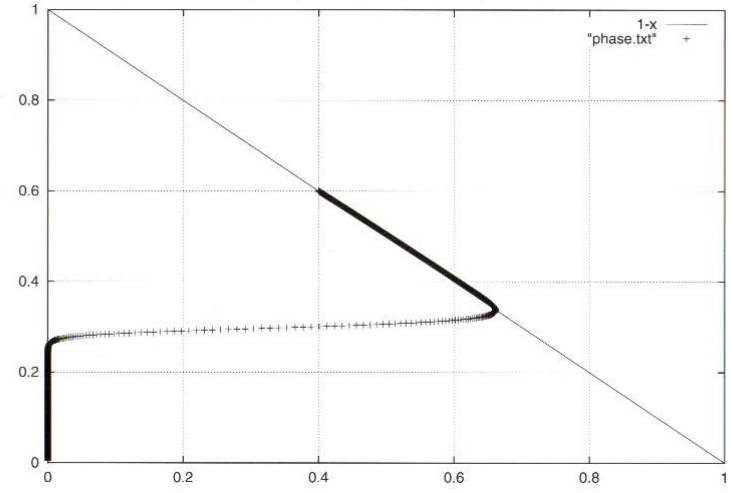
$l=50, T=1200$
 $h=0.002, k=0.00005$
 $d1=0.0001, d2=1$
 $a1=1, a2=2.5$
 $b1=1, b2=0$
 $r1=1, r2=1.0$
 $bairitsu=1$



$l=50, T=1200$
 $h=0.002, k=0.00005$
 $d1=0.0001, d2=1$
 $a1=1, a2=2.5$
 $b1=1, b2=0$
 $r1=1, r2=1.0$
 $bairitsu=1$



Predator-Prey Model($d1=0.001, d2=1, r2=1, a2=2.5, h=0.002, k=0.00005$)



6. Type I wave for $b > 0$ and $d_1 > d_2$.

$$(PPI) \quad \begin{cases} u_t = d_1 u_{xx} + r(1 - u - v)u \\ v_t = d_2 v_{xx} + (-1 + au - bv)v \end{cases}$$

Assumption: $a > 1$

$$\Rightarrow \begin{aligned} (u, v) &= (1, 0) = Q: \text{unstable} \\ (u, v) &= (u^*, v^*) = P: \text{stable} \end{aligned}$$

$$\text{where } u^* = (b+1)/(a+b), \quad v^* = (a-1)/(a+b),$$

$$(BC1) \quad (u(-\infty, t), v(-\infty, t)) = (u^*, v^*), \quad (u(\infty, t), v(\infty, t)) = (1, 0).$$

There exists an invariant rectangle

$$D = \{(u, v) \mid 0 \leq u \leq 1, \quad 0 \leq v \leq \frac{a-1}{b}\}.$$

The formal singular perturbation analysis.

Consider the case: $d_1 = 1$, $d_2 = \varepsilon^2$, $c = \sigma\varepsilon$.

The traveling wave equations of (PP) are

$$(TPP) \quad \begin{cases} U'' + \varepsilon\sigma U' + r(1 - U - V)U = 0 \\ \varepsilon^2 V'' + \varepsilon\sigma V' + (-1 + aU - bV)V = 0 \end{cases}$$

$$\text{Put } \varepsilon = 0. \quad \begin{cases} U'' + r(1 - U - V)U = 0 \\ (-1 + aU - bV)V = 0 \end{cases}$$

Define

$$V = k_\alpha(U) \equiv \begin{cases} \frac{1}{b}(aU - 1) & (u^* \leq U < \alpha) \\ 0 & (\alpha < U \leq 1) \end{cases}$$

Outer Problem :

$$(RI) \quad \begin{aligned} U'' + f(U, k_\alpha(U)) &= 0, \\ U(-\infty) = u^*, U(\infty) &= 0, U(0) = \alpha. \end{aligned}$$

Lemma 3 (RI) has a unique solution only for $\alpha = \alpha^* \in (u^*, 1)$

where α^* is a unique zero of

$$J(\alpha) = \int_{u^*}^1 f(s, k_\alpha(s)) ds.$$

Inner Problem : stretched variable $\xi = z/\varepsilon$.

$$(I-I) \quad \begin{aligned} \ddot{V} + \sigma \dot{V} + (a\alpha^* - 1 - bV)V &= 0, \\ V(-\infty) = (a\alpha^* - 1)/b, V(\infty) &= 0. \end{aligned}$$

Lemma 4 (I-I) has a unique monotone solution for each

$$\sigma \geq \sigma_1^* \equiv 2\sqrt{a\alpha^* - 1},$$

except for modulo translation.

Remark 3 : This formal singular perturbation analysis may suggest

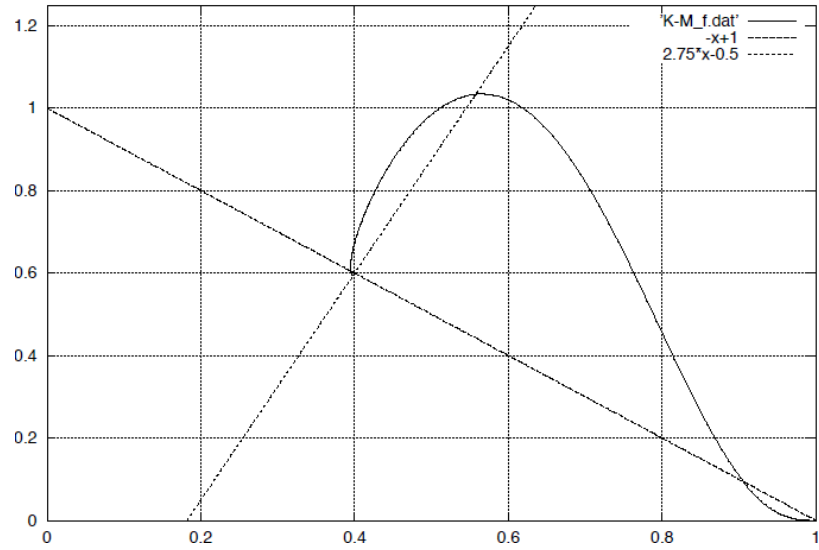
[1] type I waves exist for any $c \geq \varepsilon \sigma_1^*$ with $\sigma_1^* \equiv 2\sqrt{a\alpha^* - 1}$.

However, this is not true since type I waves exist only for

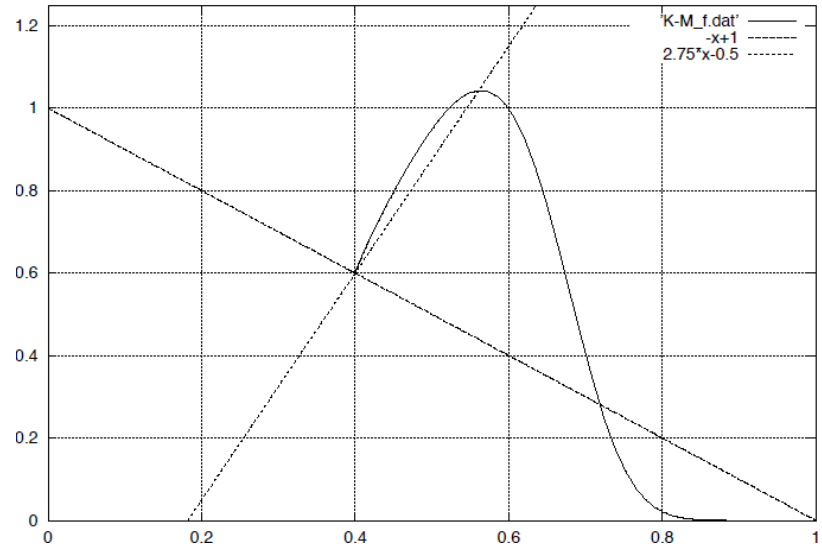
$$c = \varepsilon \sigma \geq c_1^* \equiv 2\sqrt{a - 1}.$$

[2] The profile of a predator is not monotone because the internal layer $V(\zeta)$ increases monotonely w.r.t. ζ from 0 to $(a\alpha^* - 1)/b > v^*$.

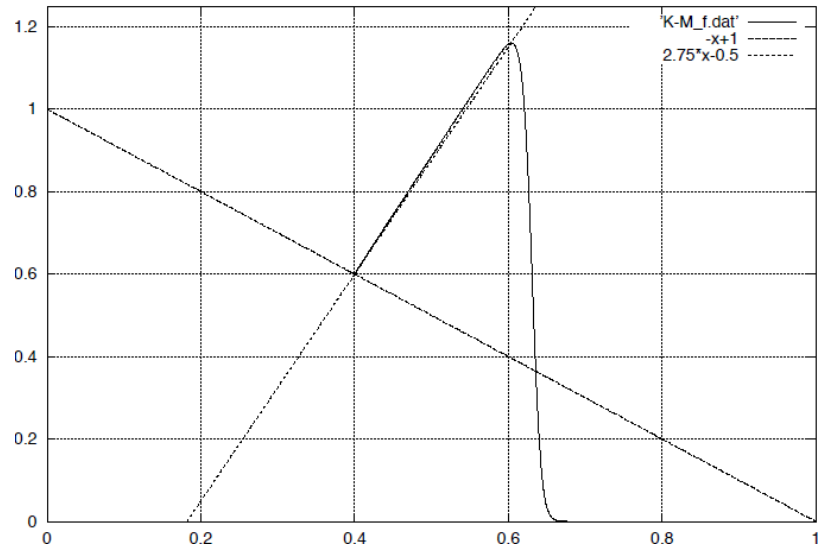
Lotka-Volterra predator-prey $d=0.1, h=0.05, k=0.05$



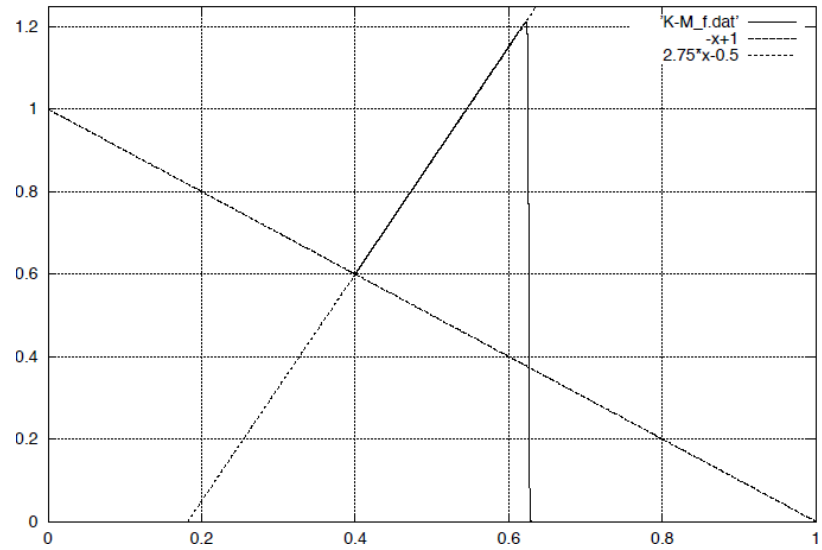
Lotka-Volterra predator-prey $d=0.01, h=0.05, k=0.05$



Lotka-Volterra predator-prey $d=0.0001, h=0.01, k=0.01$



Lotka-Volterra predator-prey $d=0.000001, h=0.001, k=0.001$



The behavior of the profile as $b \rightarrow 0$

We now fix (u^*, v^*) and let the slope of the nullcline : $v = \frac{a}{b}u - \frac{1}{b}$
 be infinity. Let $\kappa = \frac{a}{b}$ and $\alpha^*(\kappa)$ be the zero of $J(\alpha)$:

$$\begin{aligned} J(\alpha) &= \int_{u^*}^1 f(s, k_\alpha(s)) ds \\ &= \int_{\alpha}^1 (1-s)s ds + \left(\frac{a}{b} + 1\right) \int_{u^*}^{\alpha} (u^* - s)s ds \end{aligned}$$

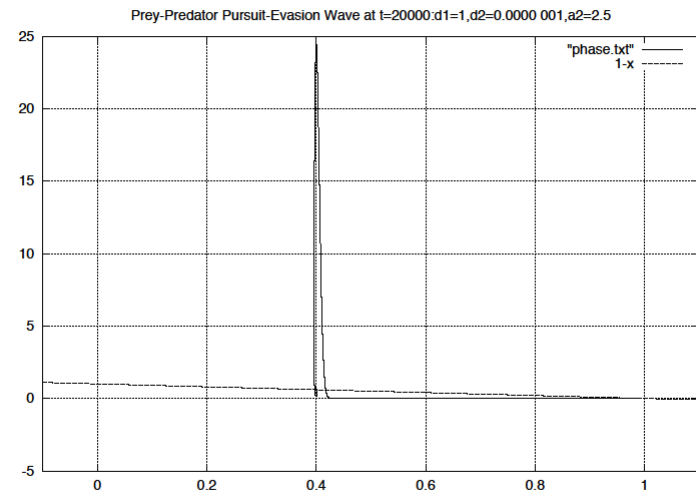
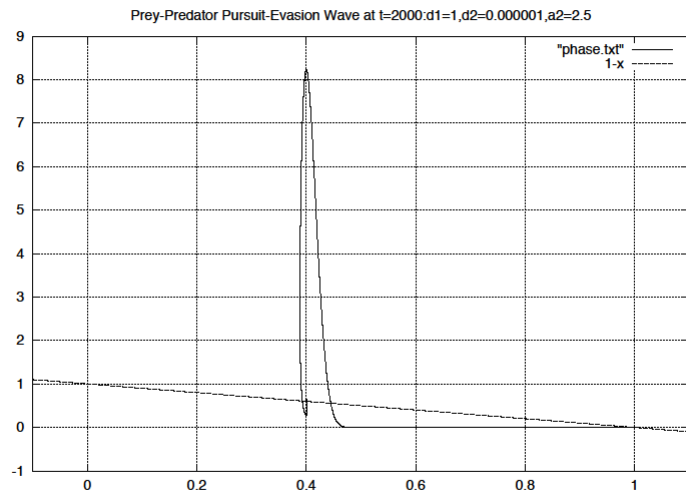
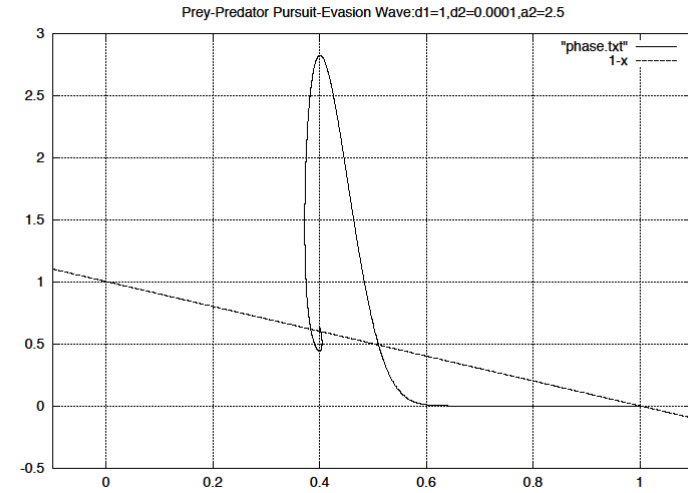
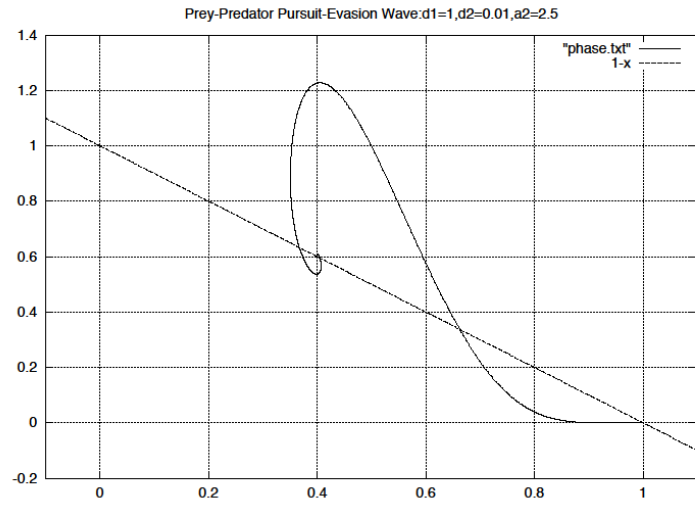
Then,

$$\lim_{\kappa \rightarrow \infty} \alpha^*(\kappa) = u^*, \quad \lim_{\kappa \rightarrow \infty} (a\alpha^*(\kappa) - 1)/b = +\infty$$

This implies that the profile of the predator becomes unbounded as b tends to zero.

Remark 4 : For the degenerate case (D), the reduced problem of the singular perturbations w.r.t. $c = \varepsilon$ is the same as (R-I).

$$b = 0$$



Conjecture :

If $c_1^* < c_2^*$, type II waves exist for any c satisfying $c_1^* \leq c < c_2^*$,

and type I waves exist only for c satisfying $c \geq c_2^*$.

Furthermore, there exists no non-monotone type II wave for $c \geq c_2^*$.

If $c_1^* > c_2^*$, non-monotone type II waves do not exist for any $c > 0$,

and type I waves exist only for c satisfying $c \geq c_2^*$.

Here, $c_1^* = 2\sqrt{d_2(a-1)}$, $c_2^* = 2\sqrt{d_1r}$.

Numerical speeds of the pursuit-evasion waves (type I waves)

For $r = O(1)$, let us consider the case that

d is sufficiently small

d	c	state	time	h
10^{-2}	$2.4252 * 10^{-1}$	↑	100	0.01
10^{-4}	$2.4360 * 10^{-2}$	↑	1000	0.005
10^{-6}	$2.2399 * 10^{-3}$	→	15000	0.001

$$c^* = 2\sqrt{d(a-1)} = \sqrt{6d} \approx 2.449\sqrt{d}$$

The mathematical analysis assure that there exists no travelling wave for any $c < c^*$, where

$$c^* = 2\sqrt{d(a-1)} = \sqrt{6d} \approx 2.449\sqrt{d}$$

Open problem: How can we understand the numerical results?

Other references on the invasion problem

- Fisher, R.A. (1937). The wave of advance of advantageous genes
- Skellam, J.G. (1951). Random dispersal in theoretical populations.
- Elton, C.S. (1958). *The Ecology of Invasions by Animals and Plants*
- Hengeveld, R. (1989). *Dynamics of Biological Invasions*
- Murray, J.D. (1989). *Mathematical Biology*,
Chap. 20. Geographic spread of epidemics.
- Shigesada, N. and Kawasaki, K. (1997). *Biological Invasions:
Theory and Practice*.
- Hastings, A. et al., The spatial spread of invasions: new developments in the theory and evidence, *Ecology Letters*, 8 (2005), 91-101

Population dynamics and biological dispersal

Yong-Jung Kim

Department of Mathematical Sciences, KAIST
291 Daehak-ro, Yuseong-gu, Daejeon 305-701, Korea

June 03, 2014 / Mathematics and its applications to complex phenomena arising in biology, chemistry and medicine, CIRM, Luminy

Part I

Random Migration of Biological Species

1. Random Diffusion of Brownian Particles

The linear diffusion equation is written as

$$u_t = d\Delta u.$$

The diffusivity d of a Brownian particle in \mathbf{R}^n is given by

Einstein-Smoluchowski Relation:
$$d = \frac{1}{2n} \frac{\langle X^2 \rangle}{t} = \frac{1}{2n} \frac{|\Delta x|^2}{|\Delta t|},$$

where Δx is the *mean free path* and Δt is the *mean collision time*.

What will happen if the temperature is not constant?

If Δx and Δt are nonconstant functions of $x \in \mathbf{R}^n$, the diffusivity is not constant, i.e., $d = d(x)$. Then, Fick's diffusion law give

$$u_t = \nabla \cdot (d \nabla u).$$

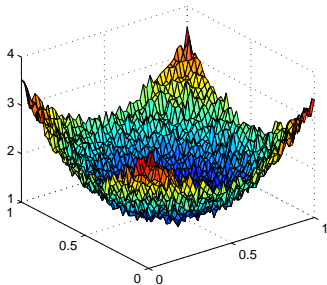
Is it correct?

2. Random Walk with spatial heterogeneity

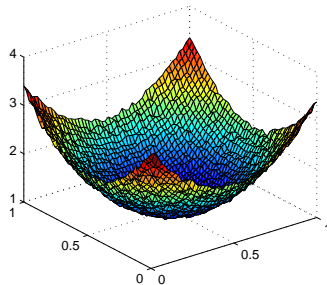
We may consider a random walk system. Let Δx and Δt be walk length and jumping time. Then the probability density function satisfies

$$u_t = \nabla \cdot \left(\frac{\Delta x}{2n} \nabla \left(\frac{\Delta x}{\Delta t} u \right) \right).$$

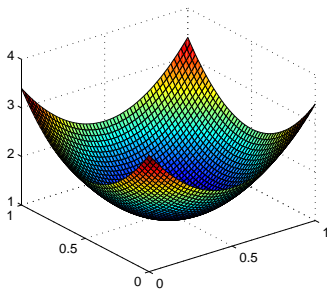
We can show the probability density function of non-uniform random walk system converges to the solution.



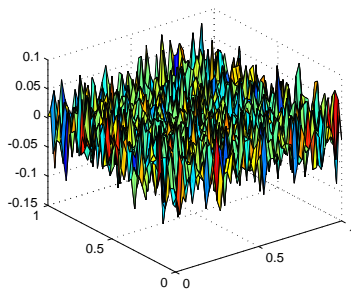
(a) 1,000,000 particles.



(b) 10,000,000 particles.



(c) theoretical steady state



(d) difference between (b) and (c).

3. Slower Diffuser Prevails!

Consider a competition model,

$$\begin{cases} u_t = d_1 \Delta u + u(m(x) - (u + v)), \\ v_t = d_2 \Delta v + v(m(x) - (u + v)), \end{cases} \quad x \in \Omega, \quad t > 0. \quad (1)$$

The initial and boundary conditions are

$$u_0(x), v_0(x) \geq 0 \text{ in } \Omega, \quad \mathbf{n} \cdot \nabla u = \mathbf{n} \cdot \nabla v = 0 \text{ on } \partial\Omega. \quad (2)$$

Let $d_1 < d_2$ i.e., u is a slower diffuser and v is a faster diffuser.

The result of this competition is rather surprising.

Theorem('98 Dockery, Hutson, Mischaikow & Pernarowski)

$$v(x, t) \rightarrow 0 \quad \text{as} \quad t \rightarrow \infty.$$

This is a paradox ! Why is this happen?

4. Random walk with respect to food, but not space

So far everybody considered random walk with respect to space. Now we consider it with respect to food.

1. Suppose that $m(x) > 0$ is the food distribution in one space dimension.
2. First define a metric

$$d(a, b) = \left| \int_a^b m(x) dx \right|.$$

3. Imbed this metric space into a Euclidean space and bring back the linear diffusion of Euclidean space. Then we obtain

$$u_t = d \left(\frac{1}{m} \left(\frac{u}{m} \right)_x \right)_x = d \left(\frac{1}{m^2} u_x - \frac{1}{m^3} u m_x \right)_x.$$

4. For multi-dimensional case, we obtain

$$u_t = d \nabla \cdot \left(\frac{1}{m} \nabla \left(\frac{u}{m} \right) \right).$$

5. Diffusion with nonconstant departing probability

In a random walk system, every particle jumps at every time step. Let $\gamma > 0$ be a *departure probability*, then the diffusion equation is

$$u_t = d\Delta(\gamma u).$$

Suppose $\gamma = \gamma(u, m) > 0$ and

$$\partial_u \gamma \geq 0 \quad \text{and} \quad \partial_m \gamma \leq 0, \quad (3)$$

then this diffusion can be called a **starvation driven diffusion**.

We may call the following a starvation measure:

$$s = \frac{u}{m} \quad \text{or} \quad s^{-1} = \frac{m}{u}.$$

If $\gamma = \gamma(s)$ is an increasing function of s , then

$$\gamma_u = \gamma'(s) \frac{1}{m} \geq 0, \quad \gamma_m = -\gamma'(s) \frac{u}{m^2} \leq 0.$$

Fick's law, Self-diffusion, Cross-diffusion and Advection

Consider

$$\begin{cases} u_t = d\Delta u + u[m(x) - u - v], \\ v_t = \Delta(\gamma(s)v) + v[m(x) - u - v]. \end{cases}$$

In this case the starvation measure is

$$s = \frac{u + v}{m}$$

and the diffusion term is written as

$$\Delta(\gamma(s)v) = \nabla \cdot \left(\gamma \nabla v + \frac{v}{m} \gamma' \nabla v + \frac{v}{m} \gamma' \nabla u - \frac{v}{m} s \gamma' \nabla m \right).$$

Four papers on starvation driven diffusion

1. E.Cho and Y.J. Kim, Starvation driven diffusion as a survival strategy of biological organisms, *Bull. Math. Biol.* 75(5) (2013) 845–870
2. Y.J. Kim, O. Kwon and F. Li, Global asymptotic stability and the ideal free distribution in a starvation driven diffusion, *J. Math. Biol.* 68 (6) (2014) 1341–1370
3. Y.J. Kim, O. Kwon and F. Li, Evolution of dispersal toward fitness, *Bull. Math. Biol.* 75(12) (2013) 2474–2498
4. C. Yoon and Y.-J. Kim, Bacterial chemotaxis without gradient-sensing, *J. Math. Biol.* (2014), published on line

6. Keller-Segel model

The Keller-Segel model for Addler's traveling wave phenomenon is

$$\begin{cases} u_t = (\mu(m)u_x - \chi(m)u m_x)_x, \\ m_t = \varepsilon m_{xx} - k(m)u, \end{cases} \quad (4)$$

where $u \geq 0$ is the population density, $m \geq 0$ is the nutrient concentration, $\varepsilon > 0$ is the diffusivity of nutrient concentration, and $k(m) \geq 0$ is the consumption rate. In the derivation of the Keller-Segel model, μ and χ satisfy

$$\chi(m) = -(1 - a)\mu'(m), \quad \mu'(m) \leq 0, \quad (5)$$

where $0 < a < 1$ is the effective body ratio.

Traveling wave solutions of (4) have been intensively studied after various simplifications. In fact, Keller and Segel by themselves broke the link between μ and χ in (5) by assuming

$$\varepsilon = \mu' = k' = 0 \quad \text{and} \quad \chi(m) = m^{-1}, \quad (6)$$

and then found explicit traveling waves. $\chi(m) = m^{-1}$ is Weber-Fechner.

7. Bacteria chemotaxis without gradient-sensing

Consider

$$\begin{cases} u_t = (\gamma u)_{xx}, \\ m_t = -k(m)u. \end{cases}$$

The first equation is written as

$$u_t = ((\gamma + u\gamma_u)u_x + u\gamma_m m_x)_x.$$

Let $\gamma = \gamma(m)$. Then, it becomes

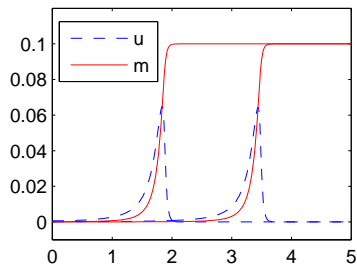
$$u_t = (\gamma(m)u_x + u\gamma'(m)m_x)_x.$$

Therefore, the corresponding chemosensitivity $\chi(m)$ and diffusivity $\mu(m)$ satisfy

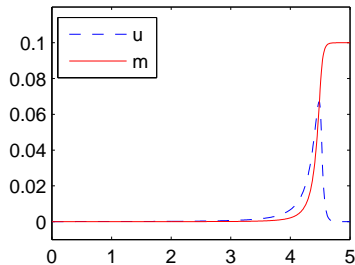
$$\chi(m) = -\mu'(m).$$

This is exactly the Keller-Segel model when $a = 0$.

Numerical Simulations for traveling waves



(a) Traveling waves at two different moments $t = 10$ and 20



(b) Pulse type traveling wave of ODE system with $c = 0.158$

Fig. 1. Traveling wave of finite mass

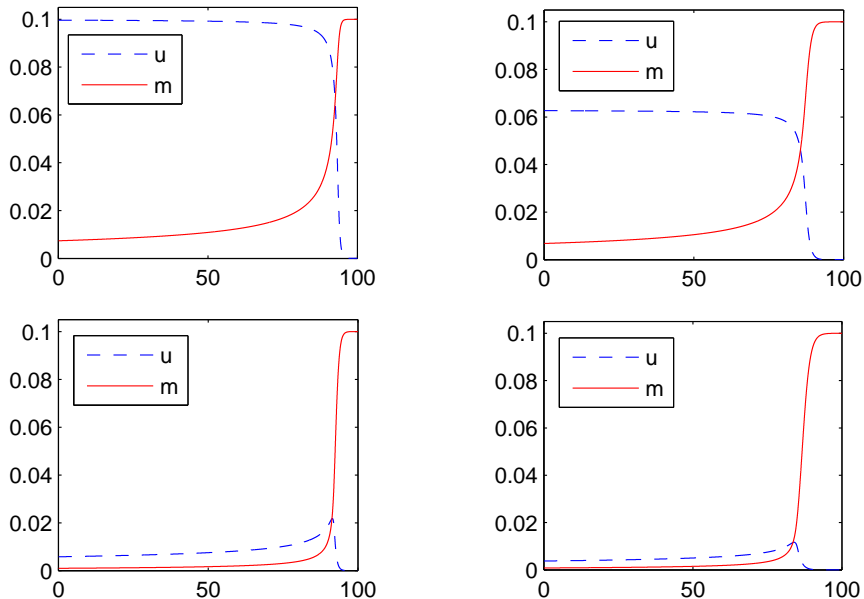


Fig. 2. Traveling waves of infinite mass

Part II

Modeling Population Reaction

8. Logistic population model

The population growth is modeled by a linear term,

$$\dot{u} = r_1 u,$$

where $r_1 > 0$ is the growth rate. If resource is limited, there exists a competition for resource, which is modeled by a quadratic term,

$$\dot{u} = r_1 u - r_2 u^2,$$

where r_2 is the self-competition rate. The ratio $m = r_1/r_2$ is called the carrying capacity and the equation can be written as

$$\dot{u} = r_1 u \left(1 - \frac{u}{m}\right), \quad m = \frac{r_1}{r_2}.$$

Now we complete the model by adding the zero-th order term:

$$\dot{u} = (r_1 u - r_2 u^2 - r_0) \chi_{\{u>0\}},$$

where $r_0 > 0$ is for the effect of constant loss.

9. Competition model beyond Lotka-Volterra

Lotka-Volterra competition model is written as

$$\dot{u} = r_1 u \left(1 - \frac{u + a_{12}v}{m_1} \right), \quad \dot{v} = r_2 v \left(1 - \frac{a_{21}u + v}{m_2} \right).$$

Let A, B, C be resources, where u consumes A, B and v consumes B, C . How to model it? If we assume

$$\frac{u_A}{A} = \frac{u_B + v_B}{B} = \frac{v_C}{C}, \quad (*)$$

the population model becomes

$$\dot{u} = r_1 u \left(1 - \frac{u + v}{M} \right), \quad \dot{v} = r_2 v \left(1 - \frac{u + v}{M} \right), \quad M = A + B + C.$$

However, (*) cannot be satisfied if

$$\frac{u}{A+B} > \frac{v}{C} \quad \text{or} \quad \frac{u}{A} < \frac{v}{B+C}.$$

Competition model beyond Lotka-Volterra

For general initial value, the system consists of three parts:

$$\begin{aligned} \dot{u} &= r_1 u \left(1 - \frac{u}{A+B}\right), & \dot{v} &= r_2 v \left(1 - \frac{v}{C}\right) & \text{if } \frac{u}{A+B} > \frac{v}{C}, \\ \dot{u} &= r_1 u \left(1 - \frac{u}{A}\right), & \dot{v} &= r_2 v \left(1 - \frac{v}{B+C}\right) & \text{if } \frac{u}{A} < \frac{v}{B+C}, \\ \dot{u} &= r_1 u \left(1 - \frac{u+v}{M}\right), & \dot{v} &= r_2 v \left(1 - \frac{u+v}{M}\right) & \text{otherwise.} \end{aligned}$$

There are infinitely many steady states:

$$u = A + tB, \quad v = C + (1-t)B, \quad 0 \leq t \leq 1.$$

The asymptotic convergence limit is decided by initial value.

Question: What will happen if there exists a spatial heterogeneity?

Thank you.

More about SI and SIR epidemic model systems with spatial structure

Michel Langlais,

Université de Bordeaux,
Institut de Mathématiques de Bordeaux.

Veronica Anaya & Mauricio Sepúlveda (Concepción, Chile)

Mostafa Bendahmane (Institut de Mathématiques de Bordeaux)

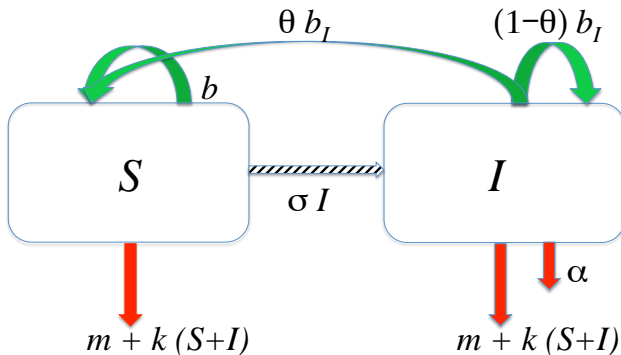
June 16, 2014

Table of contents

1 SI model system

2 SIR model system

Compartmental model for SI infectious diseases.



Flowchart for SI models

(1) Underlying ODE model system, $\theta > 0$

$$\begin{cases} S' &= -\sigma S I + b S + \theta b_I I - (m + k P) S, \\ I' &= \sigma S I + (1 - \theta) b_I I - \alpha I - (m + k P) I. \end{cases}$$

A straightforward computation yields a threshold parameter

$$\mathcal{T}_0 = \frac{\sigma K}{b + \alpha - (1 - \theta) b_I}, \quad K = \frac{b - m}{k}. \quad (1)$$

Then

when $\mathcal{T}_0 < 1$

- the semi-trivial stationary state $S = K, I = 0$ is GAS;

when $\mathcal{T}_0 > 1$

- the semi-trivial stationary state $S = K, I = 0$ is unstable,

- there exists a unique persistent stationary state,

$S^* > 0, I^* > 0$ with $0 < S^* + I^* < K$ that is GAS.

(2) Nonlinear diffusion model system, $\theta > 0$

$$\begin{cases} \partial_t S &= \Delta[d_1(S)] - \sigma S I + b S + \theta b_I I - (m + k P) S; \\ \partial_t I &= \Delta[d_2(I)] + \sigma S I + (1 - \theta) b_I I - \alpha I - (m + k P) I. \end{cases}$$

One assumes

$$0 < d_{\min} \leq \frac{d d_i}{dX}(X) = d_i'(X), \quad X \geq 0, \quad i = 1, 2; \quad d_i \in C^2([0, \infty)).$$

One prescribes no flux boundary conditions

$$d_1'(S) \nabla S(x, t) \cdot \eta(x) = d_2'(I) \nabla I(x, t) \cdot \eta(x) = 0, \quad x \in \partial\Omega, \quad t > 0$$

η being a unit normal vector to Ω along $\partial\Omega$.

Given nonnegative and bounded initial conditions, $S(0, x) = S_0(x)$ and $I(0, x) = I_0(x)$, with $S_0(x) + I_0(x) \not\equiv 0$ this PDE model system has a unique componentwise nonnegative and bounded classical solution.

Lemma

Assume $\mathcal{T}_0 > 1$.

The unique persistent stationary state of the underlying ODE system remains GAS for the nonlinear diffusion model system for those nonnegative and bounded initial conditions such that $S_0 \neq 0$ and $I_0 \neq 0$.

Usual Lyapunov function already designed for the ODE system

$$\mathcal{L}(u, v) = \nu_S \int_{\Omega} \left(u(x) - S^* - S^* \ln \frac{u(x)}{S^*} \right) dx + \nu_I \int_{\Omega} \left(v(x) - I^* - I^* \ln \frac{v(x)}{I^*} \right) dx.$$

When $\sigma > k$: rather straightforward.

When $\sigma \leq k$: a trick from Busenberg and Cooke.

1D TW solutions when $\mathcal{T}_0 > 1$

$$\begin{cases} \partial_t S &= d_1 \Delta S - \sigma S I + b S + \theta b_I I - (m + k P) S; \\ \partial_t I &= d_2 \Delta I + \sigma S I + (1 - \theta) b_I I - \alpha I - (m + k P) I. \end{cases}$$

$$S(x, t) = u(e \cdot x - c t) \text{ and } I(x, t) = v(e \cdot x - c t)$$

$$\lim_{t \rightarrow -\infty} \begin{pmatrix} u(z) \\ v(z) \end{pmatrix} = \begin{pmatrix} S^* \\ I^* \end{pmatrix}; \quad \lim_{t \rightarrow +\infty} \begin{pmatrix} u(z) \\ v(z) \end{pmatrix} = \begin{pmatrix} K \\ 0 \end{pmatrix}.$$

$$c^* = 2 \sqrt{d_2} \sqrt{(\sigma - k) K - m - \alpha + (1 - \theta) b_I}$$

Lemma

- when $\sigma < k$ for each $c \geq c^*$ there is a solution (u, v) with u increasing and v decreasing;
- when $\sigma \geq k$ and $d_1 = d_2$ for each $c > c^*$ there is a componentwise positive solution (u, v) .

(Ducrot - ML - Magal)

(3) Cross diffusion and nonlinear diffusion model system $\theta > 0$

Prototypical model system involving nonlinear and cross diffusion

$$\begin{cases} \partial_t S = \Delta[(d_1 + d_{11} S + d_{12} I)S] - \sigma S I + b S + \theta b_I I - (m + k P) S; \\ \partial_t I = \Delta[(d_2 + d_{21} S + d_{22} I)I] + \sigma S I + (1 - \theta) b_I I - \alpha I - (m + k P) I. \end{cases}$$

One assumes

- $d_1 > 0, d_2 > 0,$
- $d_{ij} \geq 0$ for $i, j = 1, 2.$

One prescribes no flux boundary conditions .

Additional set of conditions : $d_{12} = d_{21} = 1, d_{ii} > \frac{1}{2}$ for $i = 1, 2$

Given nonnegative and bounded initial conditions, $S(0, x) = S_0(x)$ and $I(0, x) = I_0(x)$, with $S_0(x) + I_0(x) \not\equiv 0$ one gets at least one (*componentwise nonnegative and bounded*) weak solution solution, (Bendahmane - ML).

Assume $\mathcal{T}_0 > 1$

Can the unique persistent stationary state $S^* > 0, I^* > 0$ of the underlying ODE system be destabilized by cross and nonlinear diffusion ?

Litterature (currently limited search, to be completed).

People in the room !

Idea : linearization and algebraic computation, numerical experiments.

No closed form expression for $S^* > 0, I^* > 0$, but for a suitable and quite restrictive parameter data set with a misleading outcome.

In that restrictive case cf. G. Gambino, M.C. Lombardo, and M. Sammartino (2012), Canrong Tian, Zhigui Lin, Michael Pedersen (2010).

#1 Linearized system assuming $\mathcal{T}_0 > 1$

Set $S = u - S^*$ and $I = v - I^*$. Linearizing yields

$$\partial_t \begin{pmatrix} u \\ v \end{pmatrix} = D^* \Delta \begin{pmatrix} u \\ v \end{pmatrix} + J^* \begin{pmatrix} u \\ v \end{pmatrix}.$$

equipped with no flux boundary conditions.

Herein D^* is the linearized diffusion matrix evaluated at (S^*, I^*)

$$D^* = \begin{pmatrix} d_1 + 2 d_{11} S^* + d_{12} I^* & d_{12} S^* \\ d_{21} I^* & d_2 + d_{21} S^* + 2 d_{22} I^* \end{pmatrix}.$$

J^* is Jacobian matrix of the ODE system evaluated at (S^*, I^*) .

One gets

$$\begin{aligned} \text{trace}(D^*) &> 0, & \det(D^*) &> 0; \\ \text{trace}(J^*) &< 0, & \det(J^*) &> 0. \end{aligned}$$

(case $\sigma \leq k$ being again somewhat trickier than case $\sigma > k$).

#1 Linearized system assuming $\mathcal{T}_0 > 1$, cont'd

Let $(\mu_j \geq 0)_{j \geq 0}$ and $(\varphi_j)_{j \geq 0}$ be the eigenvalues / eigenfunctions to

$$\begin{cases} -\Delta \varphi(x) = \mu \varphi(x), & x \in \Omega; \\ \nabla \varphi(x) \cdot \eta(x) = 0, & x \in \partial\Omega. \end{cases}$$

Looking for a solution $\begin{pmatrix} u \\ v \end{pmatrix} = \exp(\lambda t) \varphi_j(x) \begin{pmatrix} z_1 \\ z_2 \end{pmatrix}$ to

$$\partial_t \begin{pmatrix} u \\ v \end{pmatrix} = D^* \Delta \begin{pmatrix} u \\ v \end{pmatrix} + J^* \begin{pmatrix} u \\ v \end{pmatrix}$$

one gets an eigenvalue problem in \mathcal{R}^2

$$\left(\lambda Id_2 - [-\mu_j D^* + J^*] \right) \begin{pmatrix} z_1 \\ z_2 \end{pmatrix} = \begin{pmatrix} 0 \\ 0 \end{pmatrix}.$$

The question now is whether λ can be positive ?

$$M_0 = J^* - \mu_j D^*.$$

Because $\text{trace}(M_0) < 0$ instability is feasible if and only if $\det(M_0) < 0$.

#2 About $\det(M_0) < 0$, $M_0 = J^* - \mu_j D^*$, checked with Maple software !

For some linear function Θ of diffusivities (d_i, d_{ij})

$$\det(M_0) = \mu_j^2 \det(D^*) + \mu_j \Theta(d_1, d_2, d_{11}, d_{12}, d_{21}, d_{22}) + \det(J^*).$$

A necessary condition for $\det(M_0) < 0$ is to find a set of positive diffusivities implying $\Theta(d_1, d_2, d_{11}, d_{12}, d_{21}, d_{22}) < 0$.

- 1 According to previous results one has $\Theta(d_1, d_2, 0, d_{12}, d_{21}, 0) > 0$ for nonnegative $(d_1, d_2, d_{12}, d_{21})$ with $d_1 + d_2 + d_{12} + d_{21} > 0$.
- 2 Next looking at mere cross diffusivities one gets

$$\begin{cases} \Theta(0, 0, 0, d_{12}, 0, 0) &= -d_{12} (k S^* - k I^* - \sigma S^*) I^*; \\ \Theta(0, 0, 0, 0, d_{21}, 0) &= d_{21} (k S^{*2} - k S^* I^* - \sigma S^* I^* + 2\theta b_I I^*). \end{cases}$$

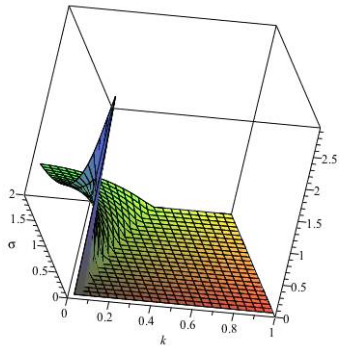
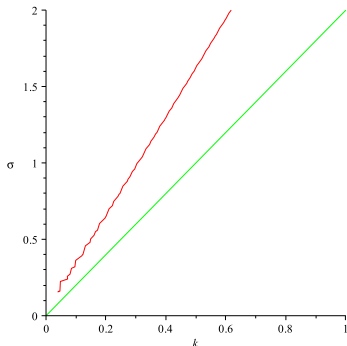
On the other hand note that when $\sigma > k$ then $\Theta(0, 0, 0, d_{12}, 0, 0) > 0$.

#2 About $\det(M_0) < 0$: Example 1

Set $b = 2$, $b_I = 0$, $m = 1$, $\alpha = 0$, $\theta = 0.3$ in which case

$$\mathcal{T}_0 = 0.5 \frac{\sigma}{k} > 1 \iff 0 < 2k < \sigma \text{ (green curve).}$$

$\Theta(0, 0, 0, 0, d_{21}, 0) = d_{21} \Theta(0, 0, 0, 0, 1, 0) < 0$ above the red one.



Assuming $\mathcal{T}_0 > 1$ it follows $\Theta(0, 0, 0, d_{12}, 0, 0) > 0$ for $d_{12} > 0$.

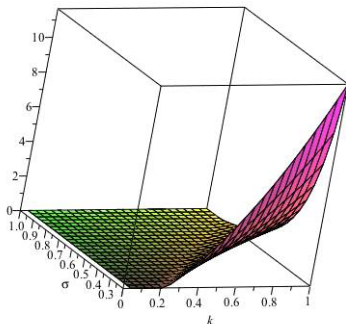
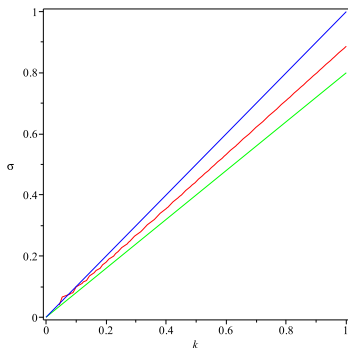
#2 About $\det(M_0) < 0$: Example 2

Set $b = b_I = 2$, $m = 1$, $\alpha = 0.2$ and $\theta = 0.3$.

When $\mathcal{T}_0 > 1$ then $\Theta(0, 0, 0, 0, d_{21}, 0) > 0$ for $d_{21} > 0$.

$$\mathcal{T}_0 = 1.25 \frac{\sigma}{k} > 1 \text{ and } \sigma < k \iff 0 < 0.8k < \sigma < k.$$

$\Theta(0, 0, 0, d_{12}, 0, 0) = d_{12} \Theta(0, 0, 0, 1, 0, 0) < 0$ between red and green curves and $\mathcal{T}_0 > 1$ above green one.

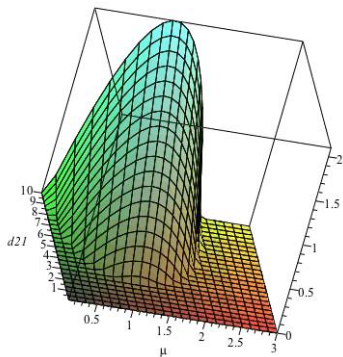
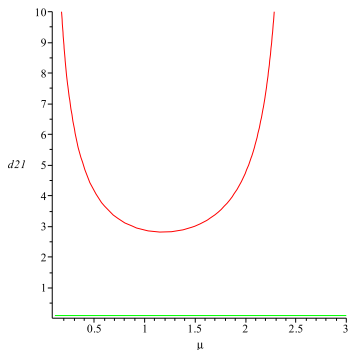


#3 Turing bifurcation : Example 1

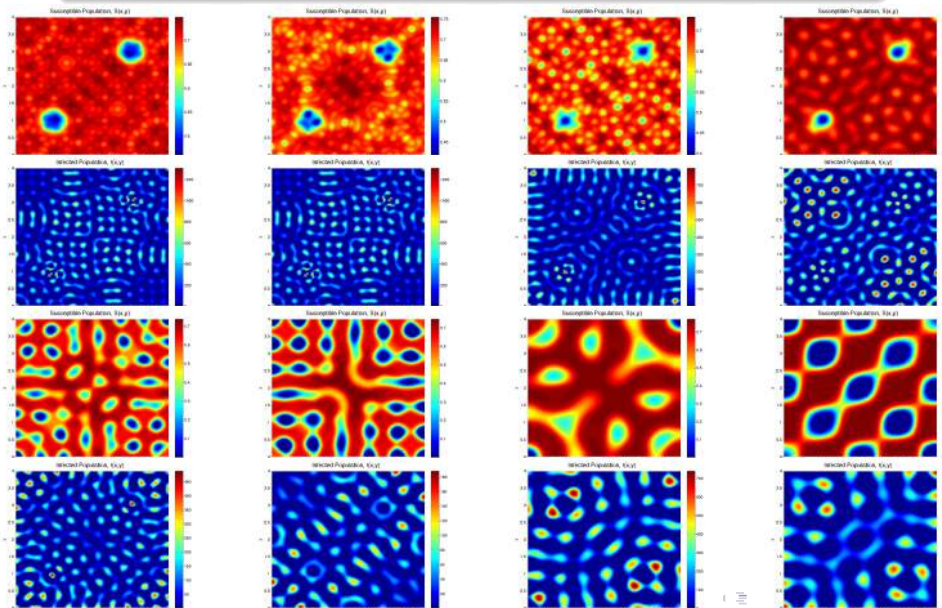
Fix $d_1 = d_2 = 0.1$, next $d_{11} = d_{22} = 0$ and last $d_{12} = 0$.

Select $k = 0.2$ and $\sigma = 0.8$ in order to get $\Theta(0, 0, 0, 0, d_{21}, 0) < 0$.

$\det(M_0) < 0$ within a wide range of the (μ, d_{21}) phase plane.



#3 Pattern formation : Example 1, $d_{21} = 190 \rightarrow 220, 300 \rightarrow 1000$



#3 Turing bifurcation : Example 2

Fix $d_1 = d_2 = 0.05$, next $d_{11} = d_{22} = 0$ and last $d_{21} = 0$.

Select $k = 0.2$ and $\sigma = 0.165$ in order to get $\Theta(0, 0, 0, d_{12}, 0, 0) < 0$.

$\det(M_0) < 0$ within a wide range of the (μ, d_{12}) phase plane.

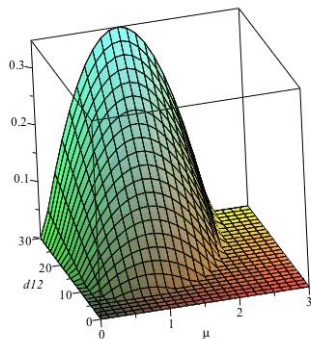
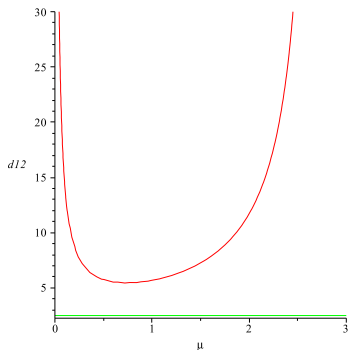
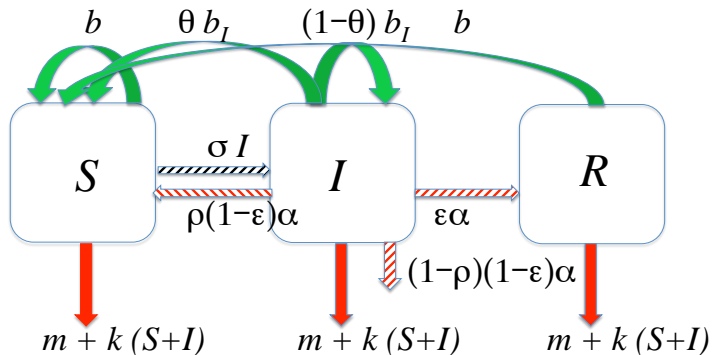


Table of contents

1 SI model system

2 SIR model system

Compartmental model for SIR infectious diseases.



Flowchart for SIR models

(1) Underlying ODE model system, $\theta > 0$

$$\begin{cases} S' &= -\sigma S I + b(S + R) + \theta b_I I + \varrho(1 - \varepsilon) \alpha I - (m + k P) S; \\ I' &= \sigma S I + (1 - \theta) b_I I - \alpha I - (m + k P) I; \\ R' &= +\varepsilon \alpha I - (m + k P) R. \end{cases}$$

Let

$$\mathcal{T}_0 = \frac{\sigma K}{b + \alpha - (1 - \theta) b_I}, \quad K = \frac{b - m}{k}.$$

Assume “*weak vertical transmission*”

$$m + \alpha - (1 - \theta) b_I > 0. \quad (2)$$

Then

$\mathcal{T}_0 < 1$ the semi-trivial stationary state $S = K, I = R = 0$ is GAS.

$\mathcal{T}_0 > 1$ - $S = K, I = R = 0$ is unstable,

- there exists a unique persistent stationary state,
 $0 < S^*, I^*, R^*, S^* + I^* + R^* < K$ that is LAS.

(2) Linear and nonlinear diffusion model system $\theta > 0$

Prototypical model system involving nonlinear and cross diffusion

$$\begin{cases} \partial_t S = \Delta[(d_1 + d_{11} S)S] \\ \quad -\sigma S I + b(S + R) + \theta b_I I + \varrho(1 - \varepsilon) \alpha I - (m + k P) S; \\ \partial_t I = \Delta[(d_2 + d_{22} I)I] + \sigma S I + (1 - \theta) b_I I - \alpha I - (m + k P) I; \\ \partial_t R = \Delta[(d_3 + d_{33} R)R] + \varepsilon \alpha I - (m + k P) R. \end{cases}$$

One assumes $d_1 > 0, d_2 > 0, d_3 > 0, d_{ij} \geq 0$, for $1 \leq i \leq 3$.

One prescribes no flux boundary conditions.

Given nonnegative and bounded initial conditions, $S(0, x) = S_0(x)$, $I(0, x) = I_0(x)$ and $R(0, x) = R_0(x)$, with $S_0(x) + I_0(x) + R_0(x) \neq 0$ one gets a unique componentwise nonnegative and bounded classical solution.

About stability ...

Quite partial results

$$\mathcal{T}_0 = \frac{\sigma K}{b + \alpha - (1 - \theta)b_I}, \quad K = \frac{b - m}{k}.$$

Assume “*weak vertical transmission*” $m + \alpha - (1 - \theta)b_I > 0$.

Then

$\mathcal{T}_0 < 1$ the semi-trivial stationary state $S = K, I = R = 0$ is GAS provided

- either $\sigma < k$;
- or $\sigma > k$, linear diffusion, $d_{ii} = 0$, with $d_1 = d_2 = d_3$.

$\mathcal{T}_0 > 1$ then

- $S = K, I = R = 0$ is unstable;
- Unique persistent stationary state “numerically” LAS,
 $0 < S^*, I^*, R^*, S^* + I^* + R^* < K$.

(3) Cross diffusion and nonlinear diffusion model system $\theta > 0$

Prototypical model system involving nonlinear and cross diffusion

$$\left\{ \begin{array}{l} \partial_t S = \Delta[(d_1 + d_{11} S + d_{12} I + d_{13} R)S] \\ \quad -\sigma S I + b(S + R) + \theta b_I I + \varrho(1 - \varepsilon) \alpha I - (m + k P) S; \\ \partial_t I = \Delta[(d_2 + d_{21} S + d_{22} I + d_{23} R)I] \\ \quad +\sigma S I + (1 - \theta) b_I I - \alpha I - (m + k P) I; \\ \partial_t R = \Delta[(d_3 + d_{31} S + d_{32} I + d_{33} R)R] \\ \quad +\varepsilon \alpha I - (m + k P) R. \end{array} \right.$$

One assumes $d_1 > 0, d_2 > 0, d_3 > 0, d_{ij} \geq 0, 1 \leq i, j \leq 3$.

One prescribes no flux boundary conditions .

Additional set of conditions : $d_{ij} = 1, i \neq j, d_{ii} > \frac{1}{2}$ for $i, j = 1, 2, 3$.

Given nonnegative and bounded initial conditions, $S(0, x) = S_0(x)$, $I(0, x) = I_0(x)$ and $R(0, x) = R_0(x)$, with $S_0(x) + I_0(x) + R_0(x) \not\equiv 0$ one gets at least one (*componentwise nonnegative and bounded*) weak solution, (Bendahmane - ML).

#1 Numerical experiments

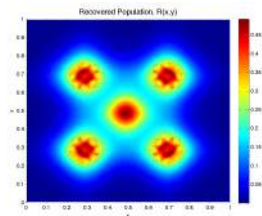
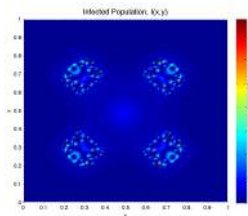
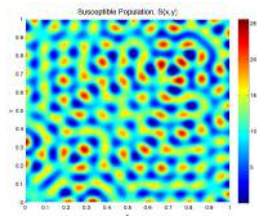
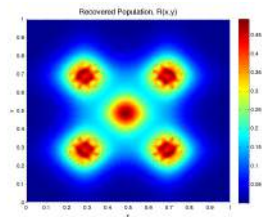
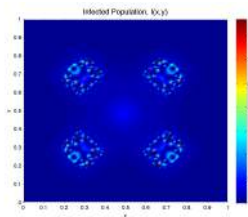
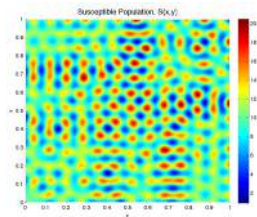
Simplified system

- $b_I = b = 0.03$, $\theta = 1$, $\varrho = 1$;
- $m = 0.01$, $k = 0.03$, $\alpha = 12$, $\varepsilon = 0.1$,
- $\sigma = 0.8$.
- $d_{ij} = 1$, for $i \neq j$ and $1 \leq i, j \leq 3$;
- varying either d_{11} or d_{22} .

$$\left\{ \begin{array}{l} \partial_t S = \Delta[(d_1 + d_{11} S + I + R)S] \\ \quad \quad \quad - \sigma S I + b P + (1 - \varepsilon) \alpha I - (m + k P) S; \\ \partial_t I = \Delta[(d_2 + S + d_{22} I + R)I] + \sigma S I - \alpha I - (m + k P) I; \\ \partial_t R = \Delta[(d_3 + S + I + d_{33} R)R] + \varepsilon \alpha I - (m + k P) R. \end{array} \right.$$

One prescribes no flux boundary conditions and nonnegative and bounded initial conditions, $S(0, x) = S_0(x)$, $I(0, x) = I_0(x)$ and $R(0, x) = R_0(x)$, with $S_0(x) + I_0(x) + R_0(x) \neq 0$.

#3 $d_{11} = 70, 90$ and $d_{22} = d_{33} = 10$



Thank you for your attention.

Perspectives

- More numerics for SI model system;
- SIR model system analysis and computations;
- ...

V. Anaya, M. Bendahmane, M.L., M. Sepúlveda. *A convergent finite volume method for a model of indirectly transmitted diseases with non-local cross-diffusion*. Submitted.

V. Anaya, M. Bendahmane, M.L., M. Sepúlveda. *Pattern formation for a reaction-diffusion system with constant and cross diffusion*. ENUMATH 2013.

A. Ducrot, M.L., P. Magal. *Qualitative analysis and traveling wave solutions for the SI model with vertical transmission*. CPAA, 11-1 (2012) 97-113.

M. Bendahmane, M.L. *A reaction-diffusion system with cross-diffusion modelling the spread of an epidemic disease*, J. Evolution Equation, 10 (2010) 883-904.

Harunori Monobe (Meiji Univ. MIMS)

joint work with

Masato Iida,

Hideki Murakawa,

Hirokazu Ninomiya

FAST REACTION LIMIT OF A TWO-COMPONENT SYSTEM WITH UNBALANCED REACTION TERMS

MATHEMATICAL AND ITS APPLICATIONS TO COMPLEX
PHENOMINA ARISING IN BIOLOGY, CHEMISTRY AND
MEDICINE, CIRM, LUMINY

June
3rd ~ 5th
2014

We consider **the fast reaction limit** of the following system :

$$\left\{ \begin{array}{ll} u_t = \Delta u - k u^{m_1} v^{m_3} & \text{in } Q_T, \\ v_t = -k u^{m_2} v^{m_4} & \text{in } Q_T, \\ \frac{\partial u}{\partial \nu} = 0 & \text{on } S_T, \\ u(x, 0) = u_0(x), \quad v(x, 0) = v_0(x) & \text{in } \Omega, \end{array} \right.$$

~ Contents ~

- (1). Motivation (some results of previous works)
- (2). Main results (the limit functions change the form depending on the combination of exponents)

1. Some results of the fast reaction limit

Let us consider the two-component system with a positive parameter k as follows :

$$\begin{cases} u_t = d_1 \Delta u + f(u) - kF(u, v), \\ v_t = d_2 \Delta v + g(v) - kG(u, v), \end{cases} \quad (1)$$

where d_1 is a positive constant, d_2 is a non-negative constant, f, g, F, G are continuous functions.

Sometimes we encounter the question :

As $k \rightarrow \infty$, what happens ?

This singular limit is called *the fast reaction limit*.

*This limit problem is helpful in the understanding of the dynamics for systems and the approximation of FBP.

1. Some results of the fast reaction limit

$$\text{Case I : } F(u, v) = G(u, v) = uv$$

$$\text{Ex. 1) } \begin{cases} u_t = \Delta u - kuv & \text{in } Q_T, \\ v_t = -kuv & \text{in } Q_T, \end{cases}$$

where $Q_T := \Omega \times (0, T)$, Ω : bounded domain with smooth boundary in \mathbb{R}^n .

* This model is related to anti-tumor therapies.

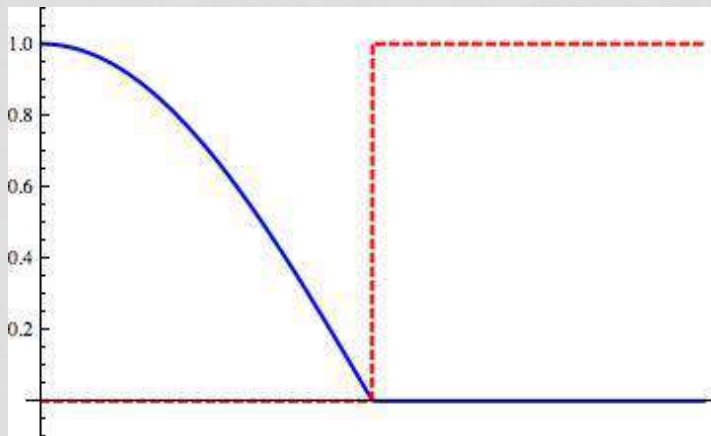
$u = u(x, t)$: Density of a medicine

$v = v(x, t)$: Density of a tumor

Q. When k is sufficiently large, how does the medicine penetrate to a tumor ?

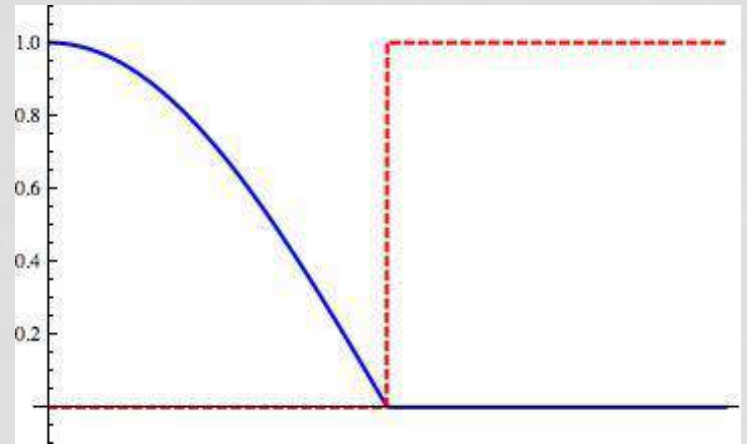
1. Some results of the fast reaction limit

(Simulation results : $k_1 \ll k_2$)



$\leftarrow k_1$

$k_2 \rightarrow$



Q. Does there exist the equation the limit functions of (u_k, v_k) satisfy ?

If there exists, what type is the equation ?

A. The limit function u_∞ satisfy **the classical one-phase Stefan problem with the latent heat** $v_\infty \equiv v_0$.
(The rigorous proof was done by D. Hilhorst et al.)

1. Some results of the fast reaction limit

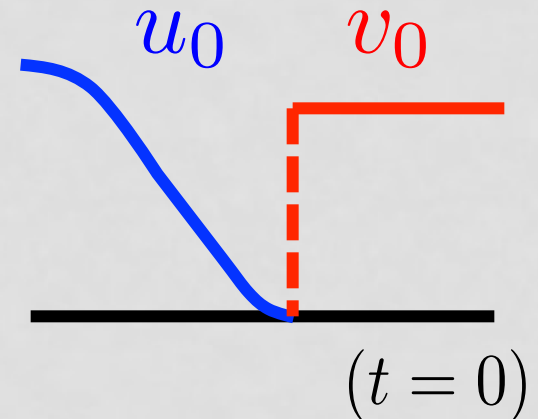
Problem setting

$$(Q)^k \begin{cases} u_t = \Delta u - kuv & \text{in } Q_T, \\ v_t = -kuv & \text{in } Q_T, \\ \frac{\partial u}{\partial \nu} = 0 & \text{on } S_T, \\ u(x, 0) = u_0, \quad v(x, 0) = v_0 & \text{in } \Omega, \end{cases}$$

where $S_T := \partial\Omega \times (0, T)$ and ν is the outer normal unit vector.

Hypothesis

- $(u_0, v_0) \in C(\overline{\Omega}) \times L^\infty(\Omega)$,
- $u_0 v_0 = 0$.



1. Some results of the fast reaction limit

Theorem 1 [Hilhorst, Mimura and Ninomiya, 2008]

(i) $\exists \{u_{k_n}\}, \{v_{k_n}\}, u_\infty, v_\infty$ s.t.

$u_{k_n} \rightarrow u_\infty$ strongly in $L^2(Q_T)$,

weakly in $L^2(0, T; H^1(\Omega))$

$v_{k_n} \rightarrow v_\infty$ strongly in $L^2(Q_T)$,

as $k_n \rightarrow \infty$.

(ii) $u_\infty v_\infty = 0$.

(iii) $\iint_{Q_T} \{-(u_\infty - v_\infty) \zeta_t + \nabla u_\infty \cdot \nabla \zeta\} dxdt = 0$

for all $\zeta \in H_0^1(Q_T)$.

1. Some results of the fast reaction limit

In Theorem 1, if the limit functions (u_∞, v_∞) are sufficiently smooth, we can confirm that **(iii) is the weak form of the classical one-phase Stefan problem** with the help of integration by parts and fundamental lemma of calculus of variations.

Notation:

$$\Omega_u(t) := \{x \in \Omega \mid u(x, t) > 0\}, \quad \Omega_v(t) := \{x \in \Omega \mid v(x, t) > 0\},$$

$$Q_T^1 := \bigcup_{0 < t < T} \Omega_u(t) \times \{t\}, \quad Q_T^2 := \bigcup_{0 < t < T} \Omega_v(t) \times \{t\},$$

$$\Gamma(t) := \Omega \setminus (\Omega_u(t) \cup \Omega_v(t)), \quad \Gamma := \bigcup_{0 < t < T} \Gamma(t) \times \{t\}.$$

\mathbf{n} : Outer normal unit vector of $\Gamma(t)$, V_n : Outer normal velocity of $\Gamma(t)$.

Theorem 2 [Hilhorst, Mimura and Ninomiya, 2008]

Suppose that

- (A1). $\Gamma(t)$ is a smooth, closed and orientable hypersurface,
- (A2). $\Gamma(t) \cap \partial\Omega = \emptyset$,
- (A3). u_∞ and v_∞ are smooth in $\overline{Q_T^1}$ and $\overline{Q_T^2}$, respectively.

Then (u_∞, v_∞) satisfies the following equation:

$$(Q)^\infty \left\{ \begin{array}{ll} u_t = \Delta u & \text{in } Q_T^1, \\ v = v_0 & \text{in } Q_T^2, \\ v_0 V_n = -\nabla u \cdot \mathbf{n} & \text{on } \Gamma, \\ u = 0 & \text{on } \Gamma, \\ \frac{\partial u}{\partial \nu} = 0 & \text{on } \partial\Omega, \end{array} \right.$$

1. Some results of the fast reaction limit

■ Other results related to the fast reaction limit of (1)

$$\begin{cases} u_t = d_1 \Delta u + f(u) - kF(u, v), \\ v_t = d_2 \Delta v + g(v) - kG(u, v), \end{cases} \quad (1)$$

Case I : $F(u, v) = G(u, v)$

Ex. 2) Hilhosrt et al. (1996, 2000, 2008)

$$\begin{cases} u_t = \Delta u - kF(u, v), & ex.) F(u, v) = u^p v^q \\ v_t = -kF(u, v), & (p, q > 1) \\ \text{B.C. and I.C.} \end{cases}$$

$\xrightarrow{k \rightarrow \infty}$ (u_∞, v_∞) satisfies the weak form of $(Q)^\infty$

1. Some results of the fast reaction limit

■ Other results related to the fast reaction limit of (1)

$$\begin{cases} u_t = d_1 \Delta u + f(u) - kF(u, v), \\ v_t = d_2 \Delta v + g(v) - kG(u, v), \end{cases} \quad (1)$$

Case I : $F(u, v) = G(u, v) = uv$

Ex. 3) Evans (1980)

$$\begin{cases} u_t = \Delta u - kuv, \\ v_t = \Delta v - kuv, \\ \text{B.C. and I.C.} \end{cases} \quad k \rightarrow \infty$$

(u_∞, v_∞) satisfies the two-phase Stefan problem with the zero latent heat.

(mathematical model in gas-liquid)

$$\begin{cases} u_t = \Delta u & \text{in } Q_T^1, \\ v_t = \Delta v & \text{in } Q_T^2, \\ \nabla u \cdot \mathbf{n} = -\nabla v \cdot \mathbf{n} & \text{on } \Gamma, \\ u = v = 0 & \text{on } \Gamma, \\ \text{B.C. and I.C.} \end{cases}$$

1. Some results of the fast reaction limit

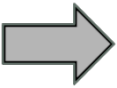
■ Other results related to the fast reaction limit of (1)

$$\begin{cases} u_t = d_1 \Delta u + f(u) - kF(u, v), \\ v_t = d_2 \Delta v + g(v) - kG(u, v), \end{cases} \quad (1)$$

Case I : $F(u, v) = G(u, v) = uv$

Ex. 4) Dancer et al. (1999), Crooks et al. (2004) etc

$$\begin{cases} u_t = d_1 \Delta u + (r_1 - a_1 u)u - kuv, & \text{(L-V system)} \\ v_t = d_2 \Delta v + (r_2 - a_2 v)v - kuv, \\ \text{B.C. and I.C.} \end{cases}$$


 $k \rightarrow \infty$

(u_∞, v_∞) satisfies the two-phase Stefan problem with the zero latent heat.

$$\begin{cases} u_t = d_1 \Delta u + (r_1 - a_1 u)u & \text{in } Q_T^1, \\ v_t = d_2 \Delta v + (r_2 - a_2 v)v & \text{in } Q_T^2, \\ \nabla u \cdot \mathbf{n} = -\nabla v \cdot \mathbf{n} & \text{on } \Gamma, \\ u = v = 0 & \text{on } \Gamma, \\ \text{B.C. and I.C.} \end{cases}$$

1. Some results of the fast reaction limit

■ Other results related to the fast reaction limit of (1)

$$\begin{cases} u_t = d_1 \Delta u + f(u) - kF(u, v), \\ v_t = d_2 \Delta v + g(v) - kG(u, v), \end{cases} \quad (1)$$

Case II : $F(u, v) = -G(u, v)$

- **Eymard et al. (2001)**
- **Bothe and Hilhosrt (2003)**
- **Bouillard et al. (2009)**
-

They considered the system with **reversible reaction terms** and showed that the system also converges the weak form of the Stefan problem as k tends to infinity.

2. Our problem and main results

Therefore we encounter the following natural question:

Q. What happens for unbalanced reaction terms, that is,

$$F(u, v) \neq \pm \ell G(u, v) \quad (\ell : \text{constant}) \quad ?$$

■ Some results for unbalanced reaction terms :

- Caffarelli et al. (2008), ▪ Dancer et al. (2012),
- Noris et al. (2014), ...

They considered the stationary **Gross-Pitaevskii equation** derived from “**Bose-Einstein condensates**”.

$$\begin{cases} -\Delta u + u^3 + kuv^2 = \lambda u, & F(u, v) = uv^2, \\ -\Delta v + v^3 + ku^2v = \lambda v, & G(u, v) = u^2v \end{cases}$$

2. Our problem and main results

We consider the fast reaction limit of the following system :

$$(P)^k \begin{cases} u_t = \Delta u - \kappa u^{m_1} v^{m_3} & \text{in } Q_T, \\ v_t = -\kappa u^{m_2} v^{m_4} & \text{in } Q_T, \\ \frac{\partial u}{\partial \nu} = 0 & \text{on } S_T, \\ u(x, 0) = u_0(x), \quad v(x, 0) = v_0(x) & \text{in } \Omega, \end{cases}$$

where $m_i \geq 1$ ($i = 1, 2, 3, 4$)

We consider the four typical combination of exponents

$$\mathbf{m} = (m_1, m_2, m_3, m_4).$$

2. Our problem and main results

(I) $\mathbf{m} = (m_1, 1, 1, 1)$ and $m_1 > 3$

⇒ u_∞ satisfies the heat equation on Ω .

(Infinite propagation)

(II) $\mathbf{m} = (1, m_2, 1, 1)$ and $m_2 > 1$

⇒ u_∞ satisfies the heat equation on $\text{supp } u_0$.

(No propagation)

(III) $\mathbf{m} = (1, 1, m_3, 1)$ and $m_3 > 1$

⇒ u_∞ satisfies the one-phase Stefan problem.

(Finite propagation)

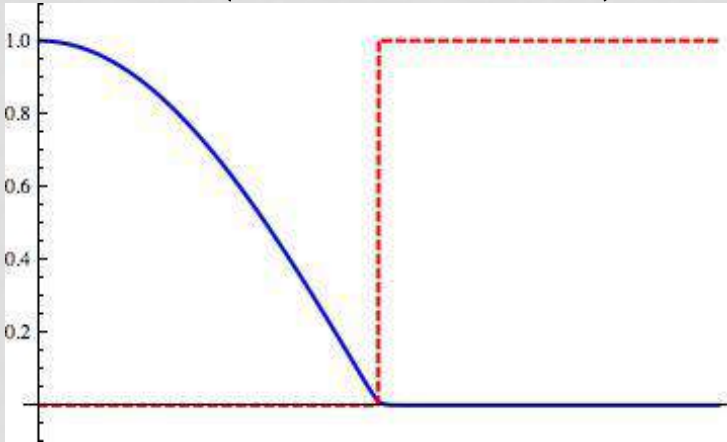
(IV) $\mathbf{m} = (1, 1, 1, m_4)$ and $2 > m_4 > 1$

⇒ u_∞ satisfies the one-phase Stefan problem.

(Finite propagation)

■ Simulation results

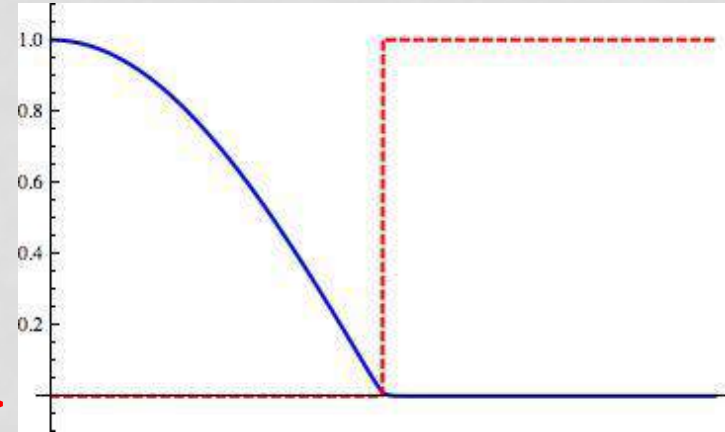
$$\mathbf{m} = (m_1, 1, 1, 1)$$



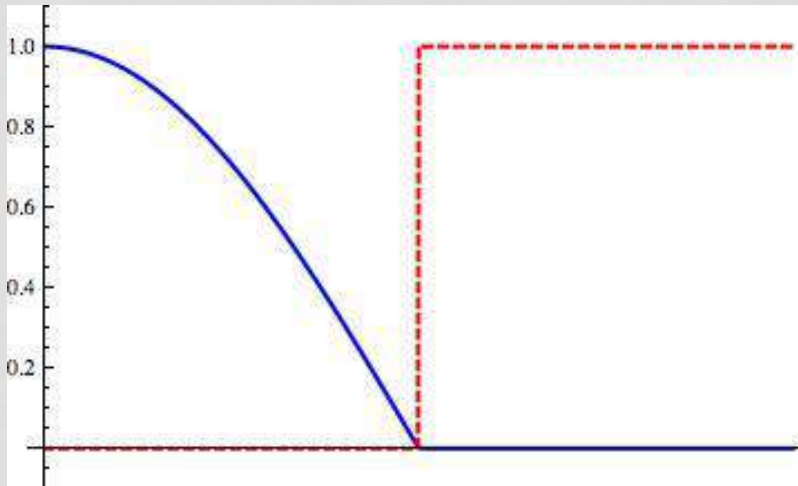
<- Infinite propagation

No propagation ->

$$\mathbf{m} = (1, m_2, 1, 1)$$



$$\mathbf{m} = (1, 1, m_3, 1) \text{ and } \mathbf{m} = (1, 1, 1, m_4)$$



<- Finite propagation

2. Our problem and main results

(I) $\mathbf{m} = (m_1, 1, 1, 1)$ and $m_1 > 3$

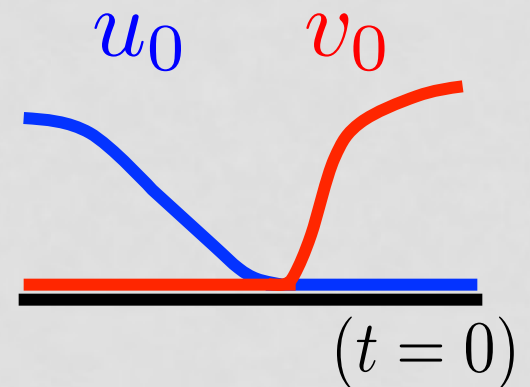
Assupmtion 1

- $(u_0, v_0) \in C^2(\bar{\Omega}) \times C^\alpha(\bar{\Omega})$, $(\alpha \in (0, 1))$
- For $x \in \Omega$,

$$u_0(x)v_0(x) = 0, \quad 0 \leq u_0(x), v_0(x) \leq M,$$

where $M := \max_{x \in \bar{\Omega}} \{u_0, v_0\}$.

- $\frac{\partial u_0}{\partial \nu} = 0$ on $\partial\Omega$



2. Our problem and main results

Main Th.1 $\mathbf{m} = (m_1, 1, 1, 1)$ and $m_1 > 3$

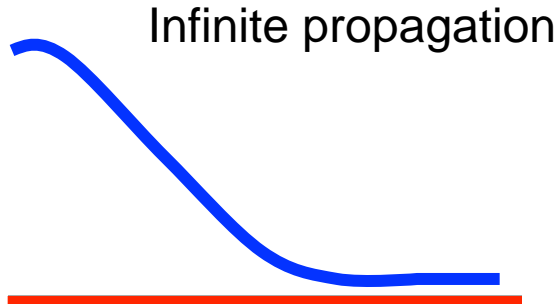
Initial data satisfy Assumption 1 $\Rightarrow \exists! u_*, v_*$ s.t.

$$u_k \rightarrow u_* \quad \text{in } C^0(\overline{Q}_T)$$

$$v_k \rightarrow v_* \equiv 0 \quad \text{in } C^0(\overline{\Omega} \times [\eta, T])$$

as $k \rightarrow \infty$.

Where η is any small positive constant and $u_*(x, t)$ is a smooth function ($C^{2,1}(\overline{Q}_T)$):

$$\left\{ \begin{array}{ll} u_t = \Delta u & \text{in } Q_T, \\ \frac{\partial u}{\partial \nu} = 0 & \text{on } S_T, \\ u(x, 0) = u_0(x) & \text{in } \Omega. \end{array} \right. \quad \begin{array}{l} \text{Infinite propagation} \\ \text{---} \\ (t > 0) \end{array}$$


Thank you for your attention !

Instability of periodic traveling wave solutions to excitable systems

Toshi OGAWA (Meiji University)
M Osman GANI (Meiji University)

ReaDiLab Conference, CIRM, Luminy, June 2014

Sudden Death by Cardiac Disease

How cardiac tissue behaves abnormally?

(1) Appearance of spiral.

(2) Spiral break-up.

Spiral waves and discordant alternans



$b=1.3$



$b=1.2$



$b=1.1$



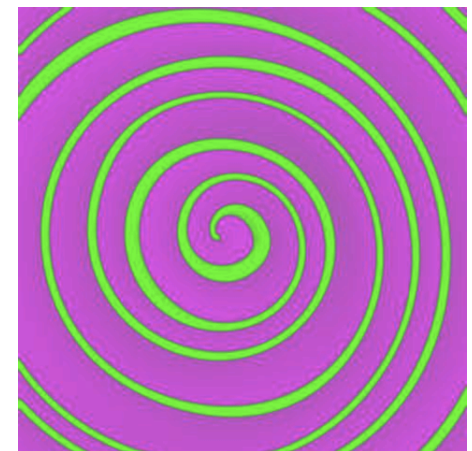
$b=1.05$



$b=1.04$



$b=1.035$



$b=1.03$

Alternant response of a single cell

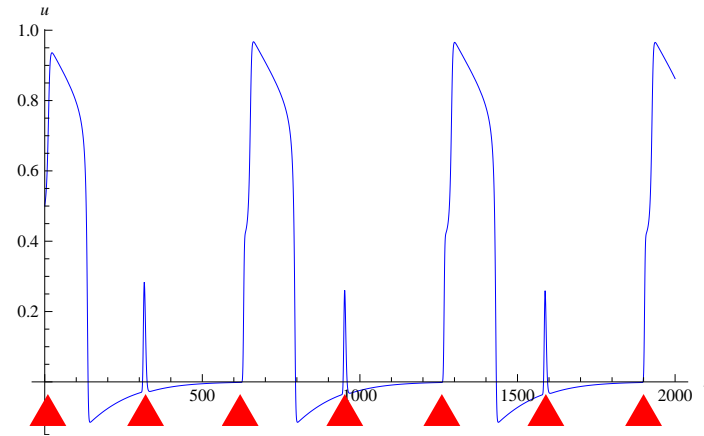
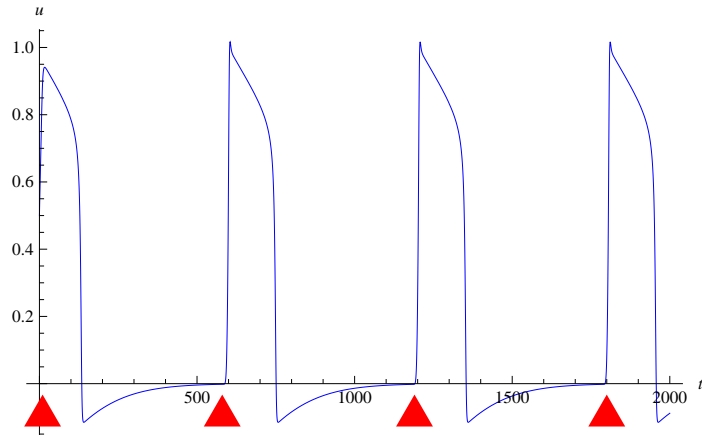
Cardiac cell as an excitable system as neuron.

Observe how an excitable cell responds to repetitive (periodic) stimulus.

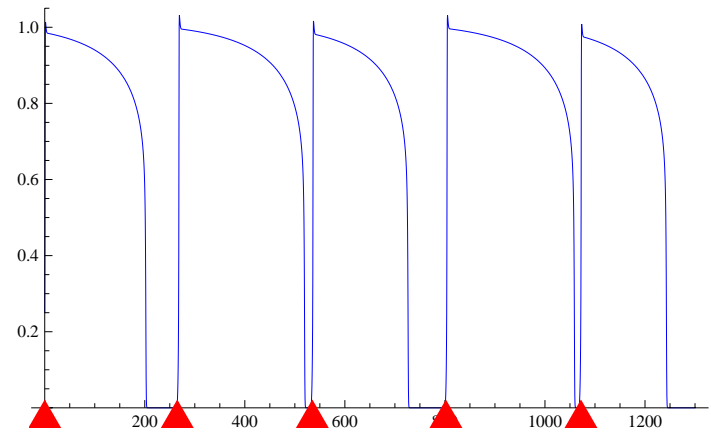
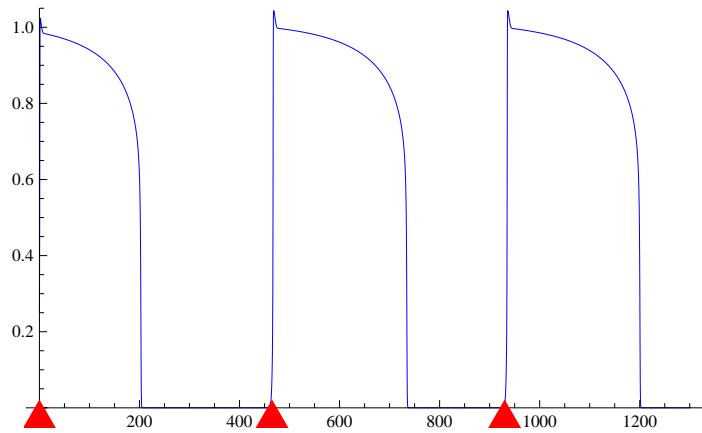
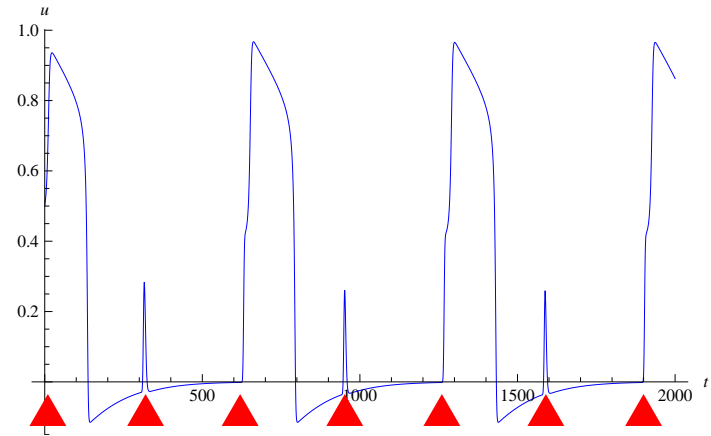
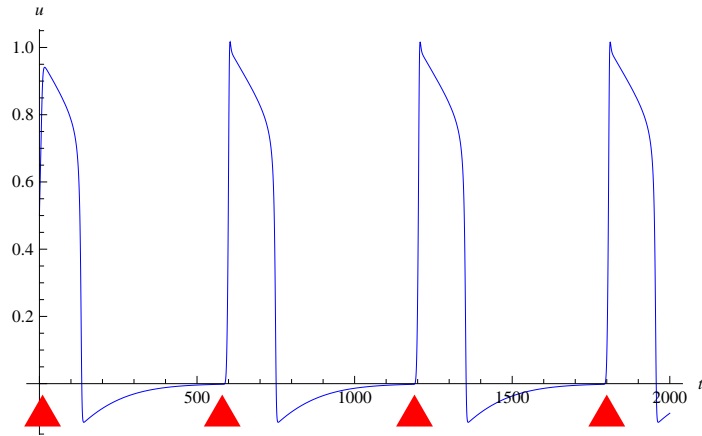
It responds precisely to each stimuli when the period is sufficiently large. While it can not follow the stimulus if the period is too short. Alternant response can be observed in a cardiac cell response.

Period doubling bifurcation, restitution curve

Increase the frequency



Alternant response



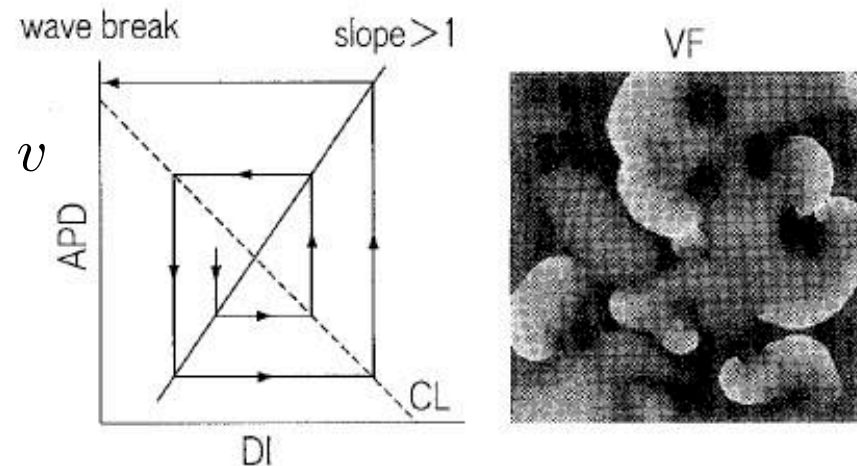
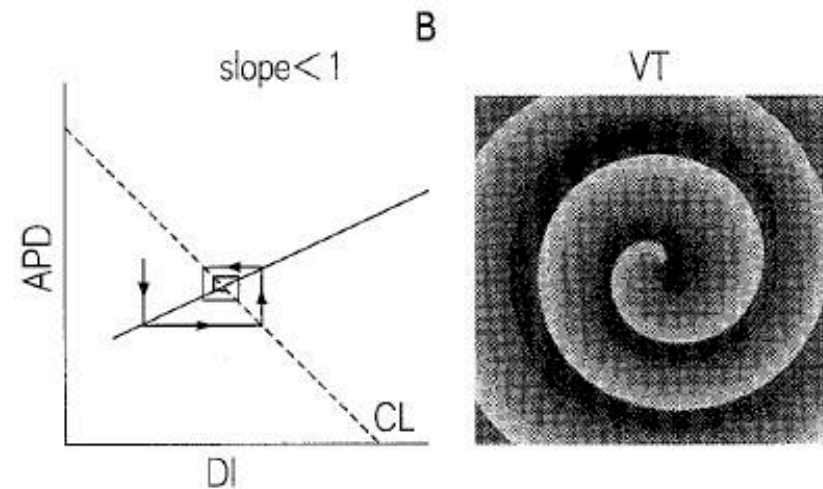
Restitution hypothesis

Pulse traveling wave and periodic traveling wave (wave train) are known to exist in a diffusively coupled system of excitable system.

Is there any relation between the alternant response by an excitable cell and the transition from VT to VF?

Study the instability of wave train in 1D (simplest case).

$$\begin{aligned}
 u_t &= D_1 u_{xx} + u(u - a)(1 - u) - v \\
 v_t &= D_2 v_{xx} + \varepsilon(u - \gamma v)
 \end{aligned}$$



Key Idea for alternant response

- Excitable system as a fast-slow system
- Restitution curve provides 1D map

Fast-slow system

FitzHugh-Nagumo system

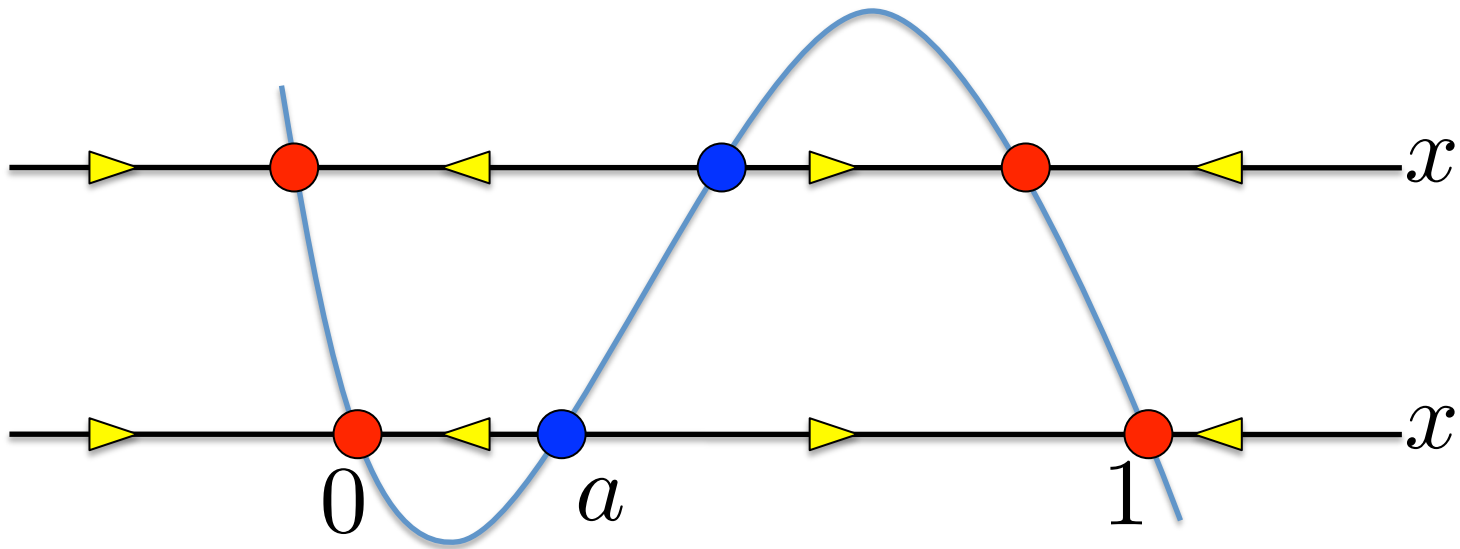
$$\begin{aligned}\varepsilon \frac{dx}{dt} &= x(x - a)(1 - x) - y \\ \frac{dy}{dt} &= x - \gamma y\end{aligned}\quad \begin{aligned}0 < a < 1/2 \\ 0 < \varepsilon \ll 1\end{aligned}$$

It is equivalent to the following by time scaling $t = \varepsilon \tau$

$$\begin{aligned}\frac{dx}{d\tau} &= x(x - a)(1 - x) - y \\ \frac{dy}{d\tau} &= \varepsilon(x - \gamma y)\end{aligned}$$

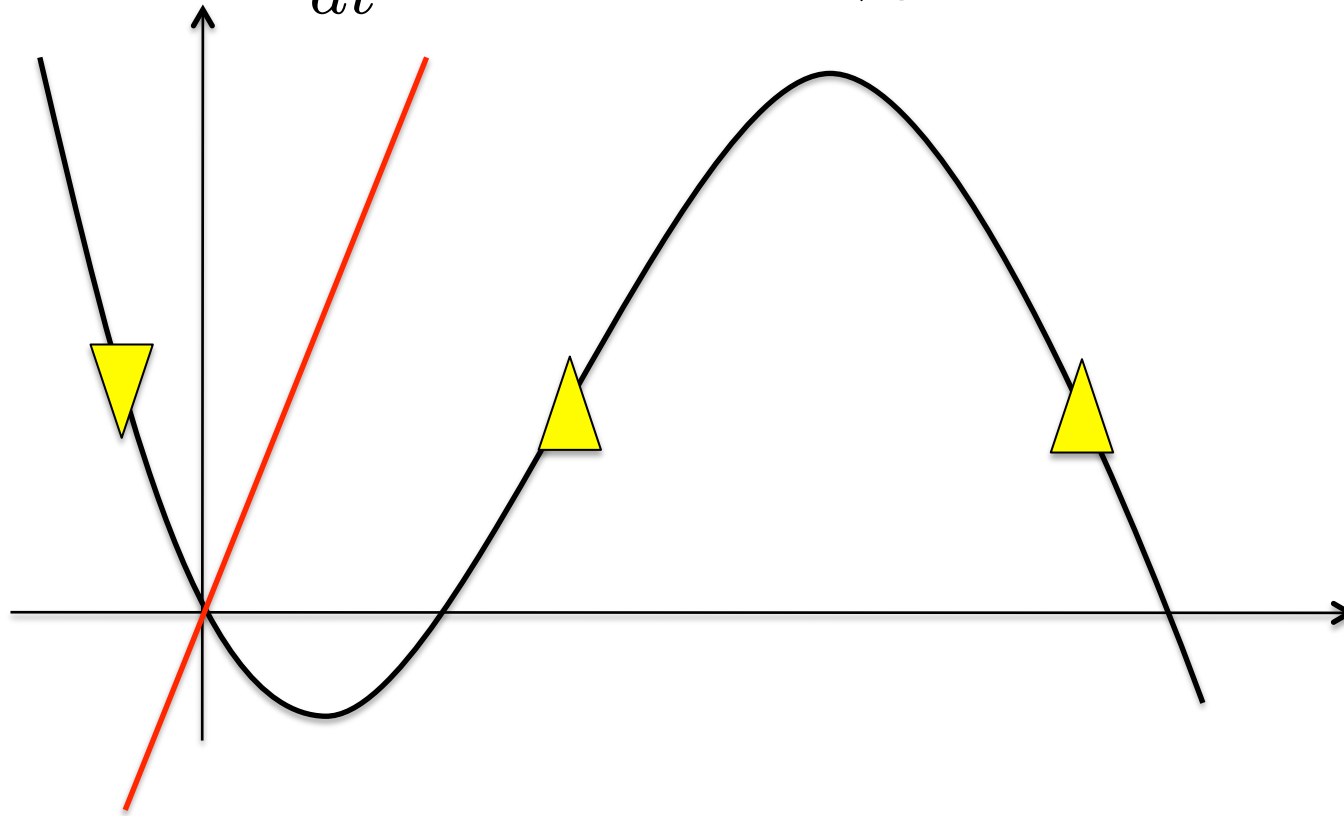
Fast Dynamics

$$\begin{aligned}\frac{dx}{d\tau} &= x(x - a)(1 - x) - y \\ y &= y_0\end{aligned}$$

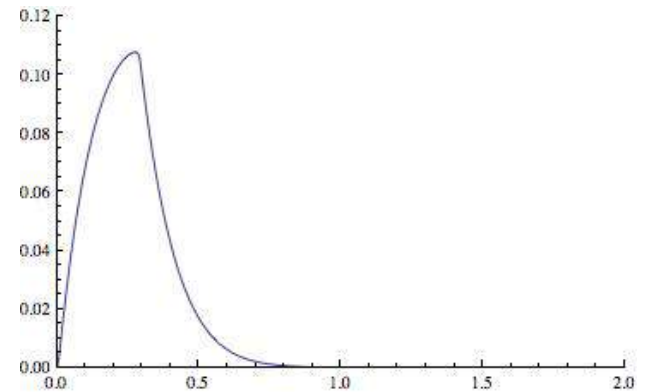
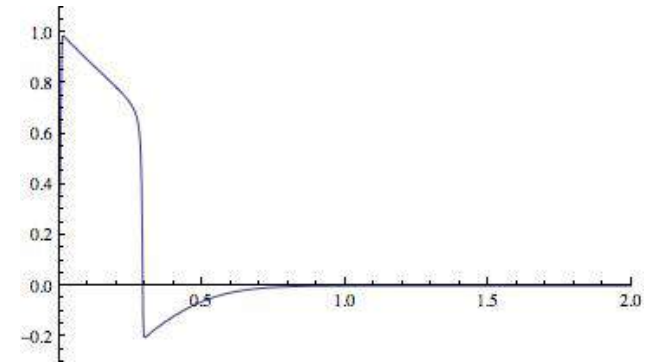
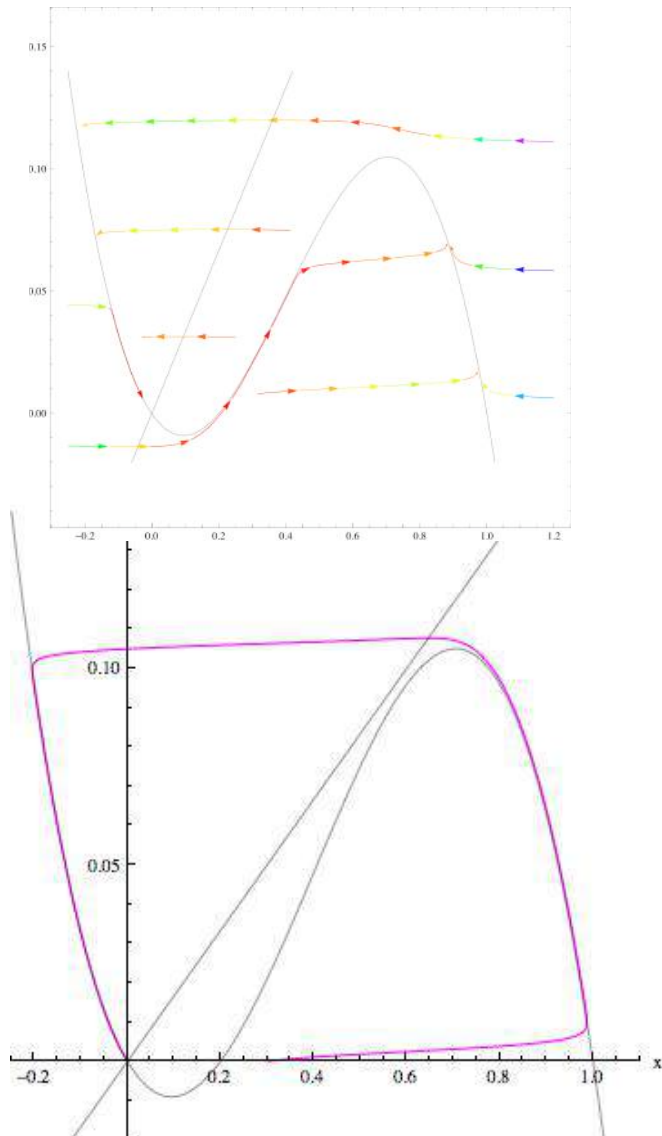


Slow Dynamics

$$x = \psi(y)$$
$$\frac{dy}{dt} = x - \gamma y$$



Dynamics of the FHN system

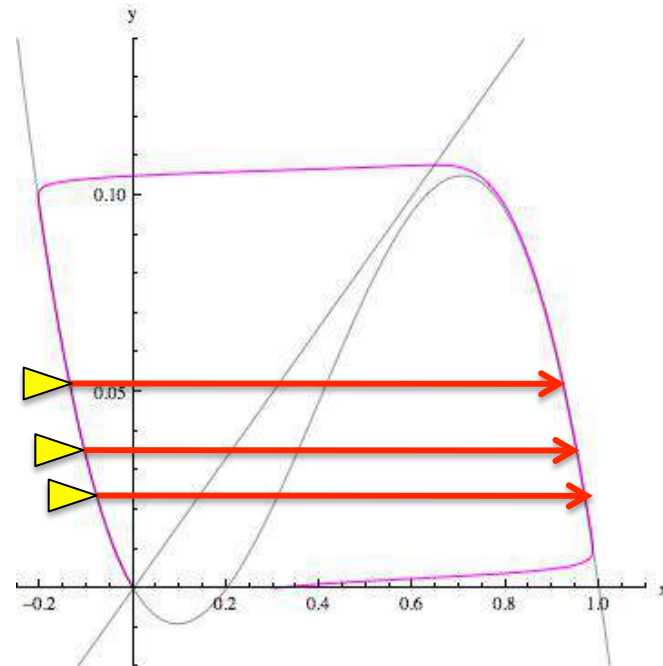


Right branch (exciting period)
Left branch (charging period)

Response to the following stimuli

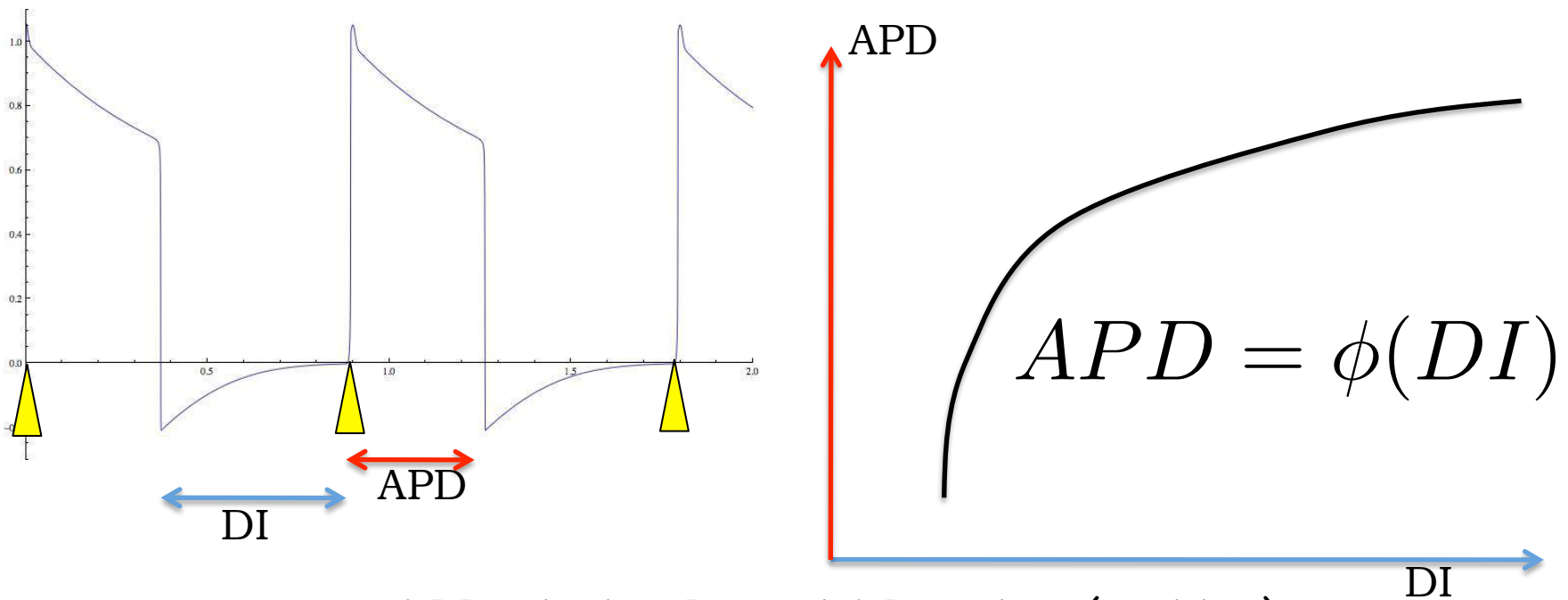
Add a next stimuli during a charging period.

Landing point on the exciting branch depends on the takeoff point on the slow charging branch.



Restitution curve

Charging period determines the following exciting period.
Longer charge leads to longer excitation.
Upper limit for the length of excitation no matter how long the previous charge.



APD : Action Potential Duration (exciting)
DI:Diastolic Interval (charging)

1D map

Sequence of pulses are obtained by adding the periodic stimulus (period: T).

$$a_n := (APD)_n$$

$$d_n := (DI)_n$$

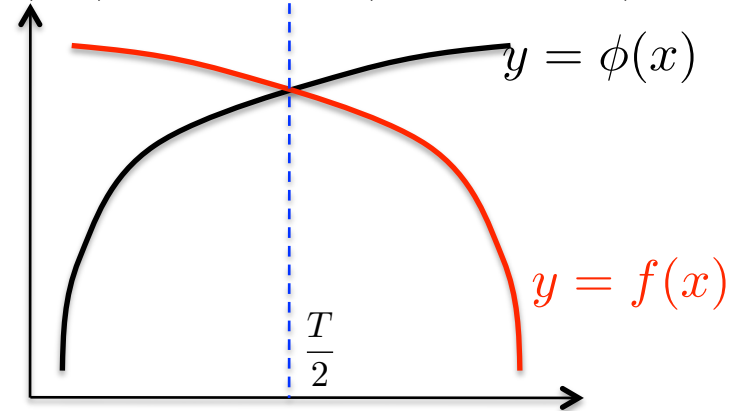
$$a_n + d_n = T$$

$$\begin{aligned} a_{n+1} &= \phi(d_n) \\ &= \phi(T - a_n) \end{aligned}$$

$$f(x) := \phi(T - x)$$

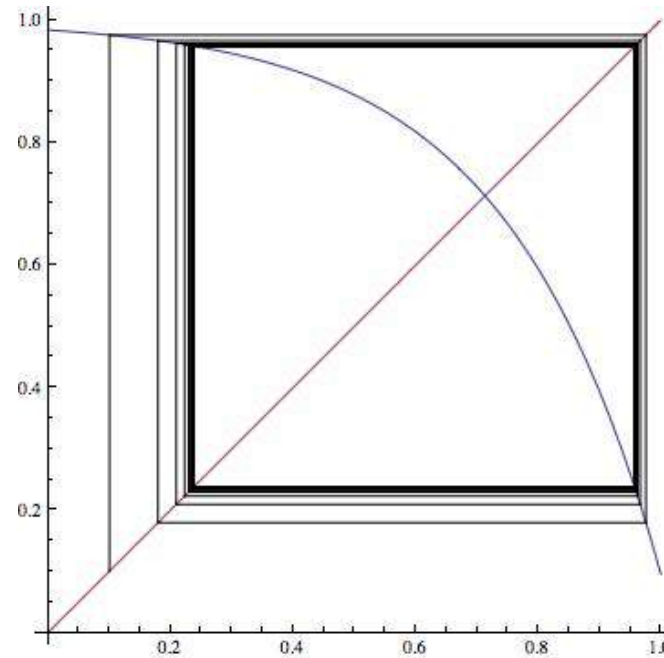
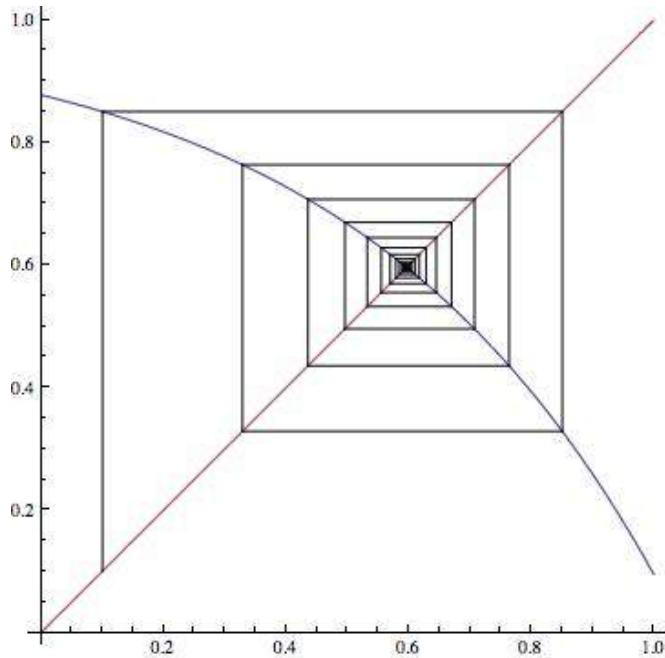
Sequence of APD satisfies the following:

$$a_{n+1} = f(a_n)$$



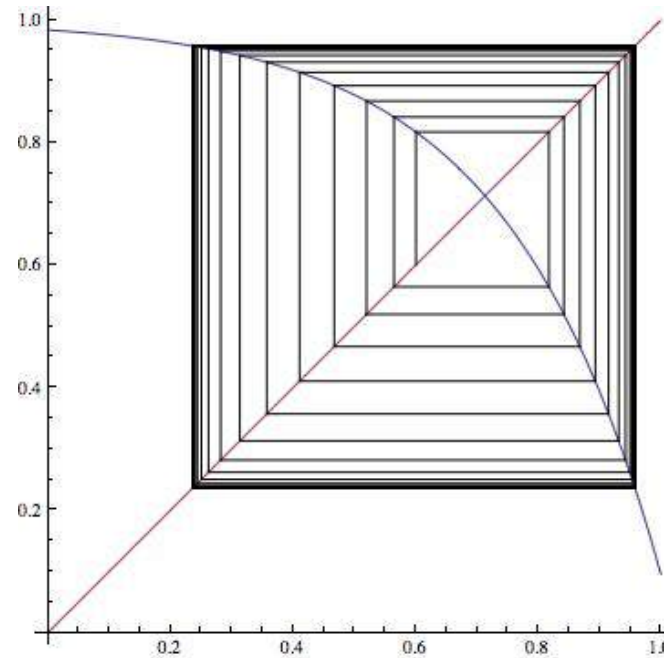
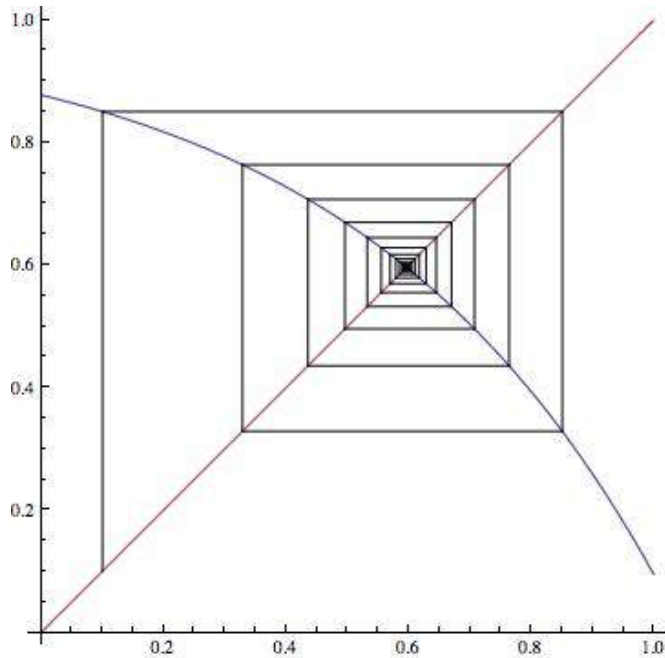
Bifurcation in the 1D map

Period doubling bifurcation occurs depending on the slope of the restitution curve.

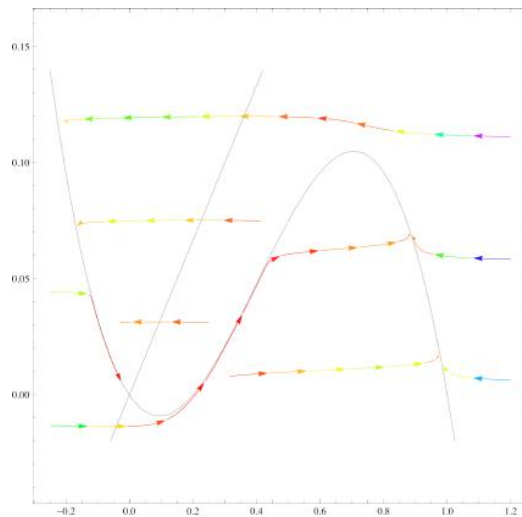


Bifurcation in the 1D map

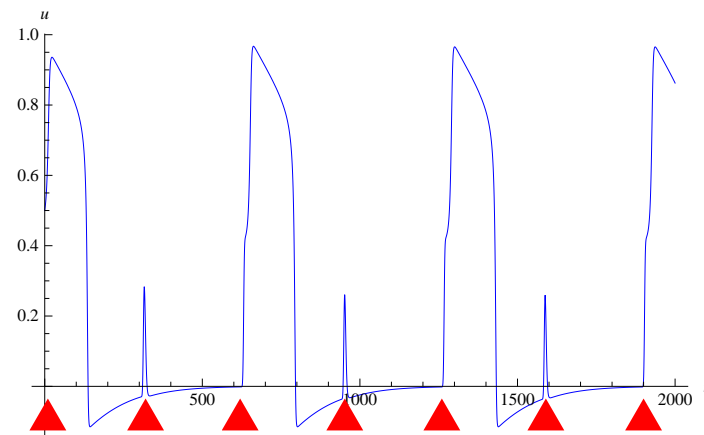
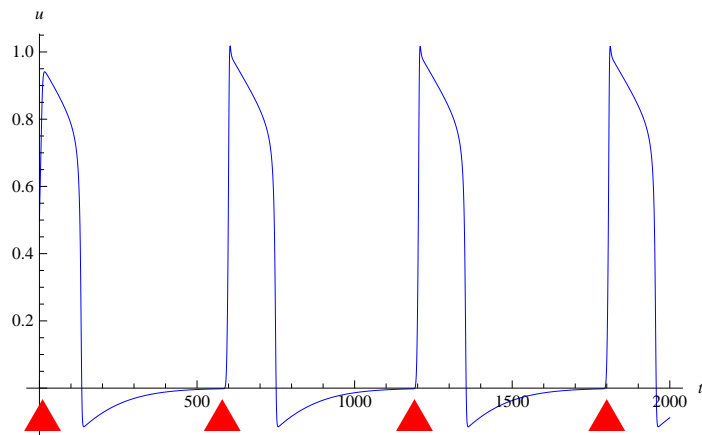
Period doubling bifurcation occurs depending on the slope of the restitution curve.



Restitution curve for FHN



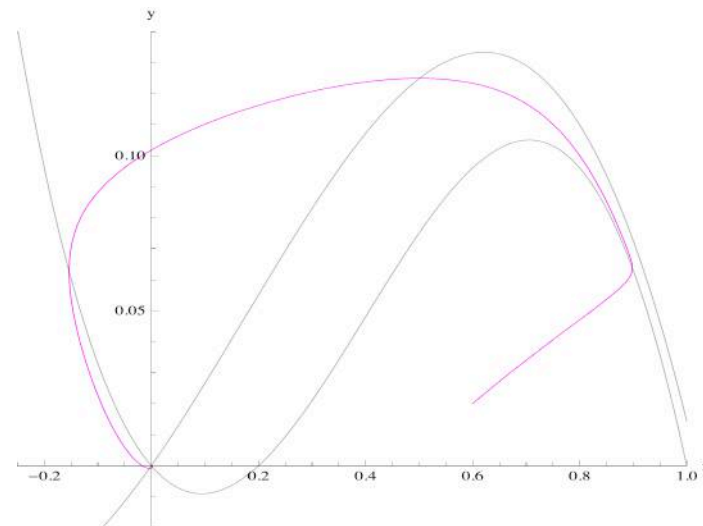
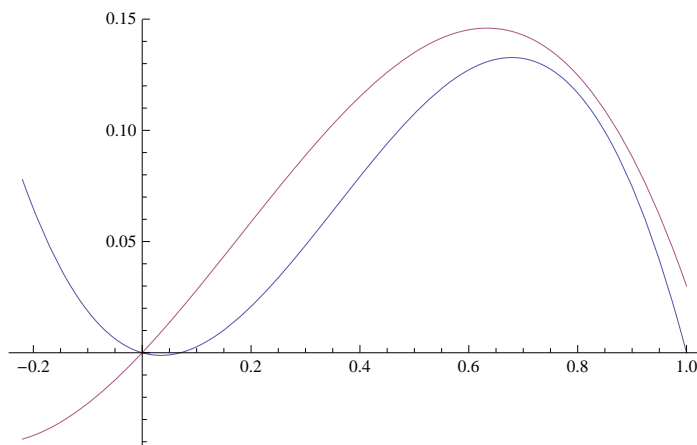
In the case of FHN the slope of the restitution curve is less than 1. So alternant response can not be observed.



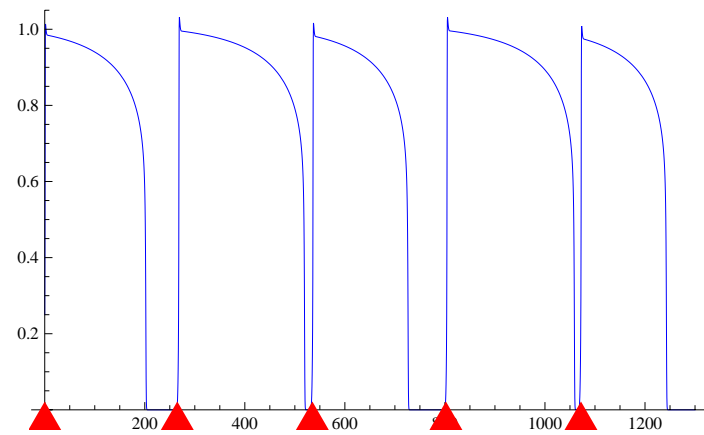
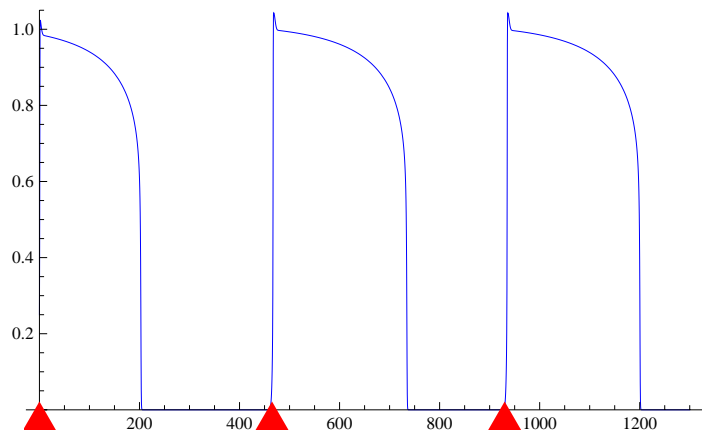
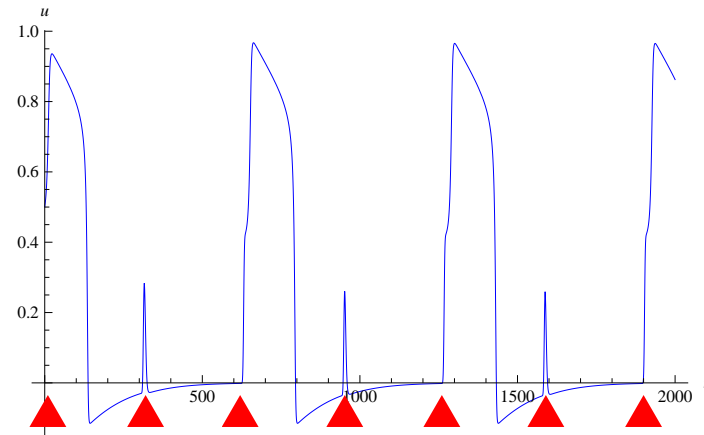
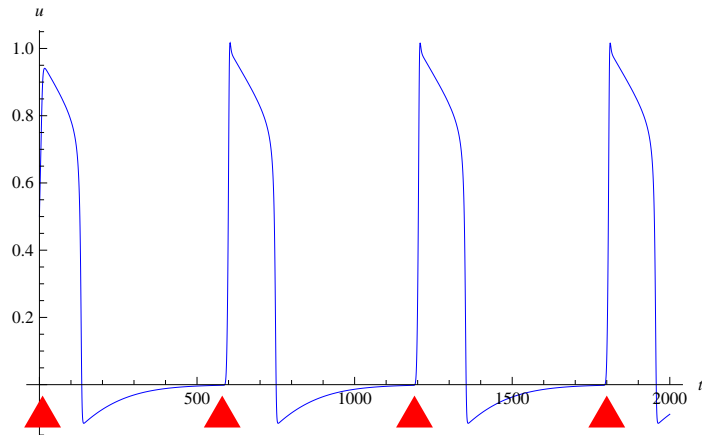
Modified FHN system

To make the restitution curve steeper the period on the exciting branch should be larger. So we modify the FHN as follows.

$$\begin{aligned}\varepsilon \frac{dx}{dt} &= x(x - a)(1 - x) - y \\ \frac{dy}{dt} &= dx(b - x)(x + c) - y\end{aligned}$$



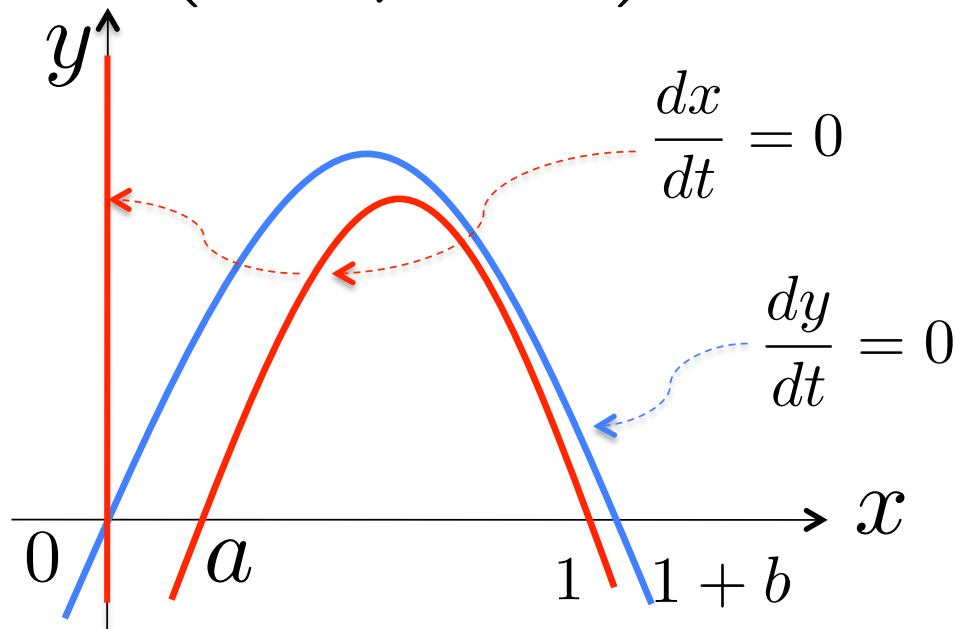
Alternant response



Aliev-Panfilov model

The Aliev-Panfilov model, one of the cardiac cell models, has a similar kind of property.

$$\begin{aligned}\frac{dx}{dt} &= Kx(x-a)(1-x) - xy \\ \frac{dy}{dt} &= \left(\varepsilon + \frac{\mu}{\mu+x} \right) (Kx(1+b-x) - y)\end{aligned}$$



1D Reaction-diffusion system

Discordant alternans seems to relate to the alternant response. But is it true?

Modified FitzHugh-Nagumo system of RD

$$\begin{aligned}u_t &= d_1 u_{xx} + u(u - a)(1 - u) - v \\v_t &= d_2 v_{xx} + \varepsilon(du(b - u)(u + c) - v)\end{aligned}$$

Study the stability for the wave train.

Stability for Wave train

- Rinzel, Keller, Biophys. J. 13, 1973
(Piecewise linear, slow-fast branches)
- Maginu, J. Math. Biology 6, 1978
(Instability on the part of the slow branch)
- Maginu, J. Math. Biology 10, 1980
(Instability for slow branch and the part of fast)
- . . .
- Gardner, J.Math.Pures Appl., 72, 1993
- Rademacher, Sandstede, Scheel, Physica D229, 2007
- Rademacher, Scheel, Int.J.Bif.Chaos 17(8),2007
- J.A. Sherratt, Applied Mathematics & Computation 218,
4684-4694 (2012) **WAVETRAN**

Essential spectra

$$u_t = Du_{xx} + cu_x + f(u) \quad u \in \mathbb{R}^n, \quad x \in \mathbb{R}$$

Suppose $\psi(x)$ is a periodic stationary solution.

$$\mathcal{L}u := Du_{xx} + cu_x + a(x)u = \lambda u \quad a(x) = a(x + L)$$

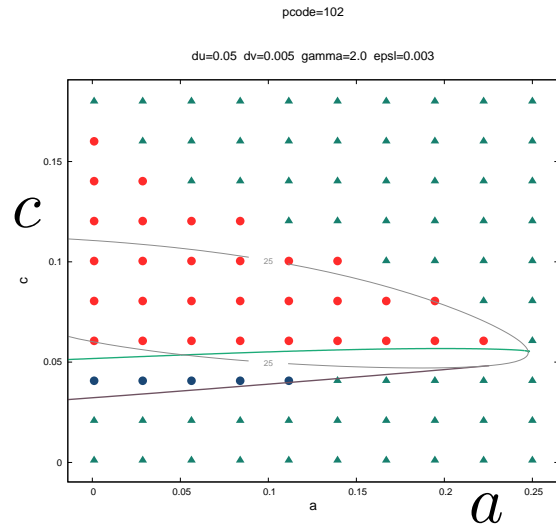
$$\mathcal{L}_\nu := D(\partial_x + \nu)^2 + c(\partial_x + \nu) + a(x)$$

Lemma[Rademacher et.al]: the followings are equivalent.

- (i) $\lambda \in \text{spec} \mathcal{L}$
- (ii) $\mathcal{L}_\nu u = \lambda u$ for some $u \in H_{per}^2(0, L)$ and some $\nu \in i\mathbb{R}$
- (iii) $\det(\Phi_\lambda - e^{\nu L}) = 0$ for some $\nu \in i\mathbb{R}$

Existence and stability of PTW solutions for the Standard FHN Model

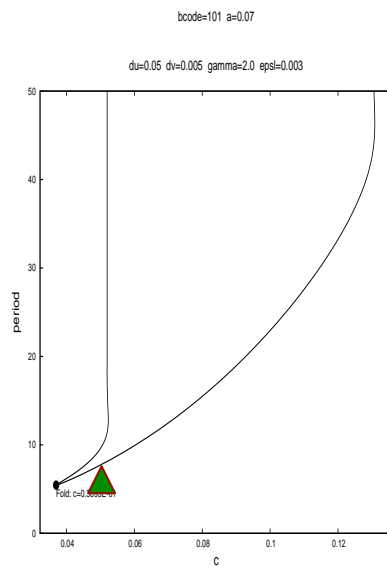
$a = \text{free}, \gamma = 2.0, \varepsilon = 0.003$



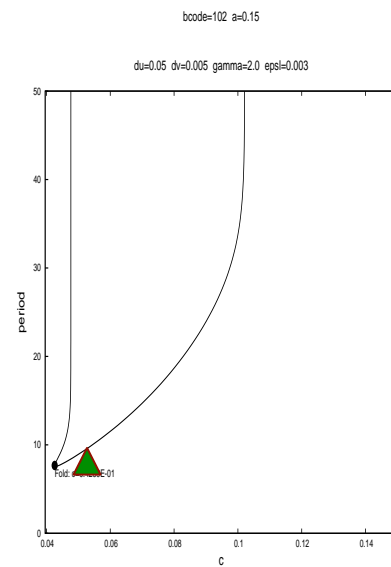
$$u_t = D_1 u_{xx} + u(1-u)(u-a) - v$$

$$v_t = D_2 v_{xx} + \varepsilon(u - \gamma v)$$

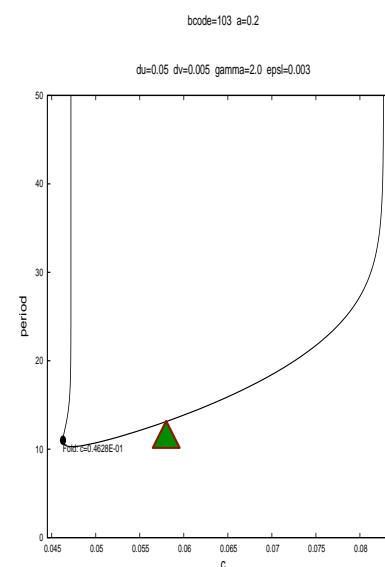
$$\varepsilon = 0.003, \gamma = 2.0$$



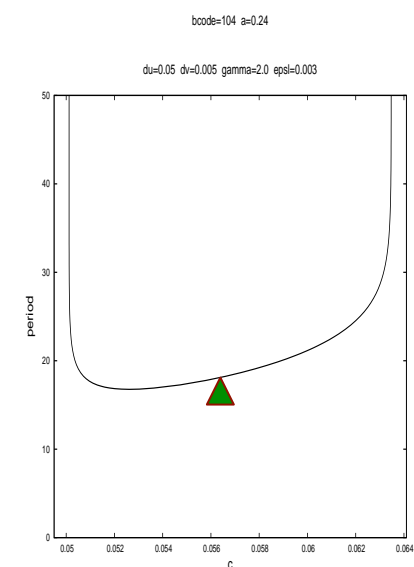
$$a = 0.07$$



$$a = 0.15$$

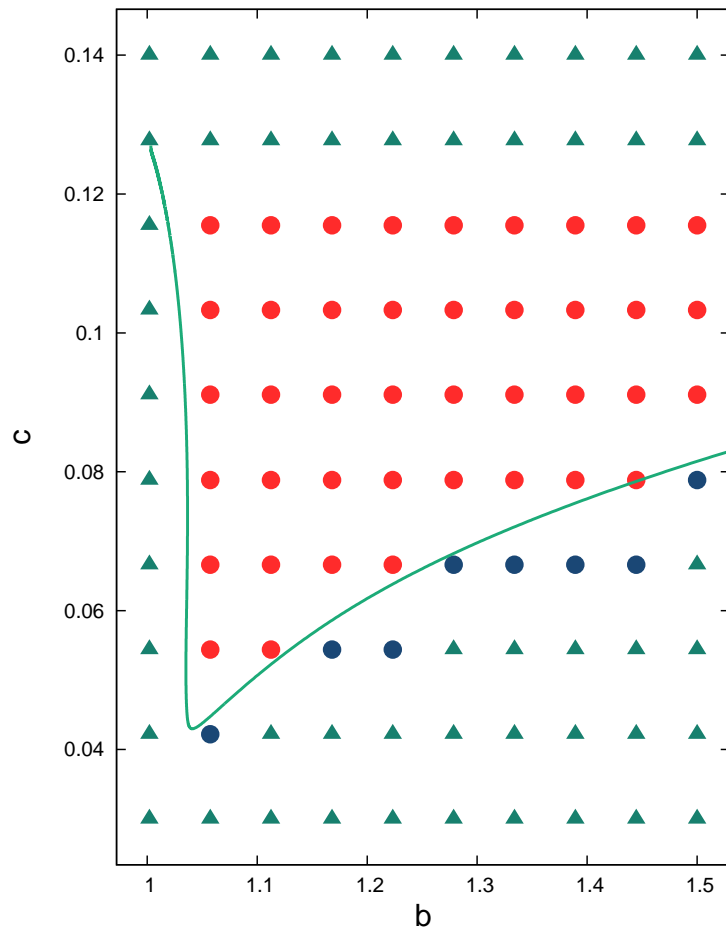


$$a = 0.2$$



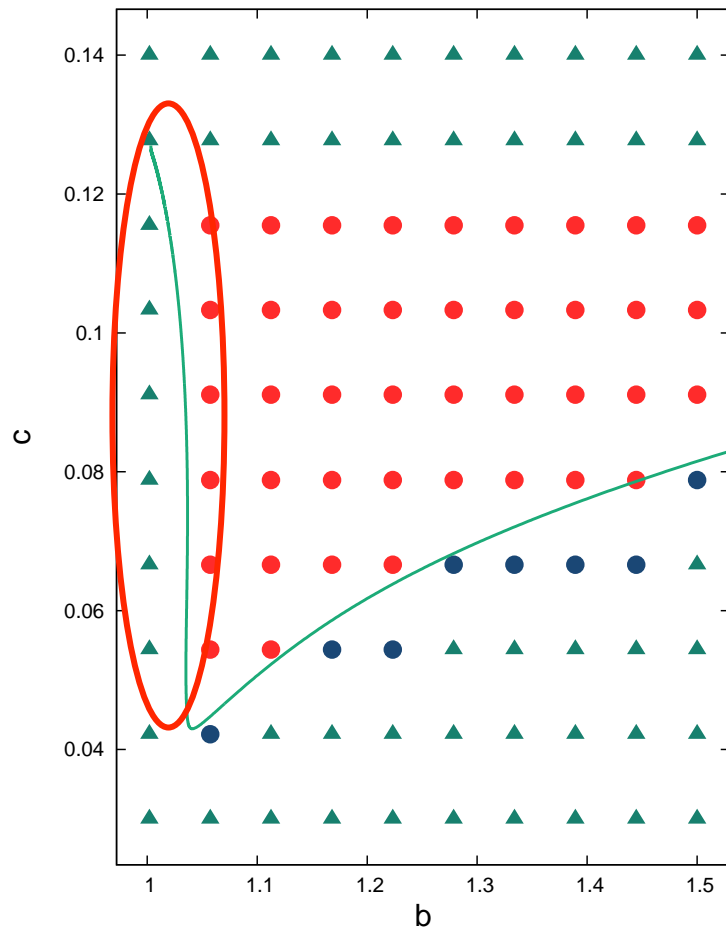
$$a = 0.24$$

Stability of PTW for modified-FHN



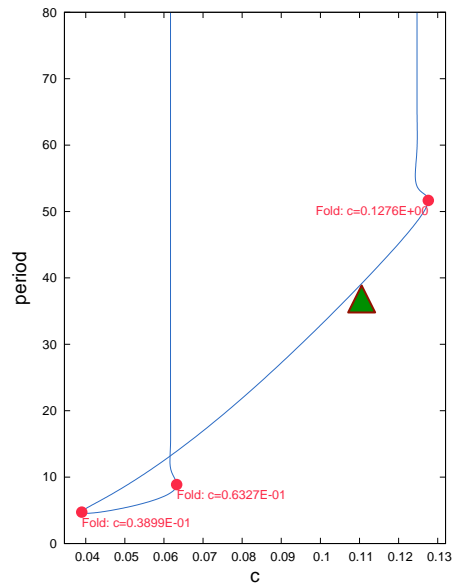
- Stable periodic traveling wave
- Unstable periodic traveling wave solution
- ▲ No periodic traveling wave
- Stability boundary (Eckhaus type)

Stability of PTW for modified-FHN

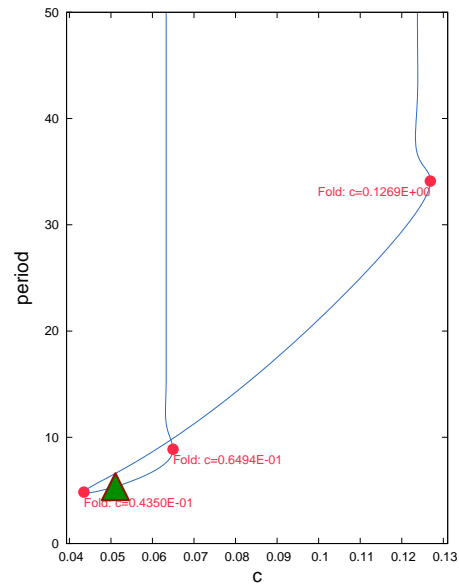


- Stable periodic traveling wave
- Unstable periodic traveling wave solution
- ▲ No periodic traveling wave
- Stability boundary (Eckhaus type)

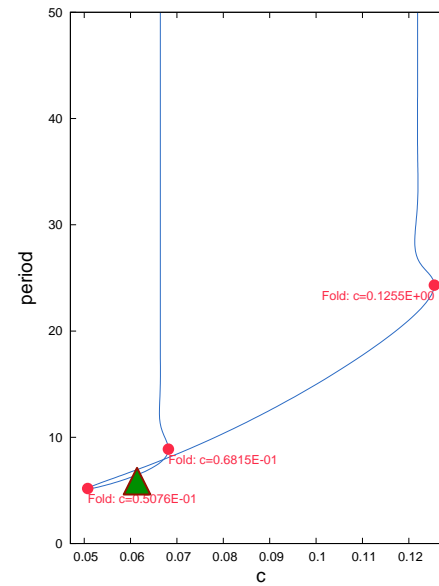
Bifurcation Diagram



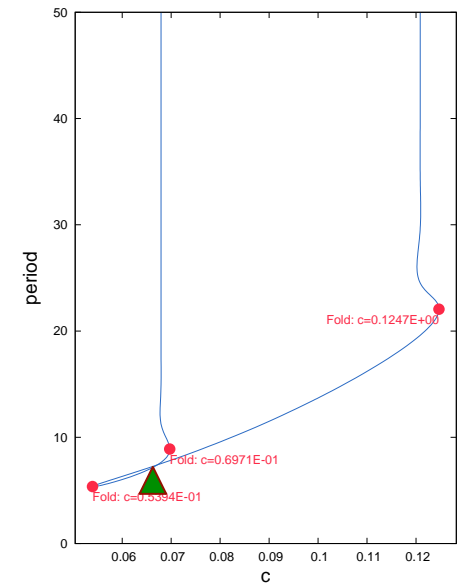
$b=1.03$



$b=1.1$

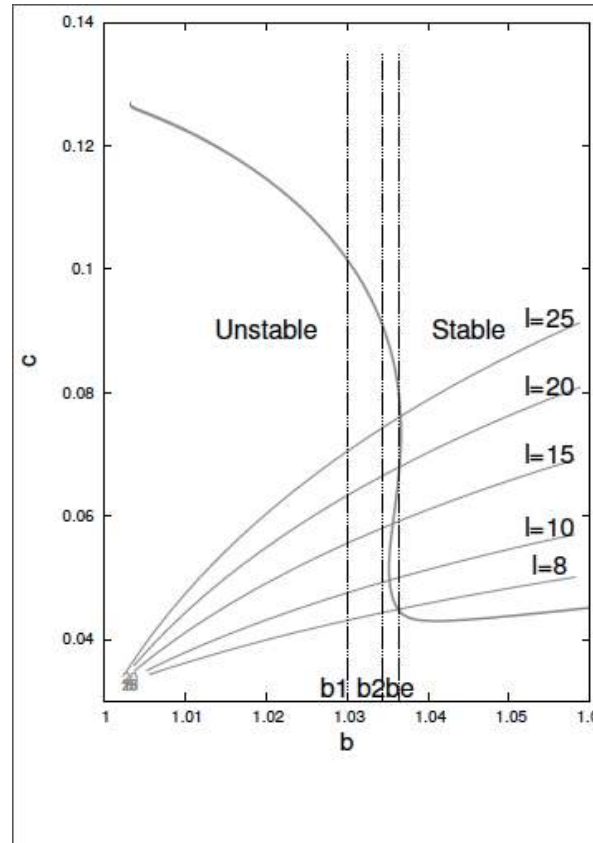
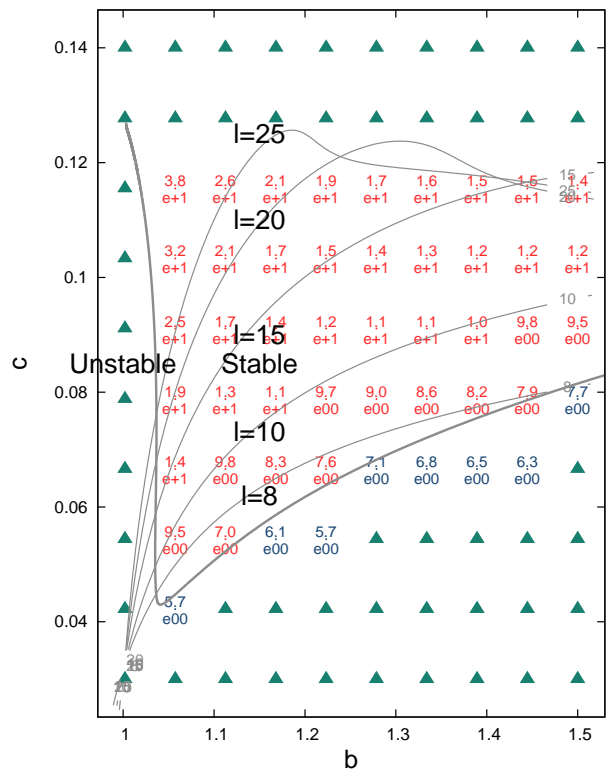


$b=1.2$

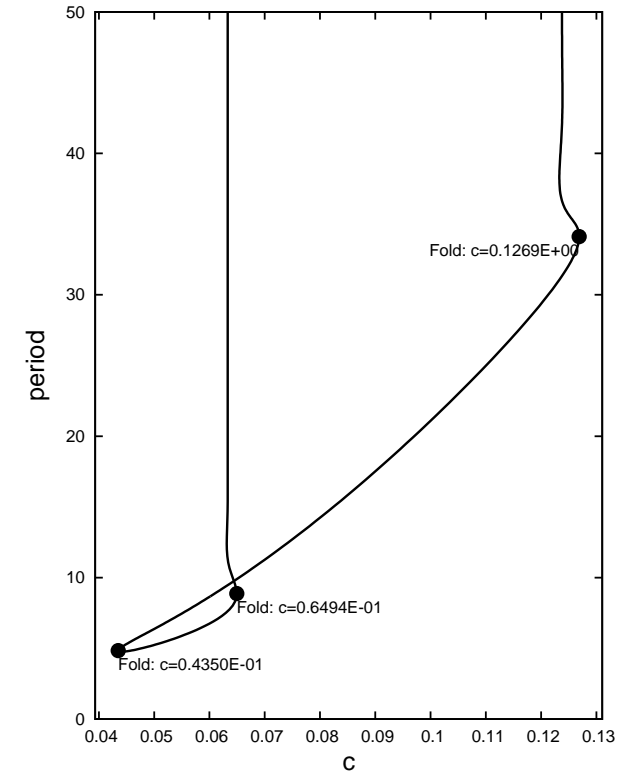


$b=1.25$

Existence and Stability of PTWs for different periods



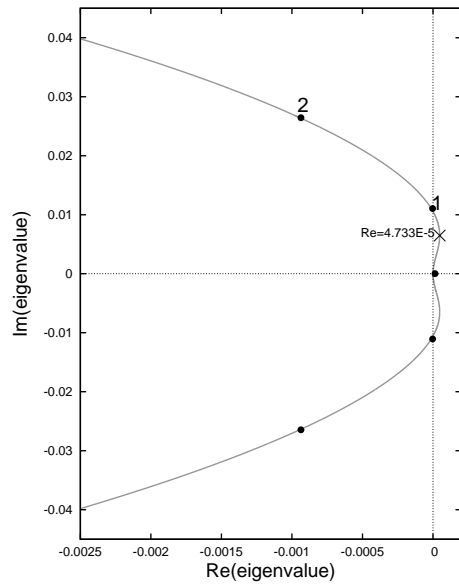
Magnification of the 1st figure



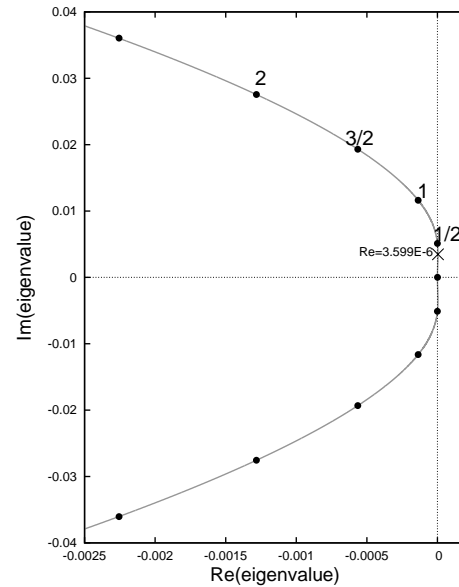
Bifurcation diagram for $b=1.1$

$$b_1 < b_2 < \dots < b_n \leq b_e$$

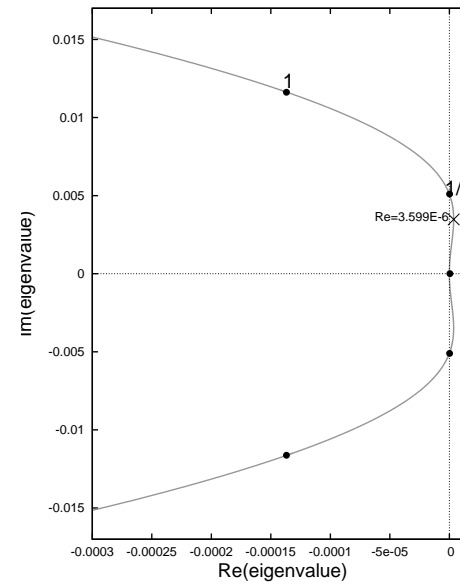
The essential spectra of four PTW solutions of our model



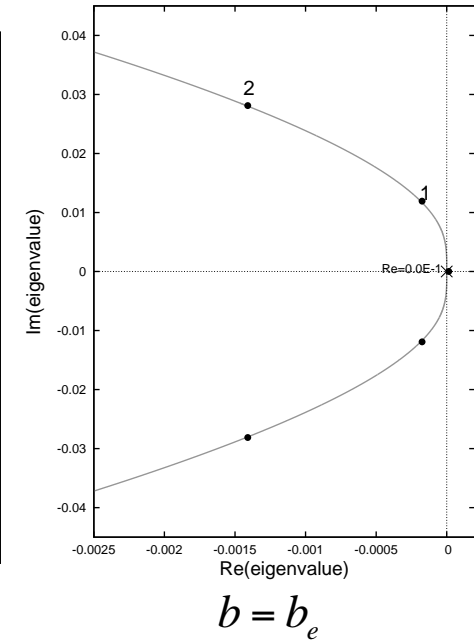
For $b=1.03$ and wave speed $c=0.07$, $L=l=25$,
PTW is Unstable
($b_1 = 1.0295$)



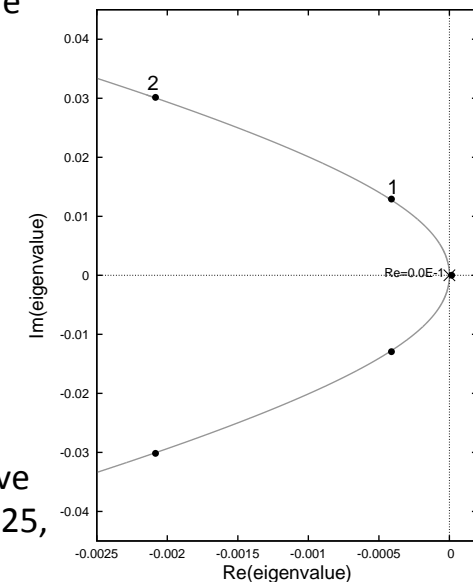
For $b=1.0495$ and wave speed $c=0.075$, $L=50$, $l=25$
PTW is Unstable
($b_2 = 1.0343$)



Closure look of 2nd figure



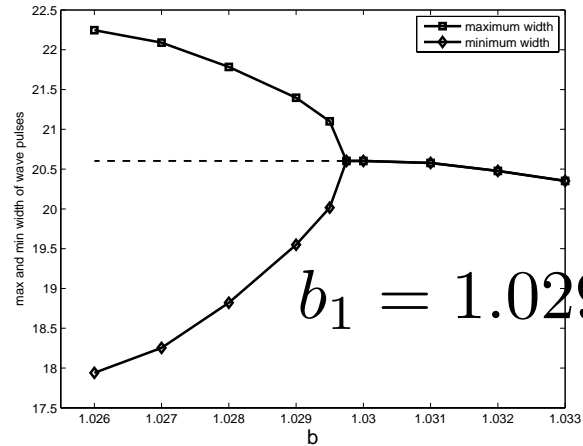
$b = b_e$



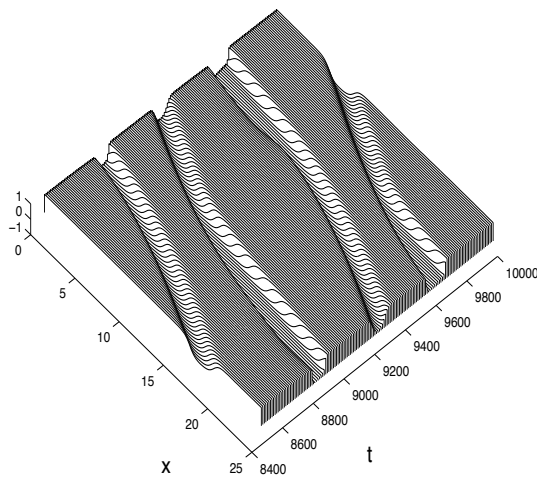
For $b=1.045$ and wave speed $c=0.082$, $L=l=25$,
PTW is stable

- ◆ The grey lines indicate the spectra and the black dots denote Eigenvalues corresponding to eigenfunctions with periods m/n of the wavelength.

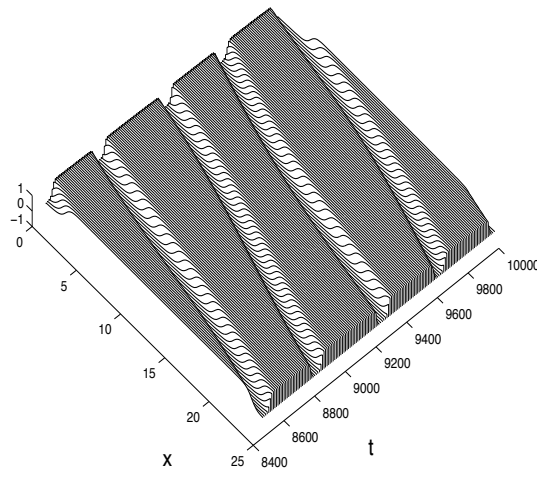
Bifurcation Diagram (L=25, l=25)



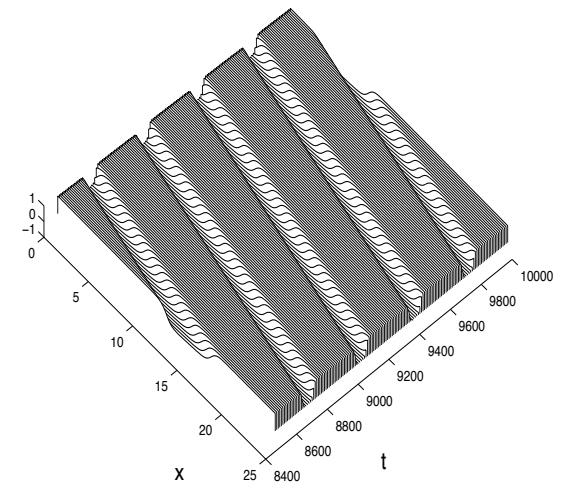
We can observe a Hopf bifurcation under periodic boundary condition with period L .



$b=1.022$

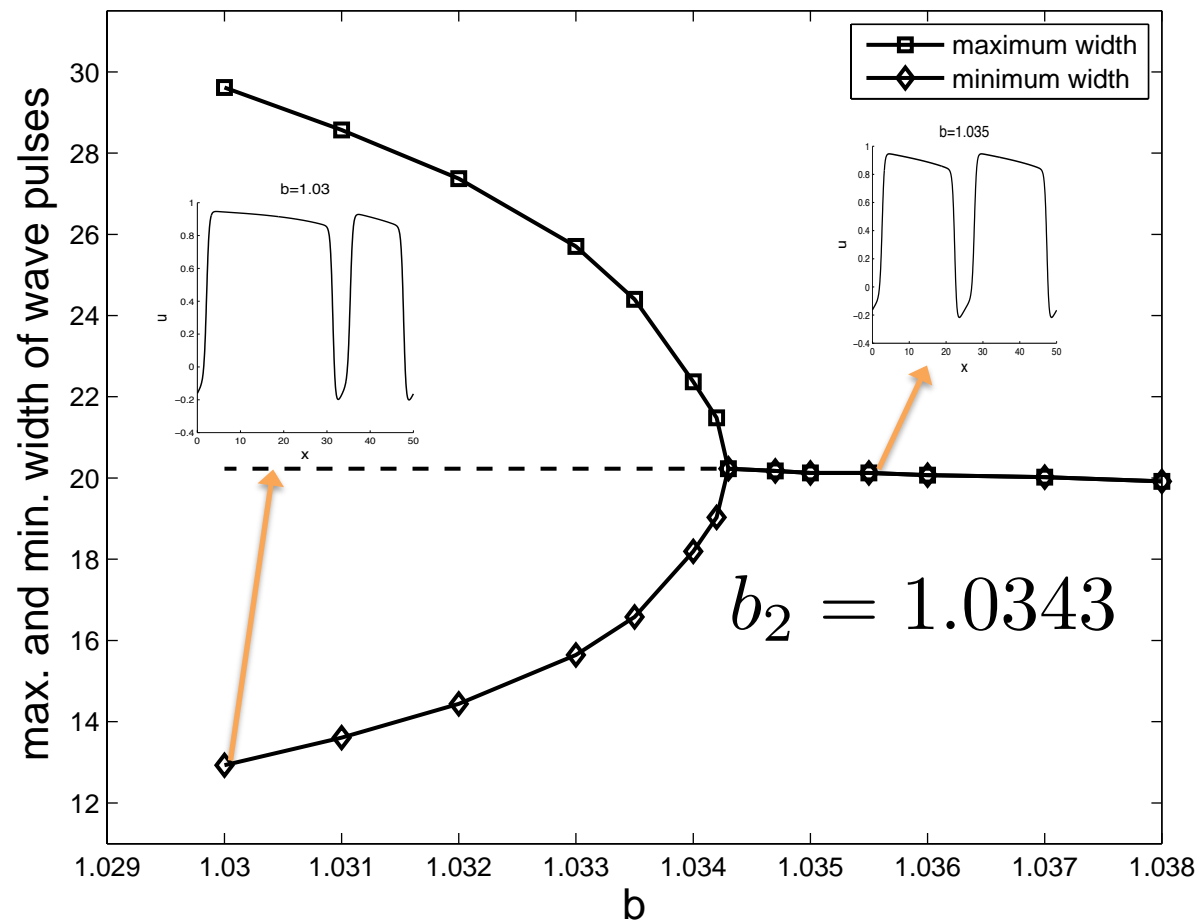


$b=1.025$



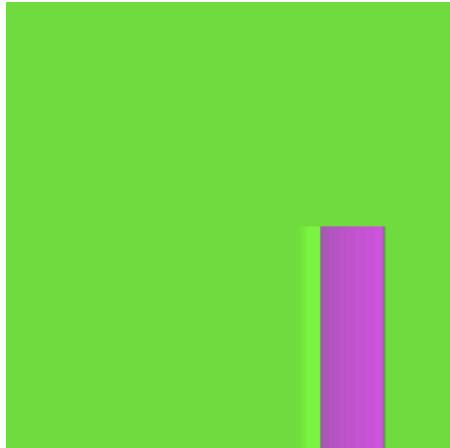
$b=1.032$

Bifurcation Diagram (L=50, l=25)



We can observe another type of Hopf bifurcation under periodic boundary condition with period L which is double the wavelength.....

Spiral pulses widths increasing as b decreased



Initial data



$b=1.3$



$b=1.2$



$b=1.1$



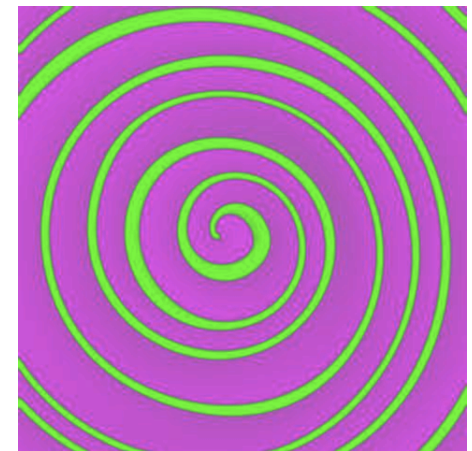
$b=1.05$



$b=1.04$



$b=1.035$



$b=1.03$

Summary

- We have studied the stability of periodic traveling wave solutions by essential spectrum from numerical continuation.
- Most of the fast periodic traveling waves become **Eckhaus** unstable by the effect of long excitation.
- We also observe a change of stability of **Hopf** type for small period.

Reference

- **S.Bauer, G.Roder and M.Bar**, Alternans and influence of ionic channel modifications: Cardiac three-dimensional simulations and one-dimensional numerical bifurcation analysis, Chaos 17, 2007
- **M.Bar and L.Brusch**, Breakup of spiral waves caused by radial dynamics: Eckhaus and finite wavenumber instabilities, New J. of Phys. 6, 2004



Contraction driven cell motility

Pierre Recho

A joint work with T. Putelat, J.-F. Joanny and L. Truskinovsky



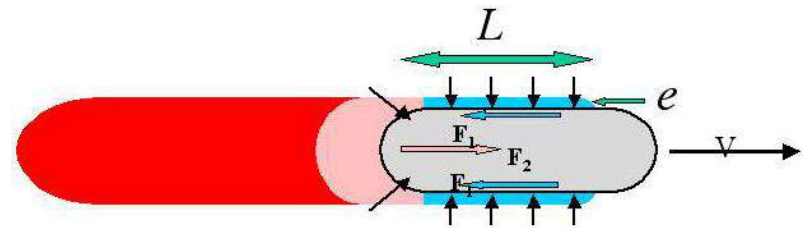
Models for cell motility

- **Polymerization-driven, macroscopic**

-A Mogilner and L Edelstein-Keshet , *Biophys. J.*, 2002

-J. Prost, J.-F Joanny, P. Lenz and C. Sykes , *In Cell Motility, Biological and Medical Physics, Biomedical Engineering*, 2008

-F. Jülicher, K.Kruse, J. Prost and J.-F. Joanny , *Phys. Rep.*, 2007



- **Turing mechanism**

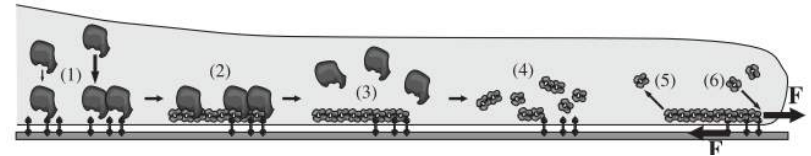
-B.Vanderlei, J.J.Feng and L.Edelstein-Keshet , *Multiscale Model. Simul.* , 2010

- **Two-phase flows**

-M.Herant and M.Dembo , *Biophys.J.*, 2010

- **Microscopic theory of active filaments**

-K. Doubrovinski and K. Kruse, *Phys. Rev. Lett*, 2011



- **Osmotic Engine Model**

-K.M. Stroka, H. Jiang, S.-H. Chen, Z. Tong, D. Wirtz, S. X. Sun, K. Konstantopoulos, *Cell*, 2014

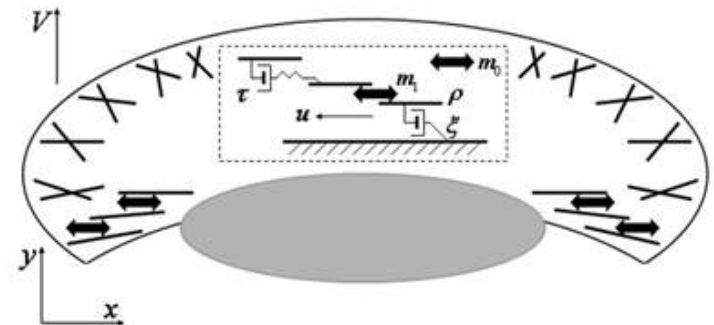
- **Comprehensive models**

-D.Shao, W.-J. Rappel and H.Levine, *Phys.Rev.Lett.*, 2010

-B. Rubinstein, M.F. Fournier, K. Jacobson, A. B. Verkhovskiy, and A. Mogilner , *Biophys J.*, 2009

-Q. Wang, X. Yang, D. Adalsteinsson, T.C.Eleston, K. Jacobson, M. Kapustina and M.G.Forest, *Comput.Model.Biol.Syst.*, 2012

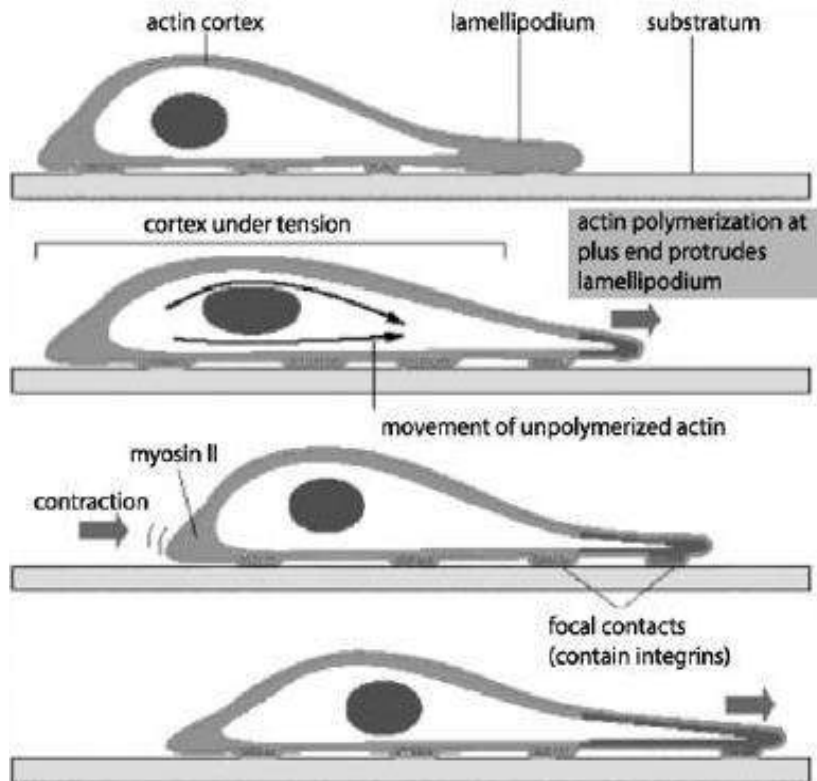
- Ziebert, F. & Aranson, I. S., *PloS one*, 2013



Crawling cells

Three main components of cell motility:

1. **Protrusion**
2. **Adhesion**
3. **Contraction**



speed \simeq one body length/min



Keratocyte

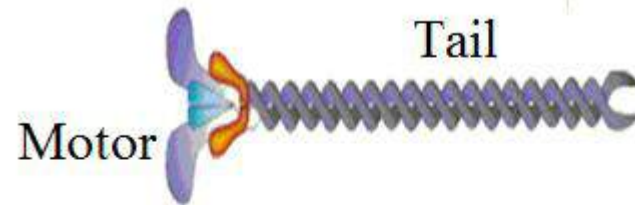


HeLa

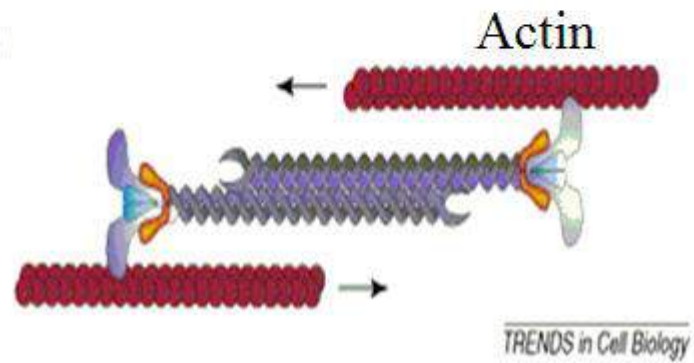
B. Alberts, et al. *Molecular biology of the cell*. 2002.

Contraction

(a)



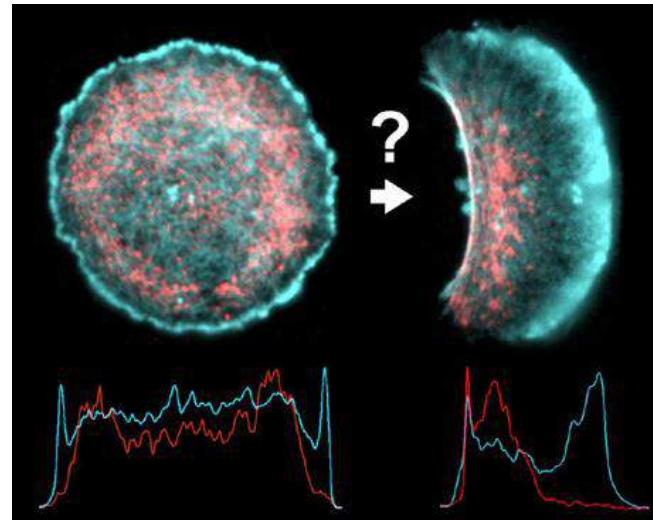
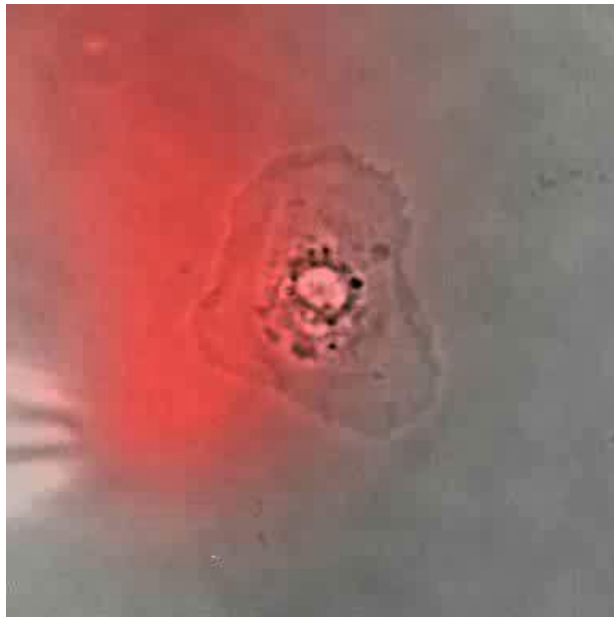
(b)



K. Clark, et al. *Trends Cell Biol.*, 17(4), 2007.

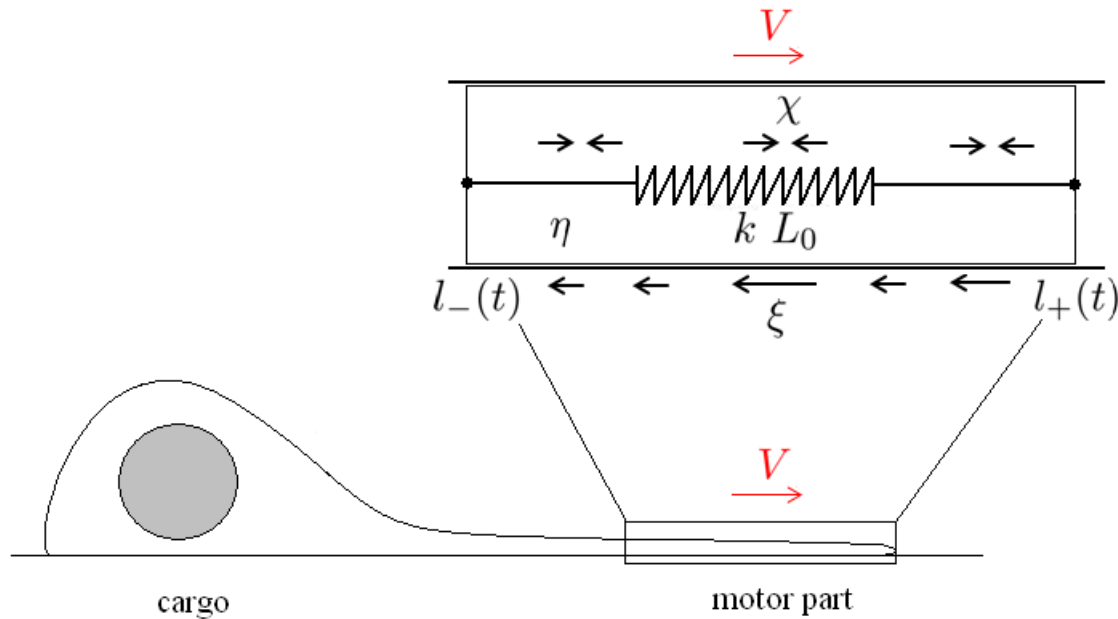
Contraction driven initiation of motility

- Verkhovsky et al. , Current Biology, 1999 : “ A **transient** mechanical **stimulus** was applied **to stationary fragments**. The stimulus induced localized contraction and the **formation of an actin–myosin II bundle at one edge** of the fragment. Remarkably, stimulated fragments started to undergo **locomotion** and the locomotion and associated anisotropic organization of the actin–myosin II system were sustained **after** withdrawal of the stimulus. ”
- Yam et al, JCB, 2007 : “ Local **stimulation of myosin activity** in stationary cells by the local application of calyculin A induced **directed motility initiation** away from the site of stimulation”



Symmetric configuration becomes unstable

Model



Cell is modeled as a viscous **active gel** with moving boundaries: $l_-(t)$ and $l_+(t)$

- Adhesion is modeled by viscous friction.
- Contraction is modeled as a distributed pre-stress.
- Cell membrane/cortex is assumed to be linear elastic.

Governing equations

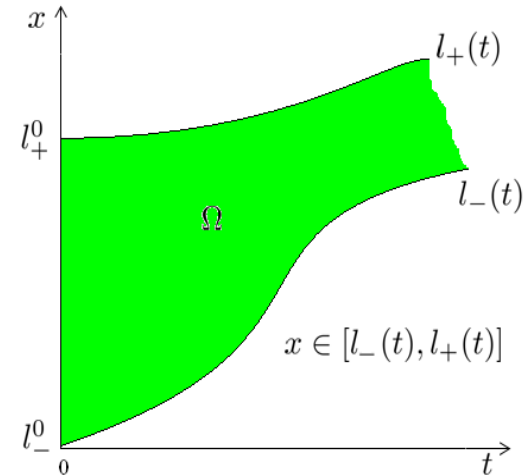
- Force Balance:
$$\begin{cases} \partial_x \sigma = \xi v & \leftarrow \text{Adhesion} \\ \sigma(l_{\pm}(t), t) = -k \frac{l_{+}(t) - l_{-}(t) - L}{L} & \leftarrow \text{Elasticity} \end{cases}$$

- Constitutive relation:
$$\sigma = \eta \partial_x v + \underbrace{\chi c(x, t)}_{\geq 0} \leftarrow \text{Contraction}$$

- Boundary kinetic:
$$\begin{cases} \dot{l}_{\pm} = v(l_{\pm}(t), t) & \leftarrow \text{Stefan-type} \\ l_{-}(0) = l_{-}^0 < l_{+}(0) = l_{+}^0 \end{cases}$$

- Myosin II:
$$\begin{cases} \partial_t c + \partial_x (cv) - D \partial_{xx} c = 0 \\ D \partial_x c(l_{\pm}(t), t) = 0 \\ c(x, 0) = c^0(x) \end{cases} \leftarrow \text{Convection-diffusion}$$

- Actin:
$$\begin{cases} \partial_t \rho + \partial_x (\rho v) = 0 \\ \rho(x, 0) = \rho^0(x) \end{cases} \leftarrow \text{uncoupled}$$



Unknowns: $l_{-}(t), l_{+}(t), \underbrace{\sigma(x, t)}_{\text{axial stress}}, \underbrace{v(x, t)}_{\text{velocity}}, \underbrace{\rho(x, t)}_{\text{actin density}}$ and $\underbrace{c(x, t)}_{\text{myosin concentration}}$

Non-dimensionalization

$$\text{Limit } k \rightarrow \infty: \begin{cases} l_+(t) - l_-(t) = L \\ \text{residual stress } \sigma_0(t) = - \lim_{k \rightarrow \infty} \frac{l_+(t) - l_-(t) - L}{L} \\ \text{velocity } V(t) = \dot{l}_\pm(t) \end{cases}$$

$$\text{Mass conservation: } c_0 = L^{-1} \int_{l_+}^{l_-} c(x, t) dx$$

Non-dimensional variables: $\sigma/(c_0\chi)$, c/c_0 , $x/\sqrt{\eta/\xi}$ and $t/(\eta/(c_0\chi))$

$$\text{Mapping: } y = x/L - 1/2$$

Keller-Segel dynamics

non-local recruitment

$$\overbrace{-\mathcal{L}^{-2}\partial_{yy}\sigma + \sigma} = c$$

$$\partial_t c + \underbrace{\mathcal{L}^{-2}\partial_y(c[\partial_y\sigma - \mathcal{L}V])}_{\text{convection}} - \underbrace{\frac{\mathcal{L}^{-2}}{\lambda}\partial_{yy}c}_{\text{diffusion}} = 0$$

$$\sigma(-1/2, t) = \sigma(1/2, t) \stackrel{\text{def}}{=} \sigma_0$$

$$\partial_y\sigma(-1/2, t) = \partial_y\sigma(1/2, t) \stackrel{\text{def}}{=} V$$

$$\partial_y c(\pm 1/2, t) = 0$$

Non dimensional parameters: $\mathcal{L} = \frac{\sqrt{\xi}L}{\sqrt{\eta}}$, $\lambda = \frac{c_0\chi}{\xi D}$

$$V = -\frac{\mathcal{L}}{2} \int_{-\frac{1}{2}}^{\frac{1}{2}} \frac{\sinh(\mathcal{L}y)}{\sinh(\frac{\mathcal{L}}{2})} c(y, t) dy \quad \rightarrow \quad \left\{ \begin{array}{l} \text{symmetry break} \\ V^\infty = \mathcal{L}/2 \end{array} \right.$$

Traveling wave assumption

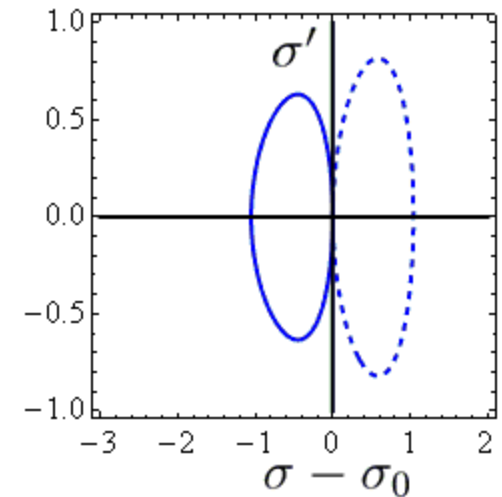
Emden equation

$$-\mathcal{L}^{-2}\sigma''(y) + \sigma(y) = \frac{e^{\lambda(\sigma(y)-V\mathcal{L}y)}}{\int_{-1/2}^{1/2} e^{\lambda(\sigma(y)-V\mathcal{L}y)} dy} \quad \rightarrow \quad \begin{cases} c(y) = \frac{e^{\lambda(\sigma(y)-V\mathcal{L}y)}}{\int_{-1/2}^{1/2} e^{\lambda(\sigma(y)-V\mathcal{L}y)} dy} \\ v(y) = \mathcal{L}^{-1}\sigma'(y) \end{cases}$$

$$\sigma(\pm\frac{1}{2}) = \sigma_0 \text{ and } \sigma'(\pm\frac{1}{2}) = \mathcal{L}V,$$

Static solutions ($V = 0$):

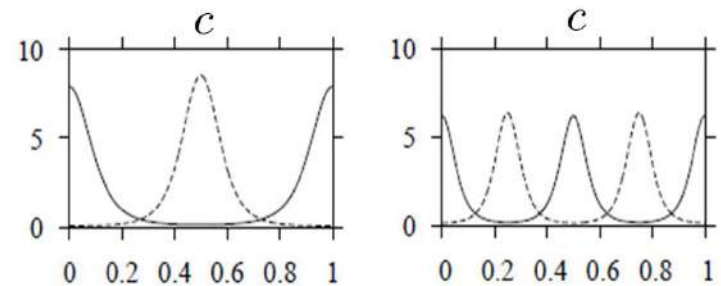
1. Trivial solution: $\sigma \equiv \sigma_0 = 1$
2. Patterned (quadratures, $\sigma'^2 = W(\sigma)$)



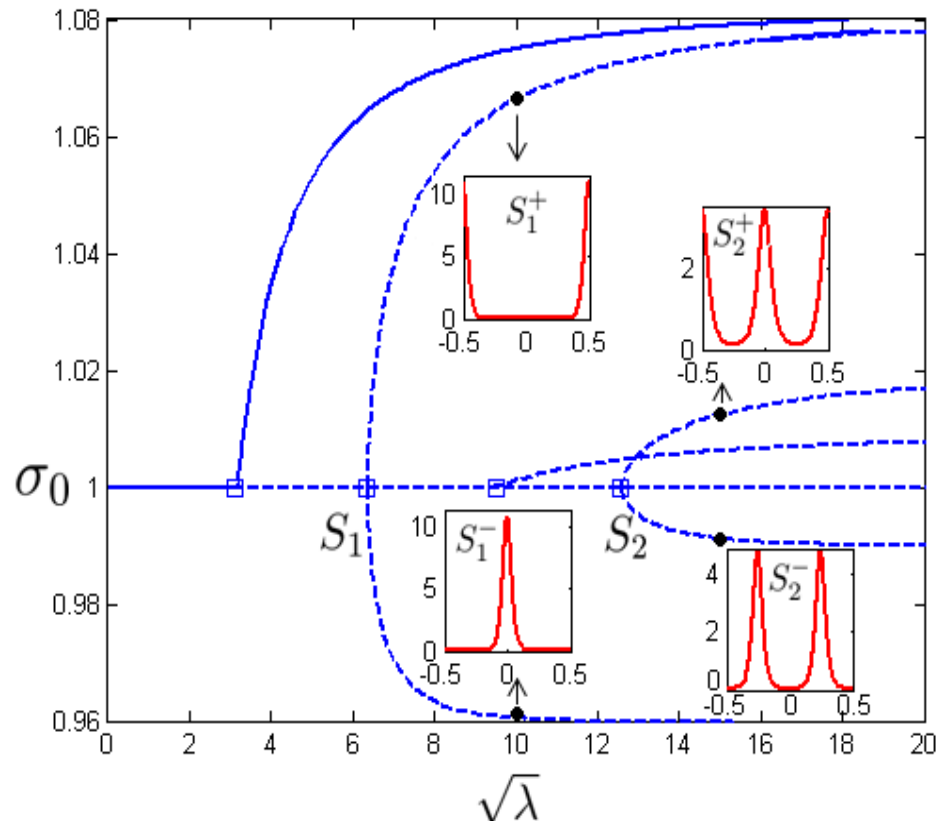
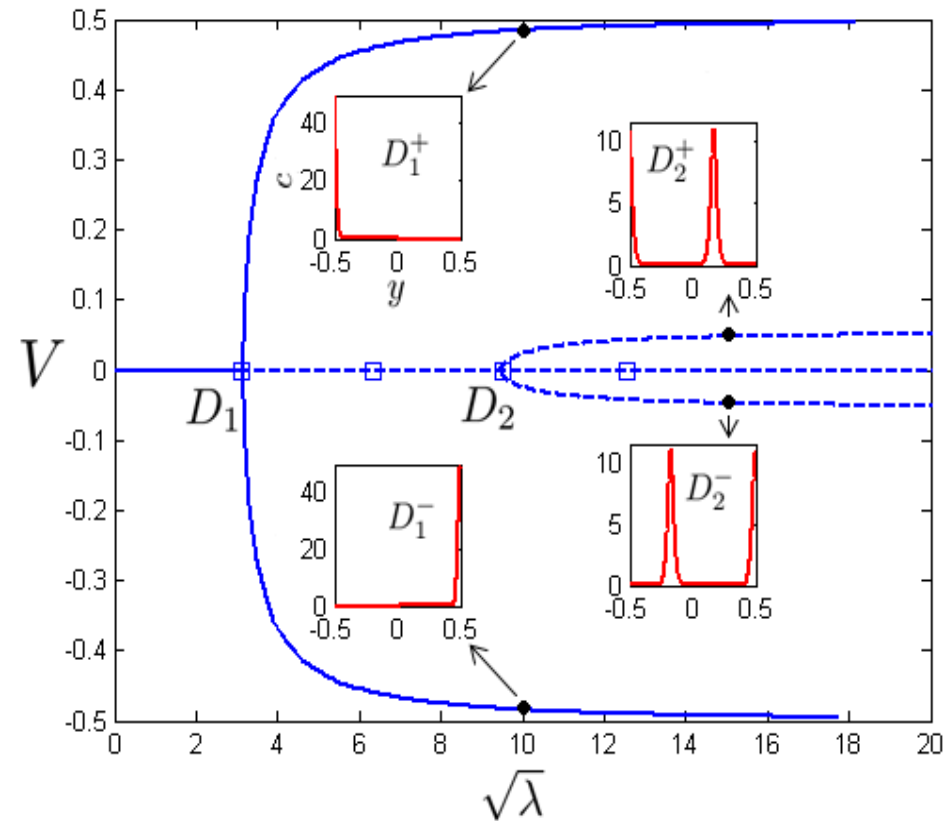
Motile solutions ($V \neq 0$):

No branching from patterned static solution

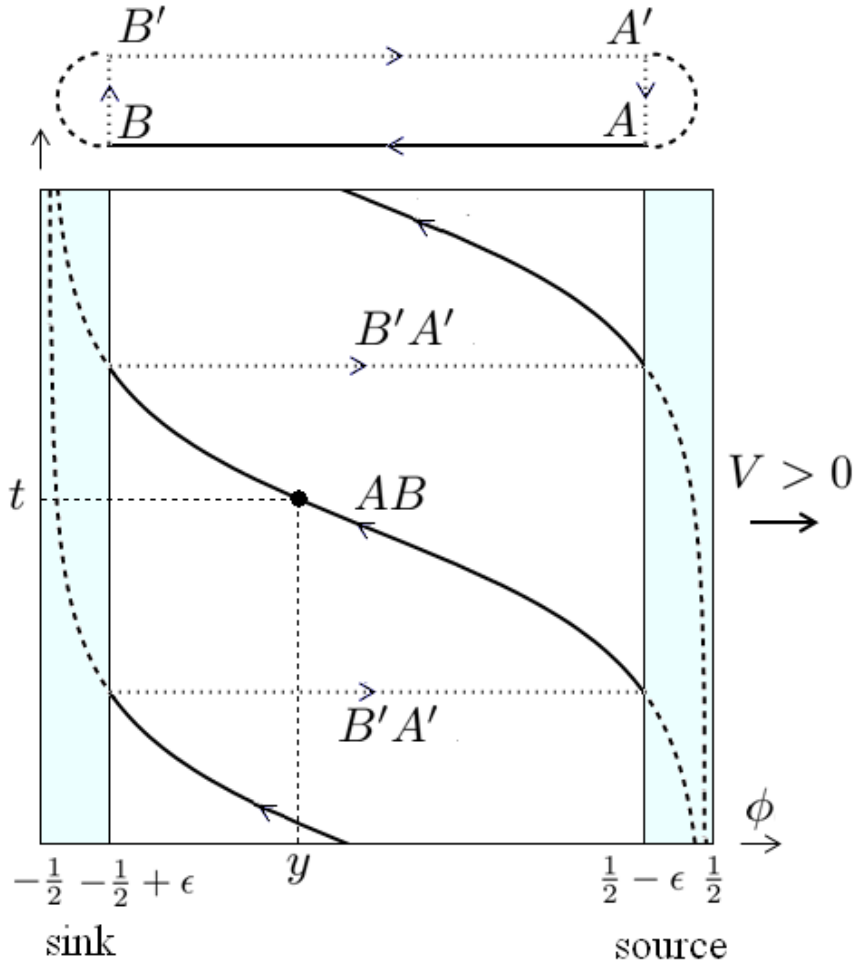
$$\int_{-1/2}^{1/2} e^{\lambda(\sigma(y)-\sigma_0-\mathcal{L}Vy)} dy = \text{sinhc}(\lambda\mathcal{L}V/2)$$



Bifurcation diagram



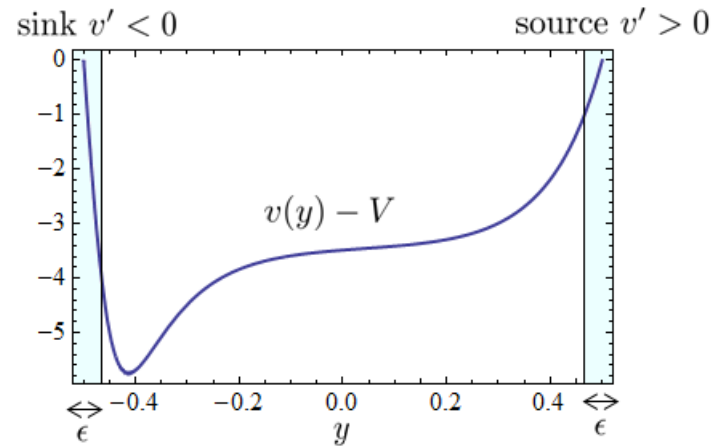
Reconstruction of actin density



$$\partial_t \rho + \mathcal{L}^{-1} \partial_y (\rho(v - V)) = 0$$

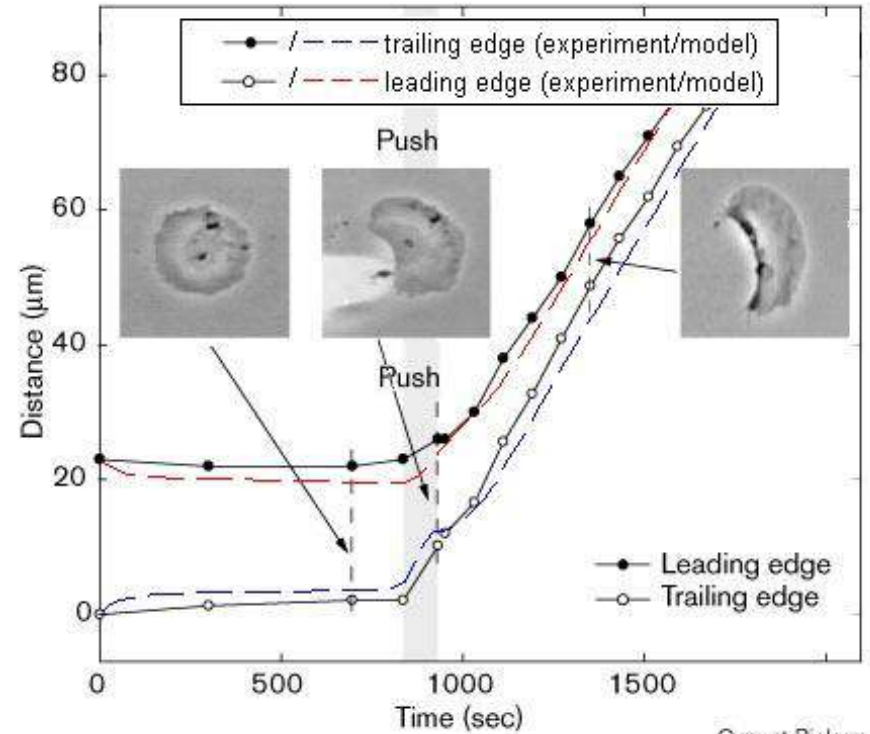
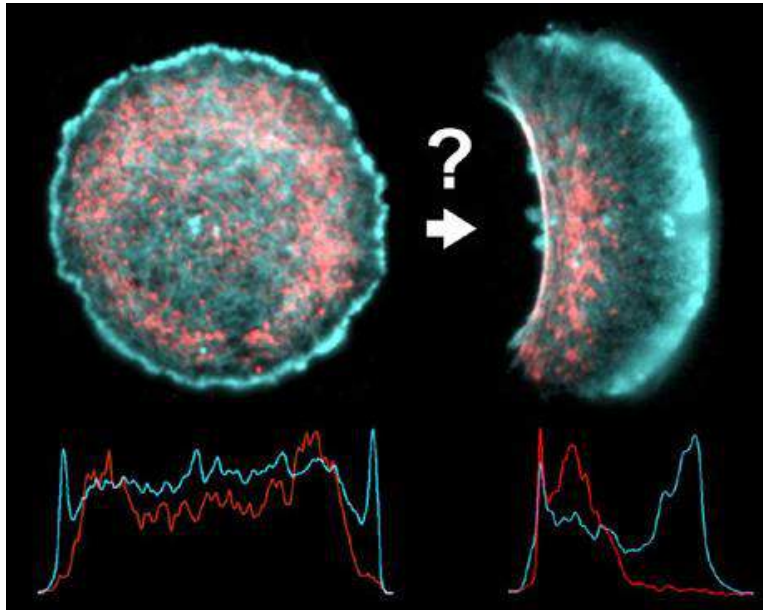
Characteristic curves:

$$\frac{d\phi}{dt} = \mathcal{L}^{-1}(v(\phi) - V)$$

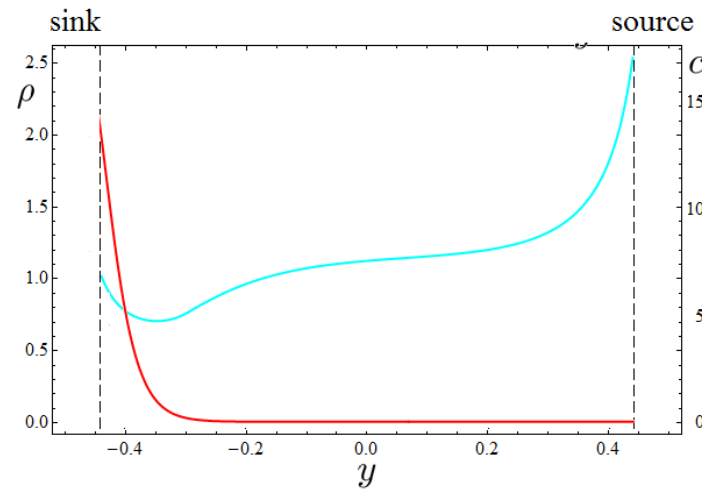
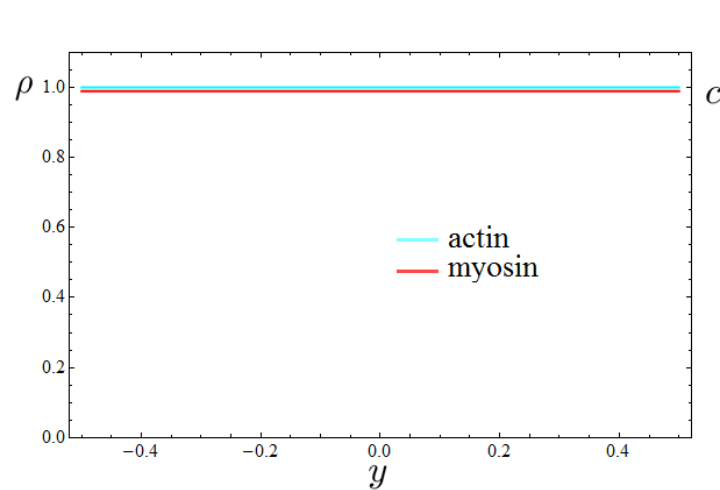


T.W. $\rightarrow \rho(y)(V - v(y)) = \dot{m} = \left(\int_{-1/2+\epsilon}^{1/2-\epsilon} (V - v(y))^{-1} dy \right)^{-1}$

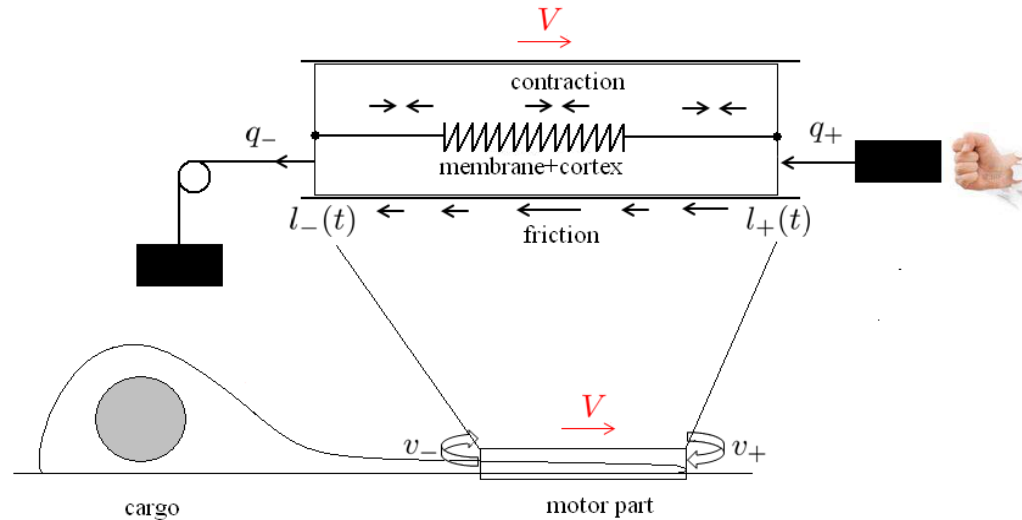
Experiments



Current Biology



Governing equations



- Force Balance:
$$\begin{cases} \partial_x \sigma = \xi v & \leftarrow \text{Adhesion} \\ \sigma(l_{\pm}(t), t) = -k \frac{l_+(t) - l_-(t) - L}{L} + q_{\pm} & \leftarrow \text{Loading} \end{cases}$$

\leftarrow Elasticity
- Constitutive relation:
$$\sigma = \eta \partial_x v + \underbrace{\chi c(x, t)}_{\geq 0} \leftarrow \text{Contraction}$$
- Boundary kinetic:
$$\dot{l}_{\pm} = v(l_{\pm}(t), t) \leftarrow \text{Stefan-type}$$

Efficiency

Balance of power

$$[\sigma v]_{l_-(t)}^{l_+(t)} = \xi \int_{-L/2}^{L/2} v^2 + \eta \int_{-L/2}^{L/2} (\partial_x v)^2 + \chi \int_{-L/2}^{L/2} c \partial_x v$$

$$\underbrace{-\chi \int_{-L/2}^{L/2} c \partial_x v}_{H^* > 0} = \underbrace{(q_- - q_+) V}_{P_m > 0} + \underbrace{\xi \int_{-L/2}^{L/2} v^2 + \eta \int_{-L/2}^{L/2} (\partial_x v)^2}_{P_d > 0}$$

$$\text{Efficiency } \Lambda = \frac{P}{H} \quad \left\{ \begin{array}{l} P = \underbrace{P_m}_{\text{work against loads}} + \underbrace{\xi L V^2}_{\text{Stokes term}} \\ H = \underbrace{H^*}_{\text{contraction}} + \underbrace{H^{**}}_{\text{"maintenance heat"}} \end{array} \right.$$

Efficiency

Balance of power

$$[\sigma v]_{l_-(t)}^{l_+(t)} = \xi \int_{-L/2}^{L/2} v^2 + \eta \int_{-L/2}^{L/2} (\partial_x v)^2 + \chi \int_{-L/2}^{L/2} c \partial_x v$$

$$\underbrace{-\chi \int_{-L/2}^{L/2} c \partial_x v}_{H^* > 0} = \underbrace{(q_- - q_+) V}_{P_m > 0} + \underbrace{\xi \int_{-L/2}^{L/2} v^2 + \eta \int_{-L/2}^{L/2} (\partial_x v)^2}_{P_d > 0}$$

$$\text{Efficiency } \Lambda = \frac{P}{H} \left\{ \begin{array}{l} P = \cancel{P_m} + \underbrace{\xi L V^2}_{\text{Stokes term}} \\ H = \underbrace{H^*}_{\text{contraction}} + \underbrace{H^{**}}_{\text{"maintenance heat"}} \end{array} \right. \Rightarrow ?$$

Energy consumption (1)

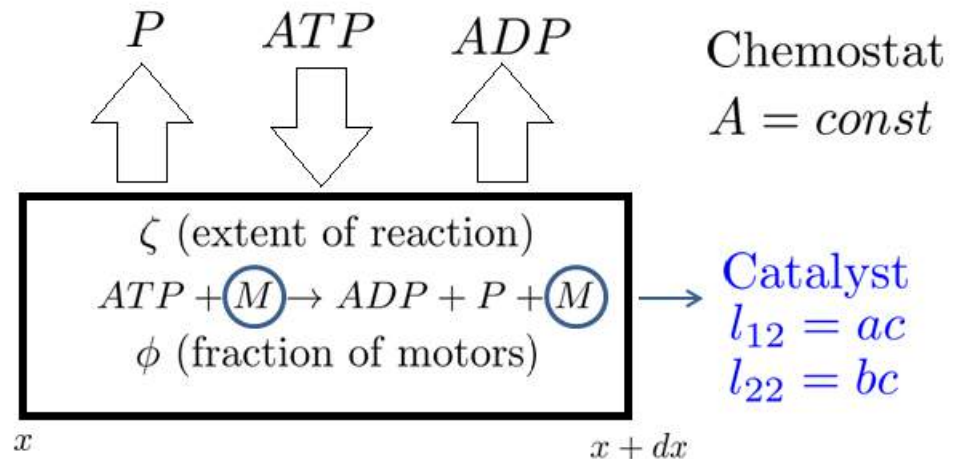
$$\underbrace{R}_{\text{Entropy production}} = \underbrace{W}_{\text{External power}} - \underbrace{\dot{F}}_{\text{Free energy rate change}}$$

$$W = \int_{-L/2}^{L/2} \sigma \partial_x v dx$$

$$\dot{F} = \int_{-L/2}^{L/2} \rho \underbrace{(-A\dot{\zeta} + \mu\dot{\phi})}_{\dot{f}(\zeta, \phi)} dx$$

$A = -\partial_\xi f$ affinity of the reaction

$\mu = \partial_\phi f$ chemical potential



$$R = \int_{-L/2}^{L/2} (\sigma \partial_x v + \rho \dot{\zeta} A + J \partial_x \mu) dx \geq 0$$

$$\begin{aligned} \sigma &= l_{11} \partial_x v + l_{12} A \\ \hat{\rho} \dot{\zeta} &= l_{21} \partial_x v + l_{22} A \\ J &= l_{33} \partial_x \mu \end{aligned}$$

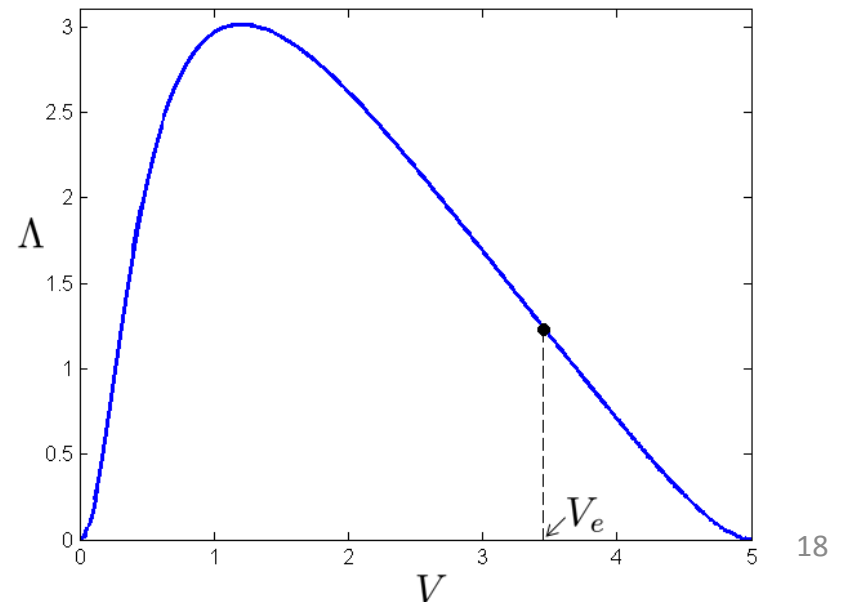
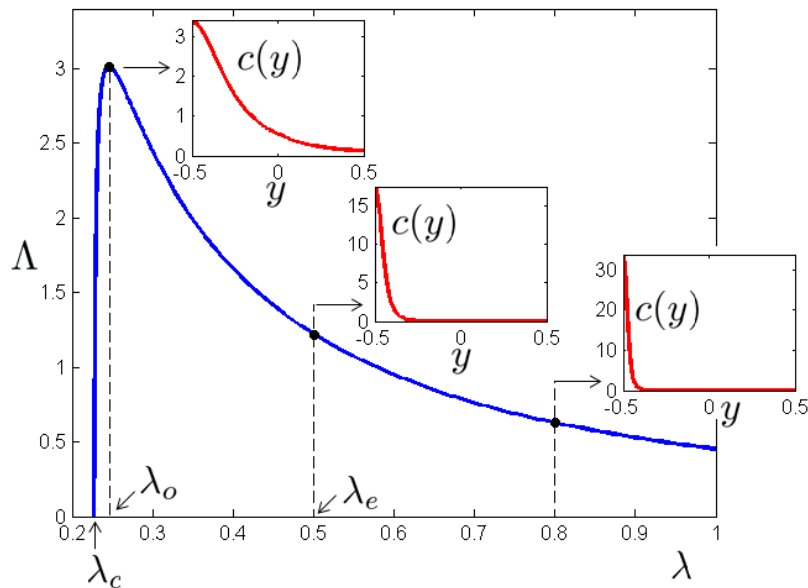
Energy consumption (2)

Efficiency $\Lambda = \frac{P}{H}$

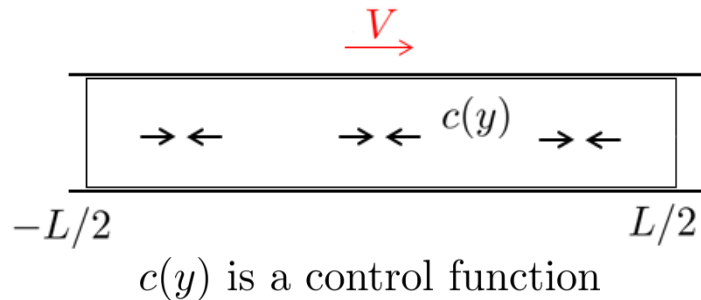
$$H = -\dot{F} = H^* + H^{**}$$

$$H^* = -\chi \int_{-L/2}^{L/2} c \partial_y v = \xi \int_{-L/2}^{L/2} v^2 dx + \eta \int_{-L/2}^{L/2} (\partial_x v)^2 dx \geq 0$$

$$H^{**} = bA^2 \int_{-L/2}^{L/2} c dx + D \frac{k_B T}{c_0} \int_{-L/2}^{L/2} (\partial_x c)^2 dx \geq 0$$

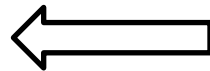


Optimization of efficiency



$$\begin{cases} -\mathcal{L}^{-2} \partial_y (\partial_y \sigma) + \sigma = c \\ \sigma(-1/2) = \sigma(1/2) \\ \partial_y \sigma(-1/2) = \partial_y \sigma(1/2) \end{cases}$$

$$\Lambda = \frac{\mathcal{L} V^2}{\underbrace{-\mathcal{L}^{-1} \int_{-1/2}^{1/2} c \partial_{yy} \sigma + \mathcal{H}^{**}}_{\mathcal{H}^*}}$$



$$V = \frac{\mathcal{L}}{2} (\partial_y \sigma(-1/2) + \partial_y \sigma(1/2))$$

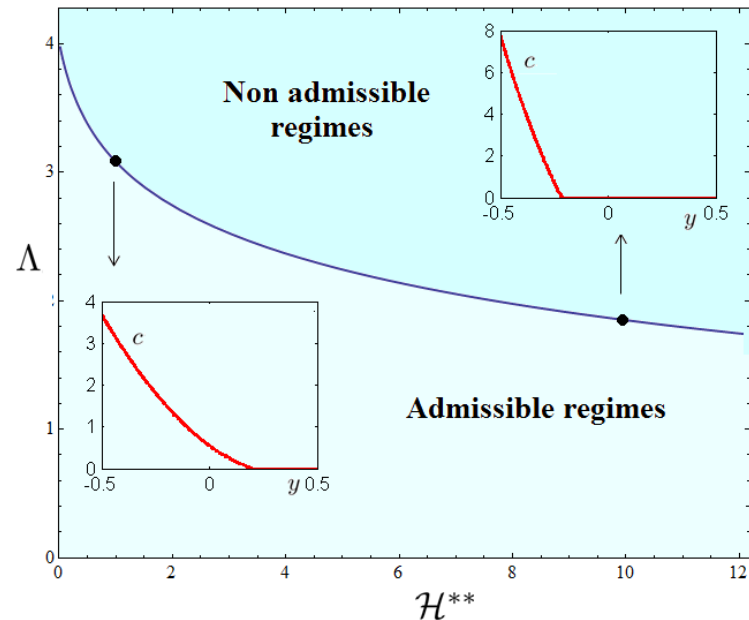
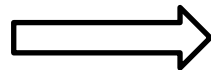
Numerator maximized by fully localized $c(y) = \delta(y + 1/2)$.
Denominator minimized by homogeneous $c(y) = 1$.



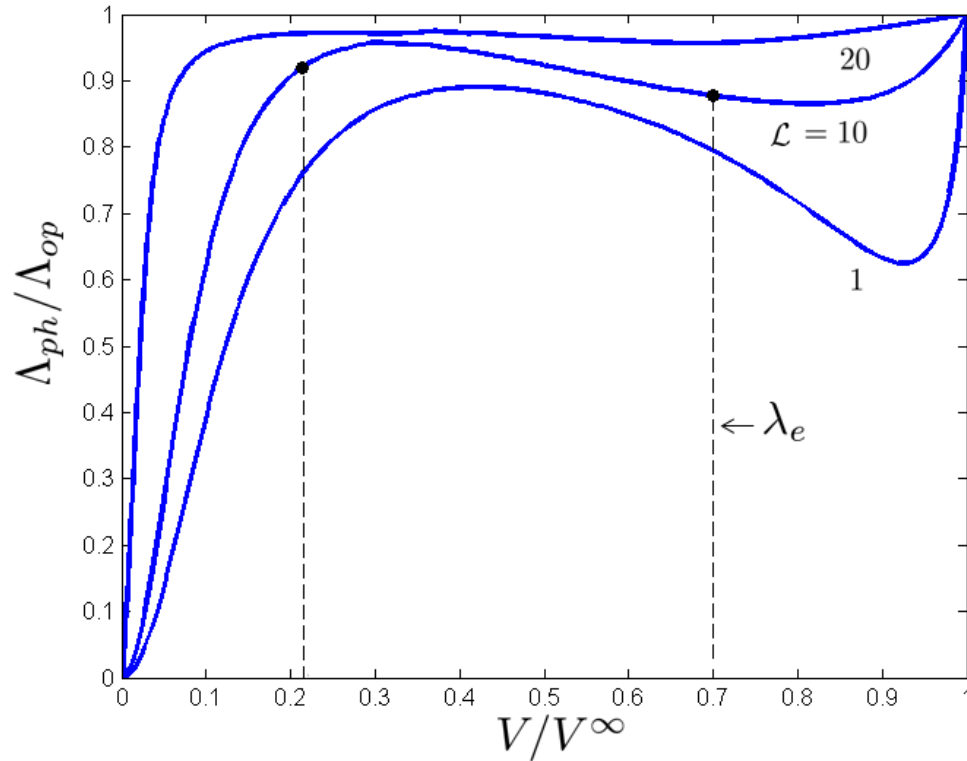
Optimization problem:

$$\begin{cases} \max_{c \in \mathcal{D}([-1/2, 1/2])} \Lambda(c) \\ \int_{-1/2}^{1/2} c(y) dy = 1 \\ c \geq 0 \end{cases}$$

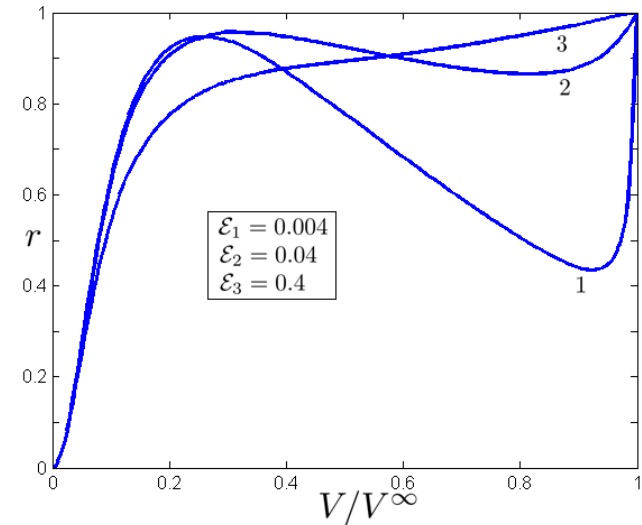
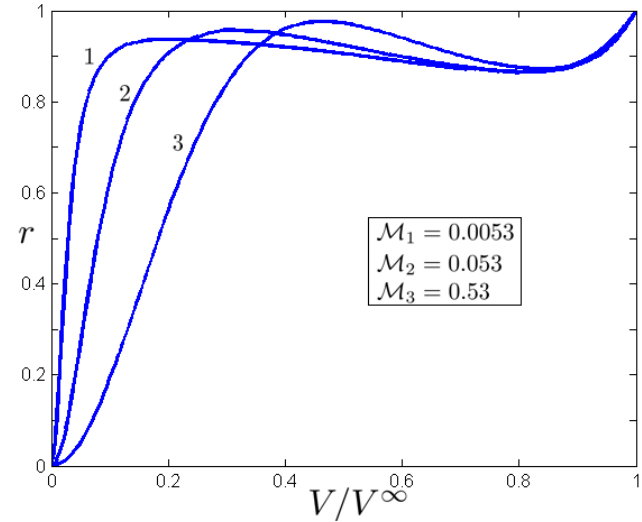
Solution:



Comparison



Robustness



Conclusions

We have shown that active contractility can generate both spontaneous polarization and steady translocation of a cell. The morphological instability is due to internal motion of the cytoskeleton which is generated by **active cross-linkers** and simultaneously transports them. The motility initiation pattern is similar to the one observed in experiments on **keratocytes fragments**. In this way myosin motors use passive actin network as a medium through which they interact and **self-organize** in a fashion that is remarkably close to the **optimal** one.

Recho P., Putlelat T., Truskinovsky L., (2013), PRL

Recho P., Joanny J.-F., Truskinovsky L., (2014), PRL

Hydrodynamic Instabilities in Tissues and Active Gels

T Risler

M Basan, P Loyer, J-F Joanny & J Prost

Epithelia and carcinomas

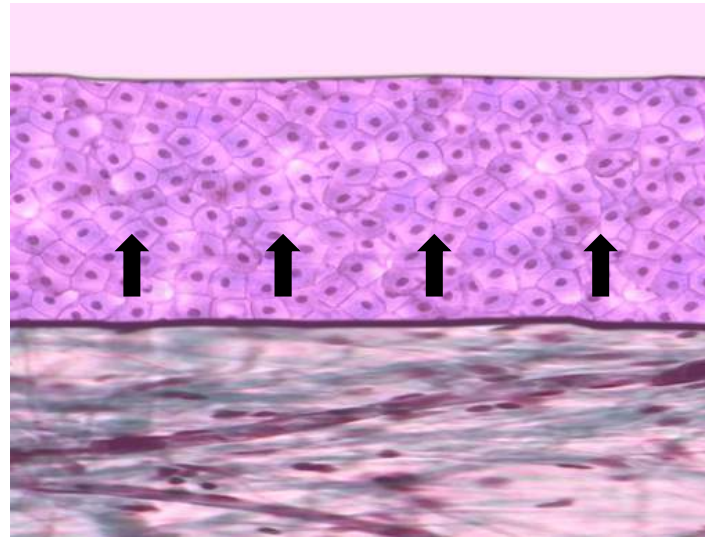
Epithelium is one of the four basic types of animal tissue:
connective ; muscle ; nervous ; epithelial

Over 80% of human tumors originate from epithelia

Multilayered, stratified epithelium

Free surface

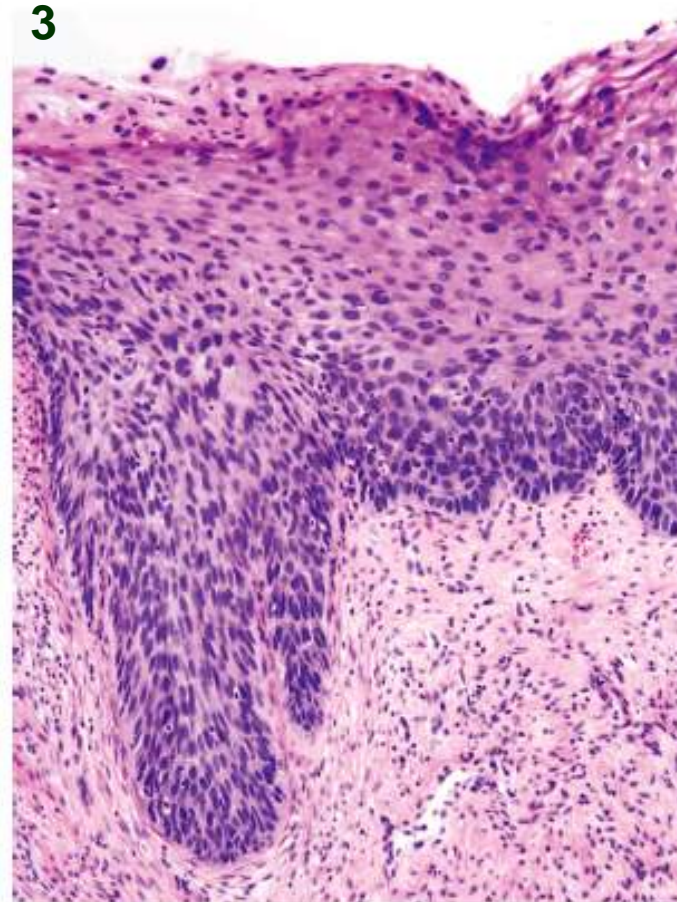
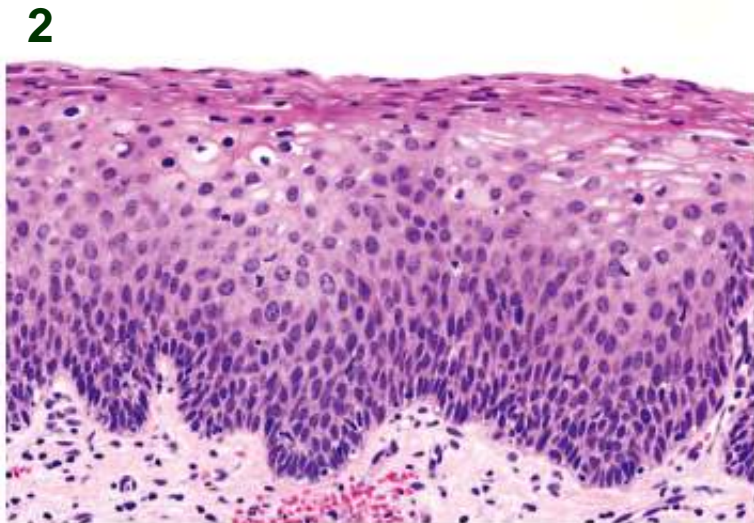
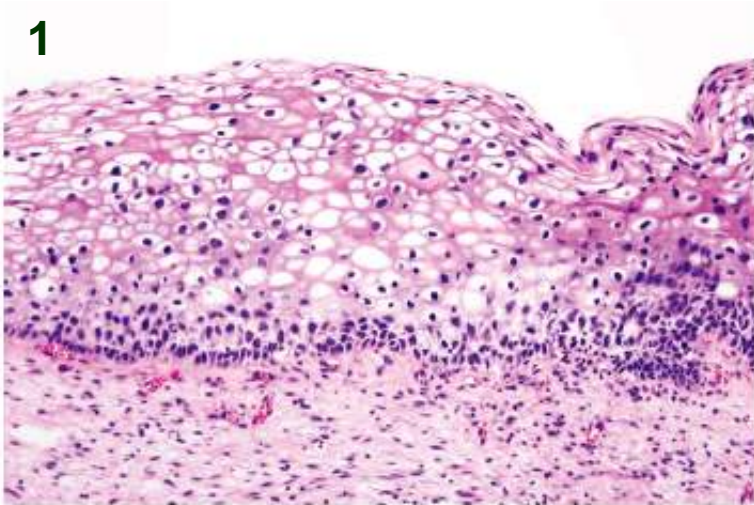
Basement
membrane



Epithelium

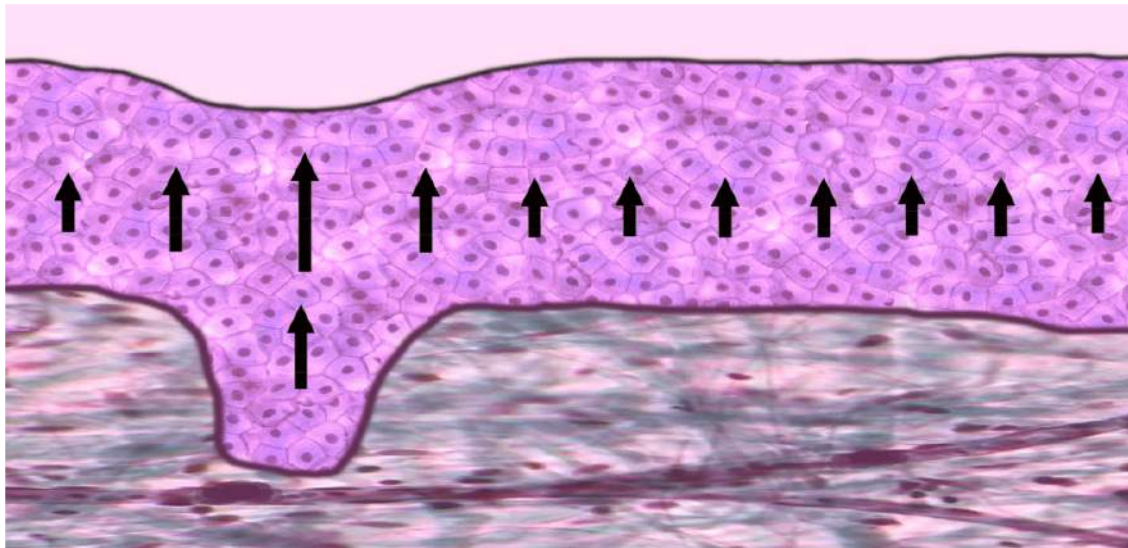
Connective
tissue

Epithelial undulations



http://en.wikipedia.org/wiki/Cervical_dysplasia

Epithelial instability

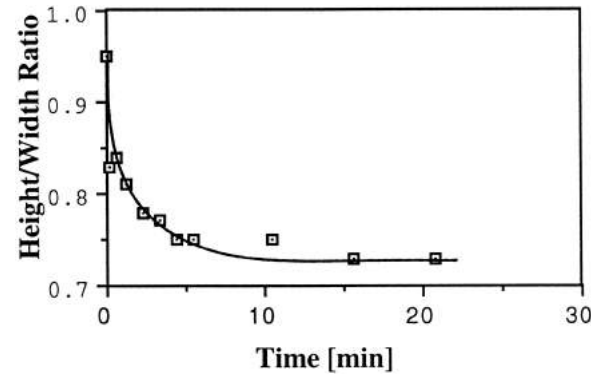
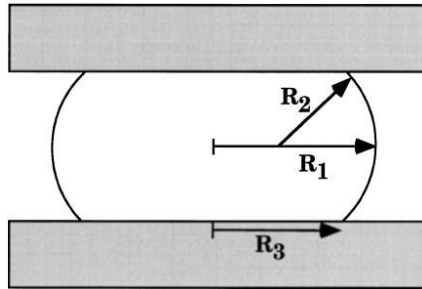


Epithelium

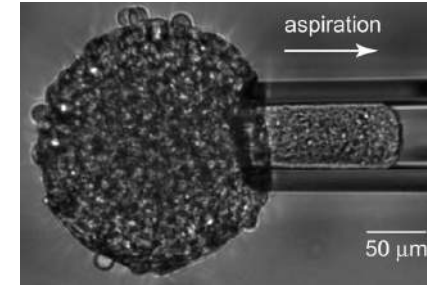
Stroma

Basan *et al.*, *PRL* (2011)

Relaxation time and rheology



Foty *et al.*, *Development* (1996)
 Forgacs *et al.*, *Biophys. J.* (1998)



Guevorkian *et al.*,
Phys. Rev. Lett. (2010)

Elastic modulus

$$E \simeq 10^2 - 10^4 \text{ Pa}$$

Viscosity

$$\eta \simeq 10^3 - 10^5 \text{ Pa} \cdot \text{s}$$

Relaxation time

$$\tau \simeq 10 \text{ s} - 10 \text{ mn}$$

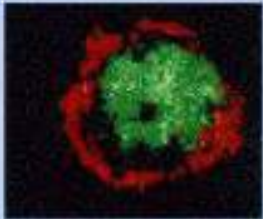
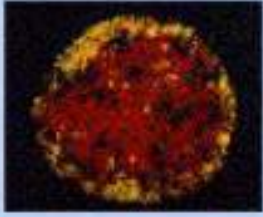
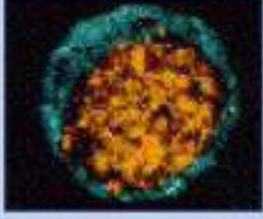
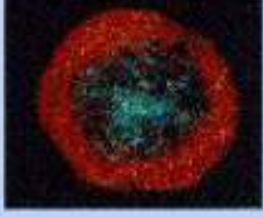
$$\tau \simeq \text{hours}$$

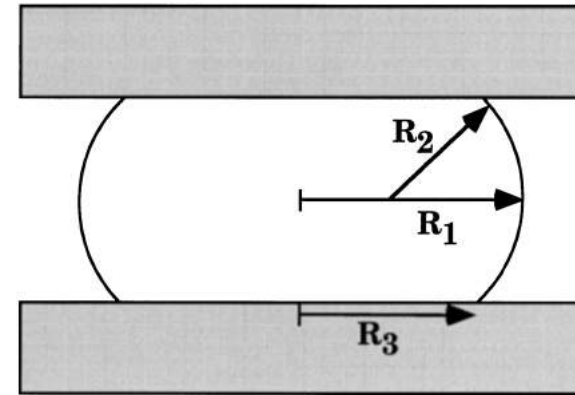
Marmottant *et al.*,
PNAS (2009)

Soft-matter models for tissues

Gonzalez-Rodriguez *et al.*,
Science (2012)

Surface tension

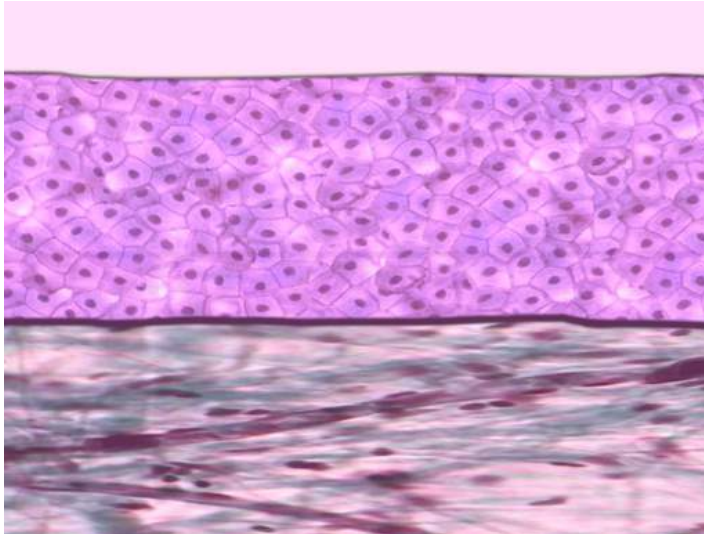
TISSUE	SURFACE TENSION (dynes/cm)	EQUILIBRIUM CONFIGURATION
Limb bud (green)	20.1	
Pigment Epithelium (red)	12.6	
Heart (yellow)	8.5	
Liver (blue)	4.6	
Neural retina (orange)	1.6	



$$\frac{F_{eq}}{\pi R_3^2} = \gamma \left(\frac{1}{R_1} + \frac{1}{R_2} \right)$$

Foty *et al.*, *Development* (1996)

Constitutive equations



Epithelium:

Viscous medium with source term

$$\partial_{\alpha} v_{\alpha} = k_d - k_a$$

$$\partial_{\alpha} \sigma_{\alpha\beta} = 0$$

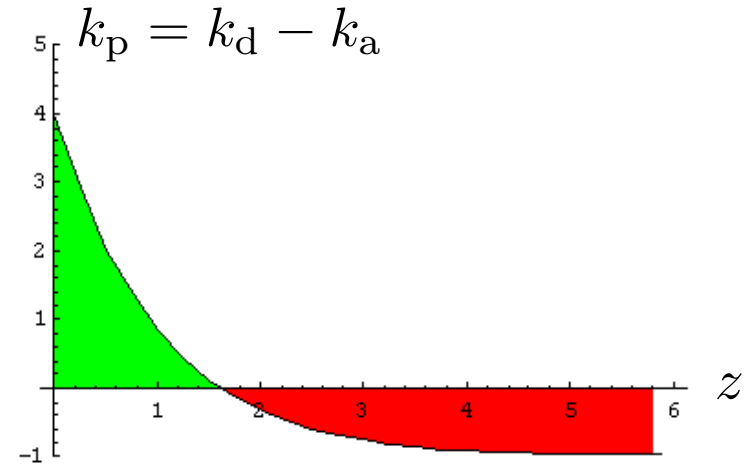
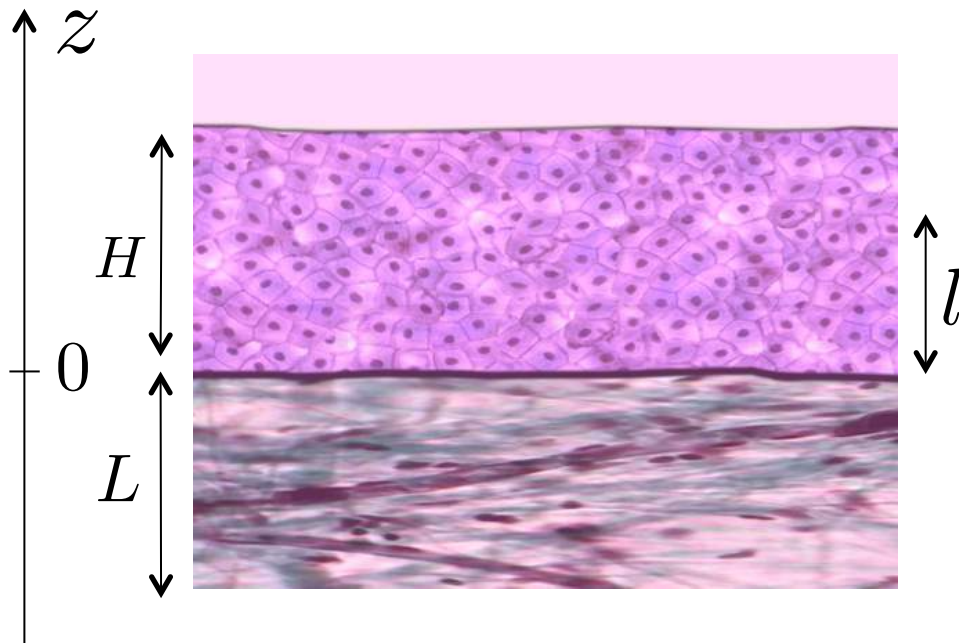
$$\sigma_{\alpha\beta} + P\delta_{\alpha\beta} = \eta (\partial_{\alpha} v_{\beta} + \partial_{\beta} v_{\alpha})$$

Supporting tissue: Passive viscoelastic medium

$$\partial_{\alpha} v_{\alpha}^s = 0 \quad \partial_{\alpha} \sigma_{\alpha\beta}^s = 0$$

$$(\tau \partial_t + 1) (\sigma_{\alpha\beta}^s + P^s \delta_{\alpha\beta}) = \eta^s (\partial_{\alpha} v_{\beta}^s + \partial_{\beta} v_{\alpha}^s)$$

Epithelial source term



$$k_p = k_d - k_a$$

$$k_p = k \exp(-z/l) - k_0$$

$$v_z^0|_{z=H} = \int_0^H k_p(z) dz = 0$$

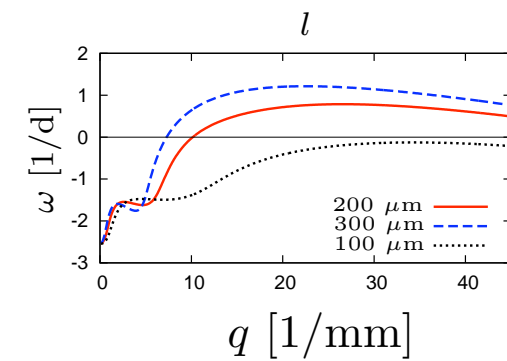
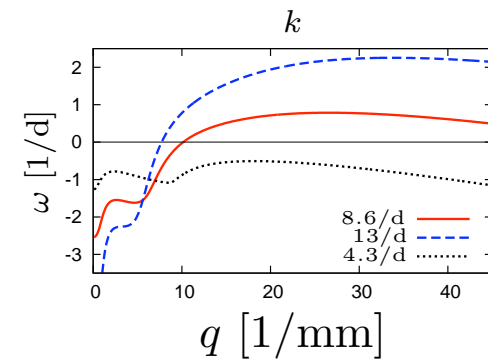
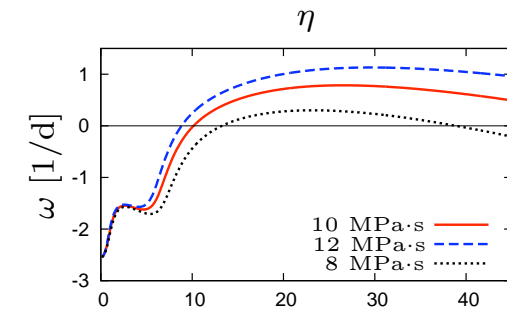
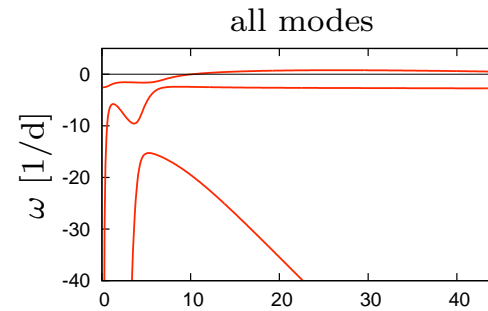
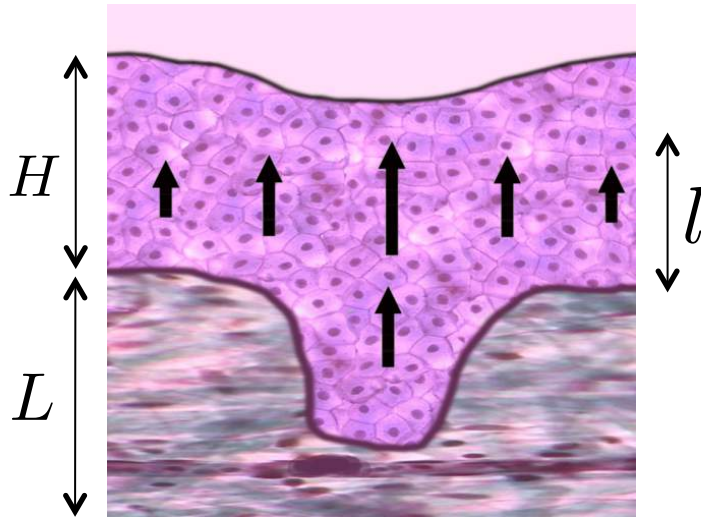
Boundary conditions

Apical surface of the epithelium $\sigma_{nt} = 0$ $\sigma_{nn} = \gamma_a \delta H''$

Interface $\sigma_{nn}^s = \sigma_{nn} + \gamma_i \delta h''$ $\sigma_{nt}^s = \sigma_{nt} = \xi(v_t - v_t^s)$

Bottom $v_\alpha^s = 0$

Elastic stroma



Basan *et al.*, *PRL* (2011)

Epithelium viscosity

η

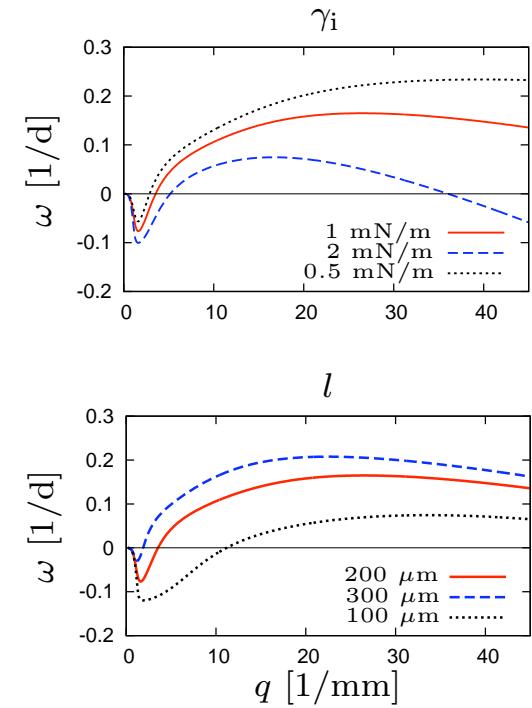
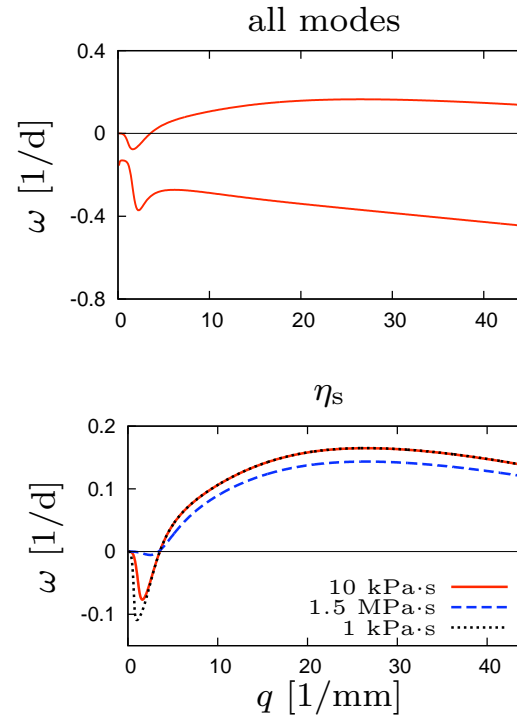
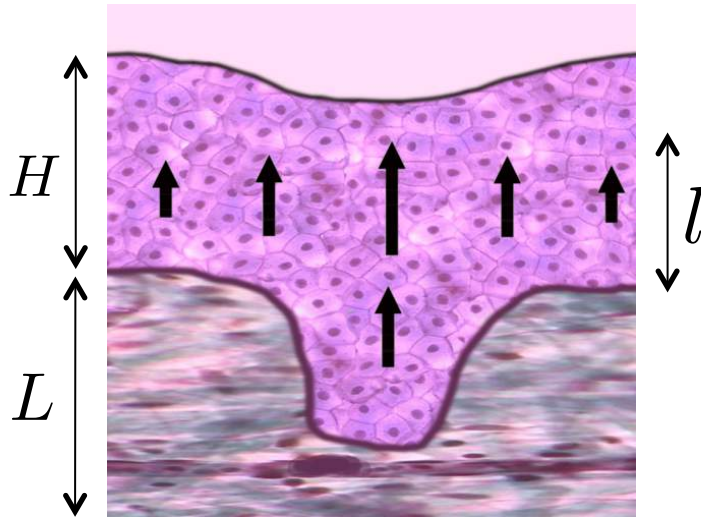
Rate of cell division

k

Thickness of dividing region

l

Viscous stroma



Basan *et al.*, *PRL* (2011)

Interfacial tension

γ_i

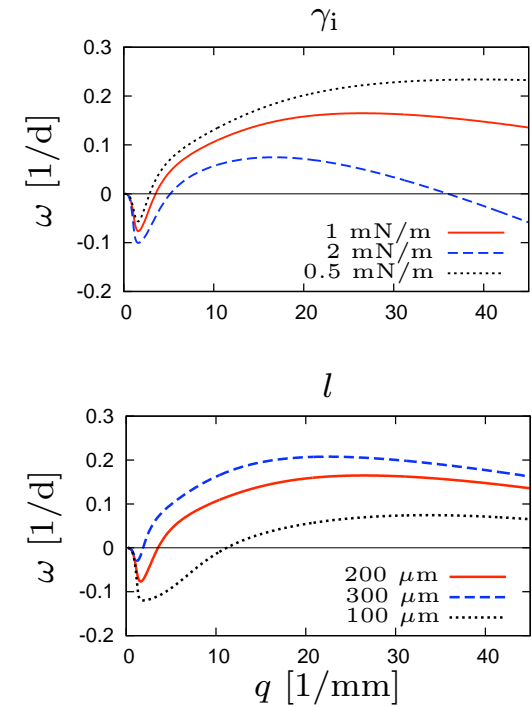
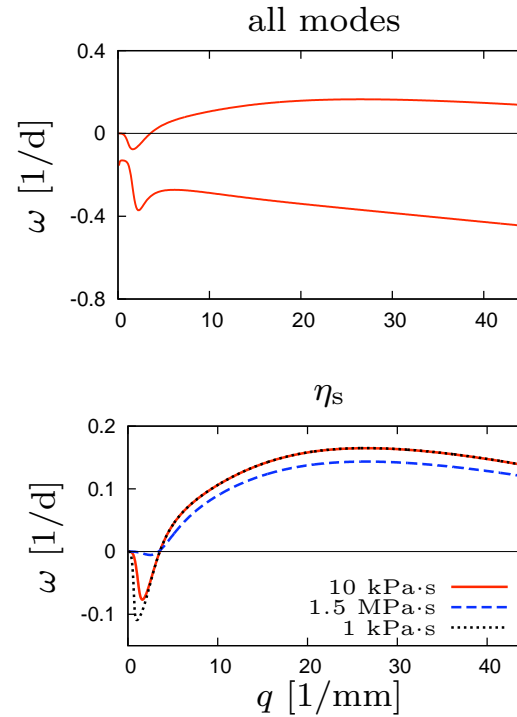
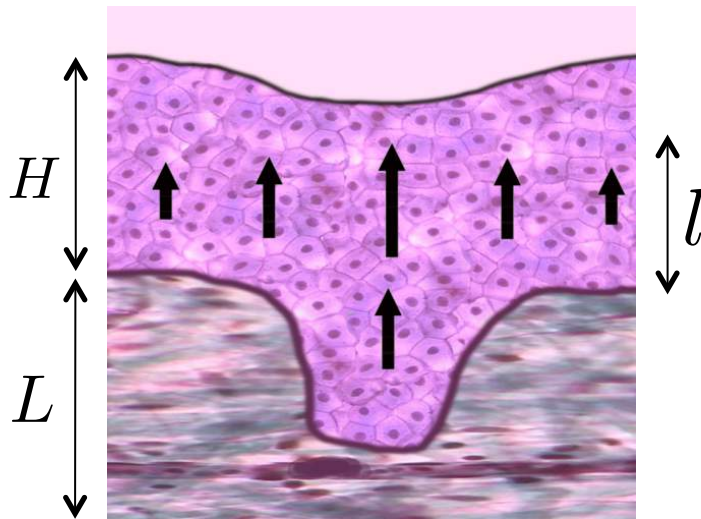
Stroma viscosity

η_s

Thickness of dividing region

l

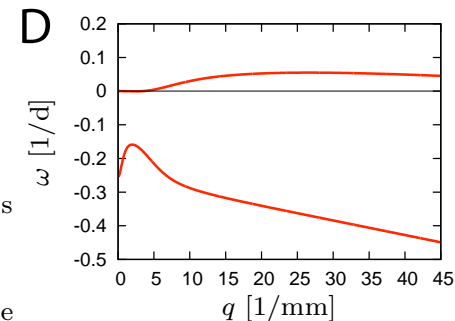
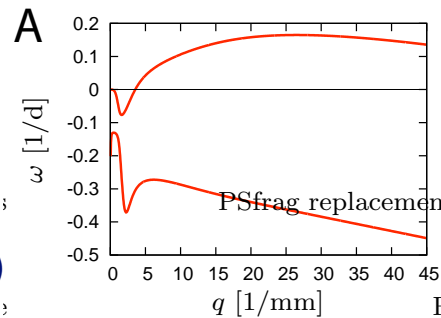
Viscous stroma



Relative viscosities $\eta = 10 \text{ MPa} \cdot \text{s}$

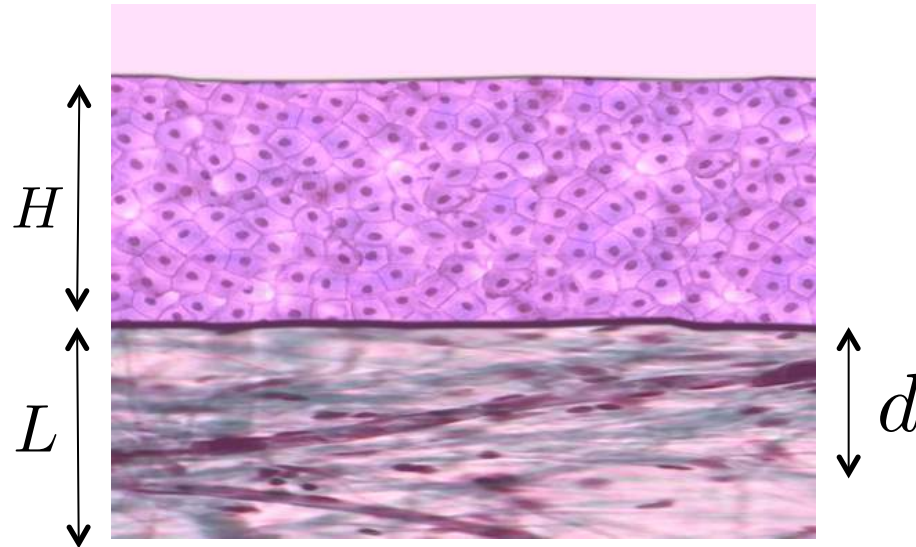
$\eta_s = 10 \text{ kPa} \cdot \text{s}$

Risler and Basan,
New J. Phys. (2013)



$\eta_s = 20 \text{ MPa} \cdot \text{s}$

Coupling to nutrient diffusion

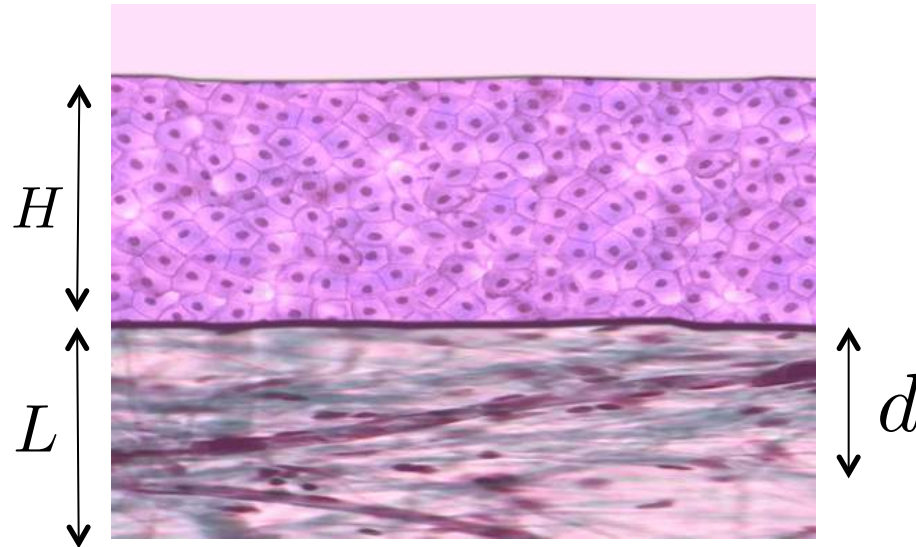


$$k_d - k_a = \kappa_1 \rho - \kappa_0$$

$$\partial_t \rho = D \nabla^2 \rho - c \rho$$

$$\partial_t \rho^s = D^s \nabla^2 \rho^s$$

Coupling to nutrient diffusion



$$k_d - k_a = \kappa_1 \rho - \kappa_0$$

$$\partial_t \rho = D \nabla^2 \rho - c \rho$$

$$\partial_t \rho^s = D^s \nabla^2 \rho^s$$

Boundary conditions

Distance d from the interface

$$\rho^s = \bar{\rho}_0$$

Apical surface of the epithelium

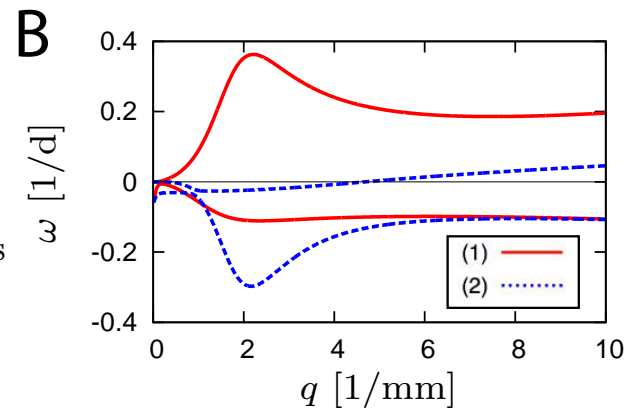
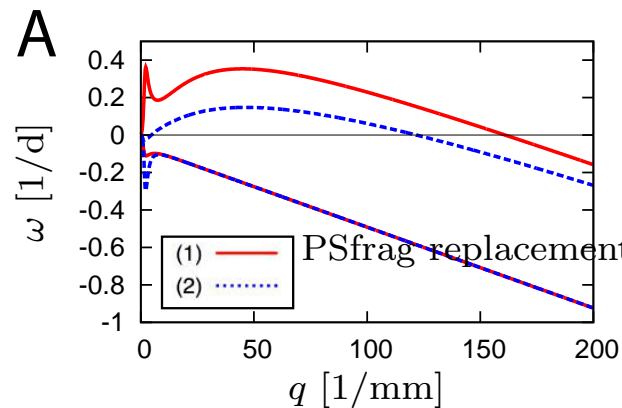
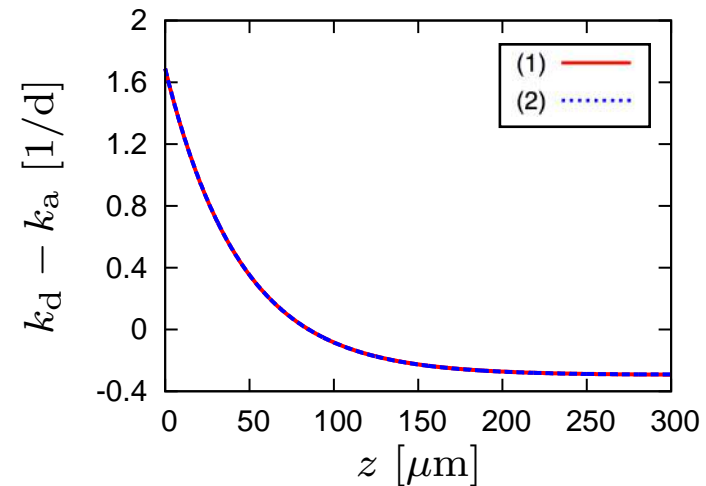
$$-D \partial_{\perp} \rho = k_{\text{off}} \rho$$

Comparison of the two models

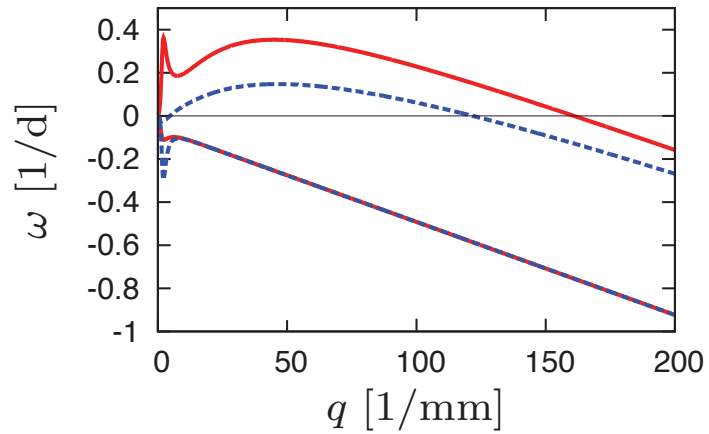
Fit the cell-production function

$$(1) \quad k_d - k_a = \kappa_1 \rho - \kappa_0$$
$$\partial_t \rho = D \nabla^2 \rho - c \rho$$
$$\partial_t \rho^s = D^s \nabla^2 \rho^s$$

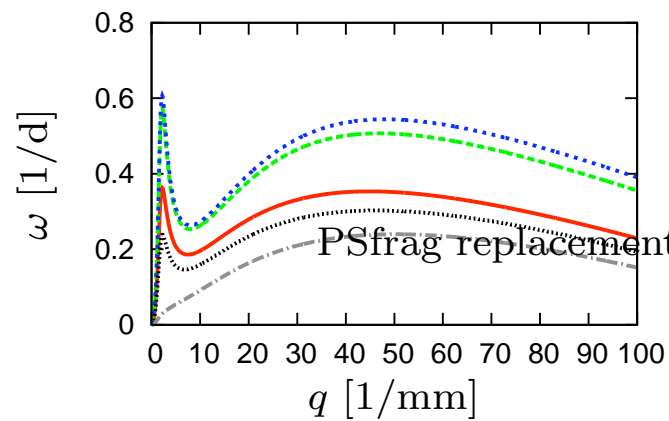
$$(2) \quad k_d - k_a = k \exp(-z/l) - k_0$$



Mullins-Sekerka-type peak



www.its.caltech.edu/~atomic/snowcrystals



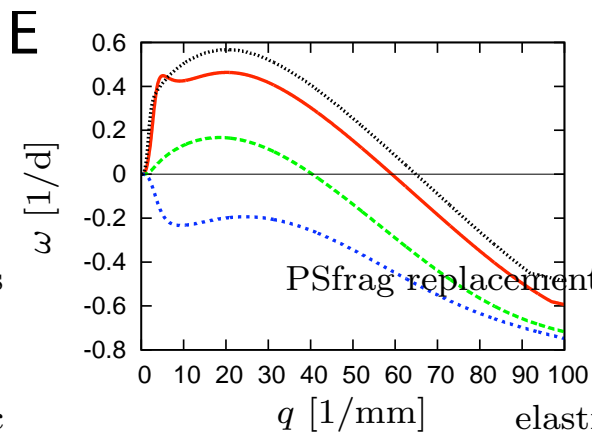
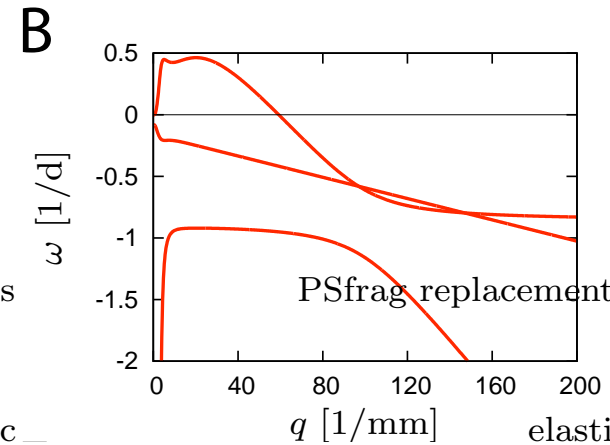
— · — · —	$D^s = 2 \cdot 10^{-11} \text{ m}^2 \cdot \text{s}^{-1}$
—	$D^s = 2 \cdot 10^{-10} \text{ m}^2 \cdot \text{s}^{-1}$
- · - · -	$D^s = 2 \cdot 10^{-9} \text{ m}^2 \cdot \text{s}^{-1}$

Risler and Basan, *New J. Phys.* (2013)

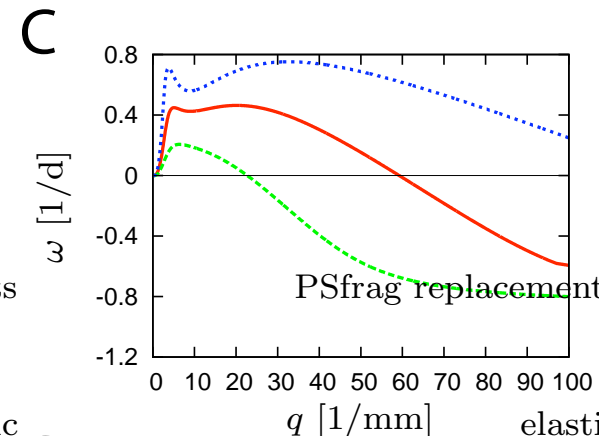
Viscoelastic stroma

Epithelium thickness $H = 300 \mu\text{m}$

Epithelium viscosity $\eta = 10 \text{ MPa} \cdot \text{s}$

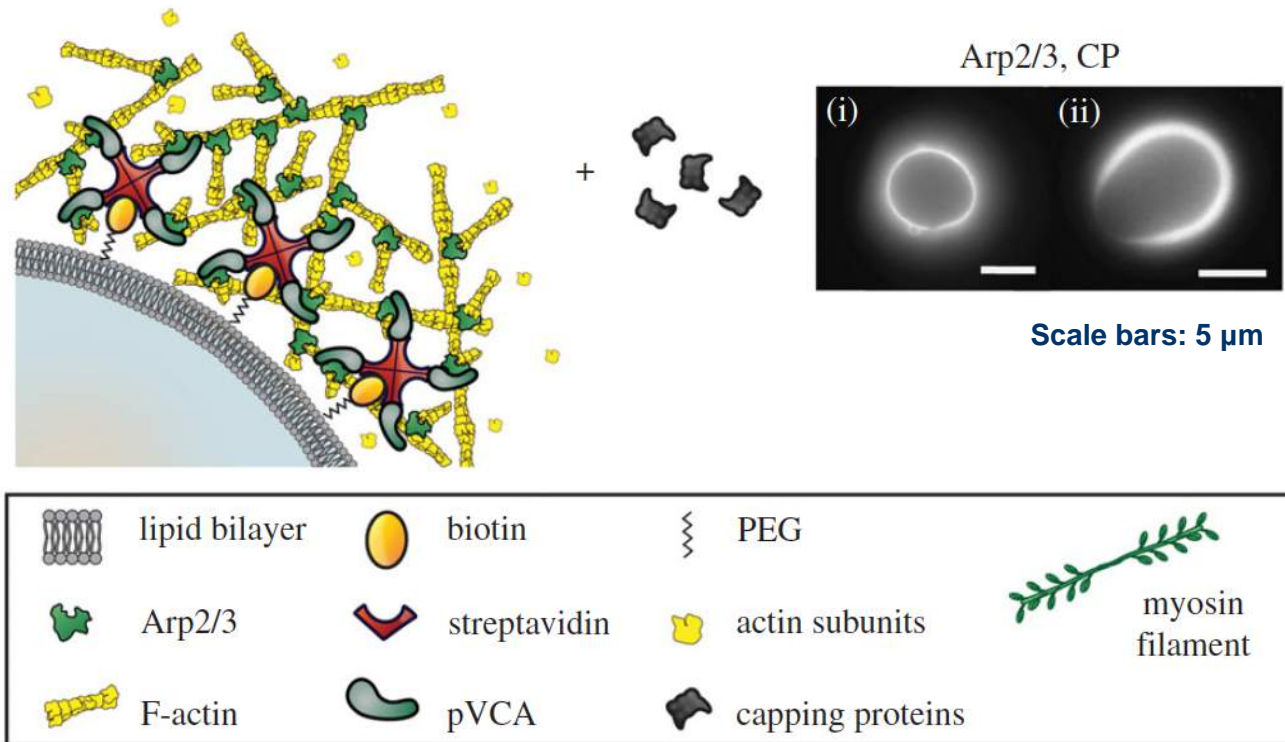


- $H = 100 \mu\text{m}$
- - $H = 50 \mu\text{m}$
- · $H = 900 \mu\text{m}$



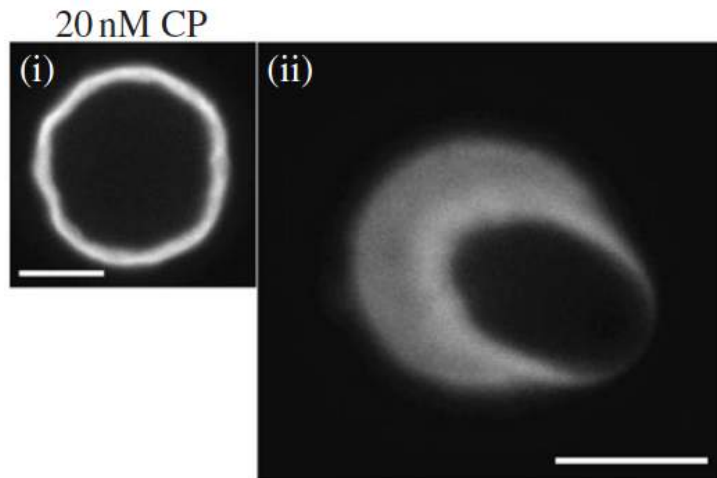
- $\eta = 5 \text{ MPa} \cdot \text{s}$
- - $\eta = 20 \text{ MPa} \cdot \text{s}$

Reconstituted membrane-cortex interaction

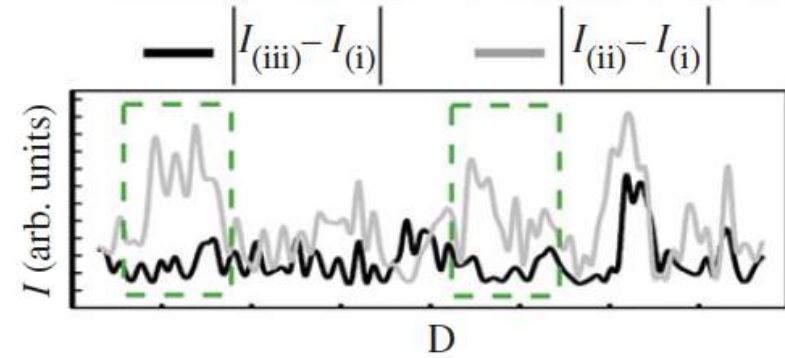
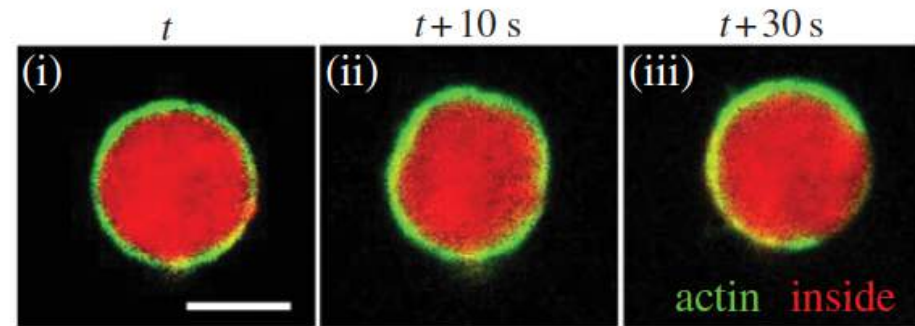


Carvalho *et al.*, *Phyl Trans R Soc B* (2013)

Membrane-cortex shape fluctuations



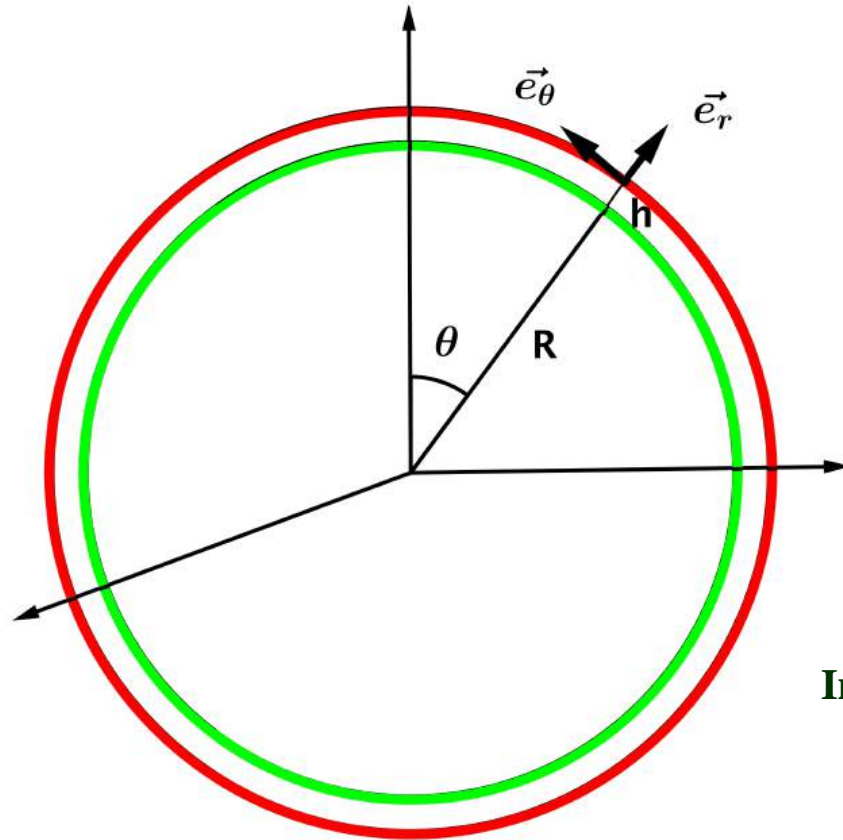
Scale bars: 10 μm



Scale bar: 5 μm

Carvalho *et al.*, *Phyl Trans R Soc B* (2013)

Model for membrane-cortex shape fluctuations



Liposome of radius R
Gel of thickness h

Cortex bulk equations

$$\partial_\alpha v_\alpha = 0$$

$$\partial_\alpha \sigma_{\alpha\beta} = 0$$

$$\sigma_{\alpha\beta} + P\delta_{\alpha\beta} = \eta (\partial_\alpha v_\beta + \partial_\beta v_\alpha)$$

Boundary conditions

Inner surface $v_n = v_p$

$$\sigma_{nt} = 0$$

$$\sigma_{nn} = -p_{lip} + \gamma C$$

Outer surface $\sigma_{nt} = \sigma_{nn} = 0$

Regulation of the gel thickness

Tension favors depolymerization

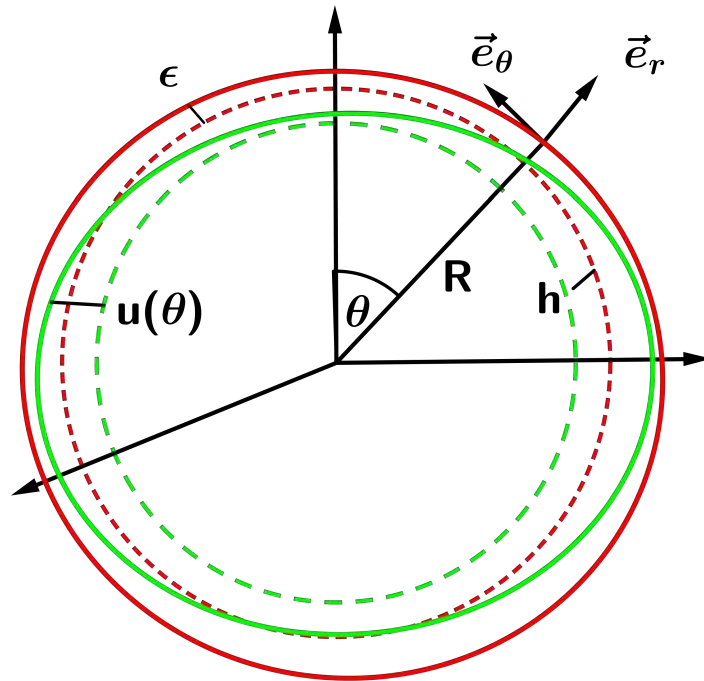
Kramers

$$r = r_0 \exp\left(\frac{Fd}{k_B T}\right)$$
$$F = \sigma_{\text{tang}} \xi^2$$
$$d = a/2$$
$$v_d = v_d^0 \exp\left(\frac{\sigma_{\text{tang}}}{\sigma_0}\right)$$
$$\sigma_0 = \frac{2k_B T}{\xi^2 a}$$

$$\frac{dh}{dt} = v_n(R + h) - v_d = 0$$

$$\frac{h}{R} = \frac{12\eta v_p - \sigma_0 R \ln(v_p/v_d^0)}{36\eta v_p - 2\sigma_0 R}$$

Model for membrane-cortex shape fluctuations



----- Unperturbed
——— Perturbed

Axisymmetric first-order expansion

$$\mathbf{v} = v_r(r, \theta) \mathbf{e}_r + \mathbf{v}_\theta(\mathbf{r}, \theta) \mathbf{e}_\theta$$

$$R + u(\theta)$$

$$h + \epsilon(\theta)$$

$$\epsilon \sim u \ll h \ll R$$

Unstable modes

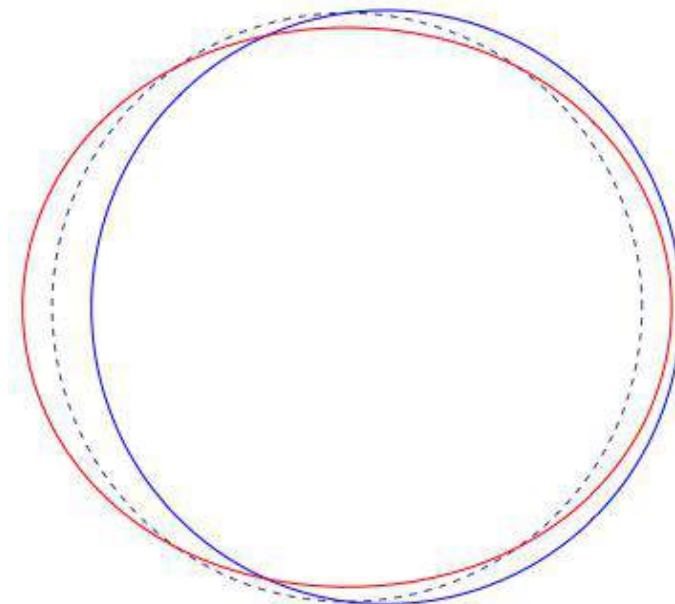
Mode n=0

Volume conservation : stable

Mode n=1

With $R = 5 \mu\text{m}$; $h = 0.5 \mu\text{m}$

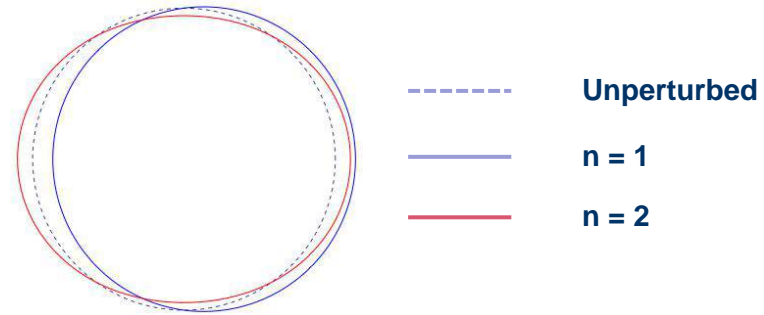
Unstable if $\frac{v_p}{v_d^0} \gtrsim 2$



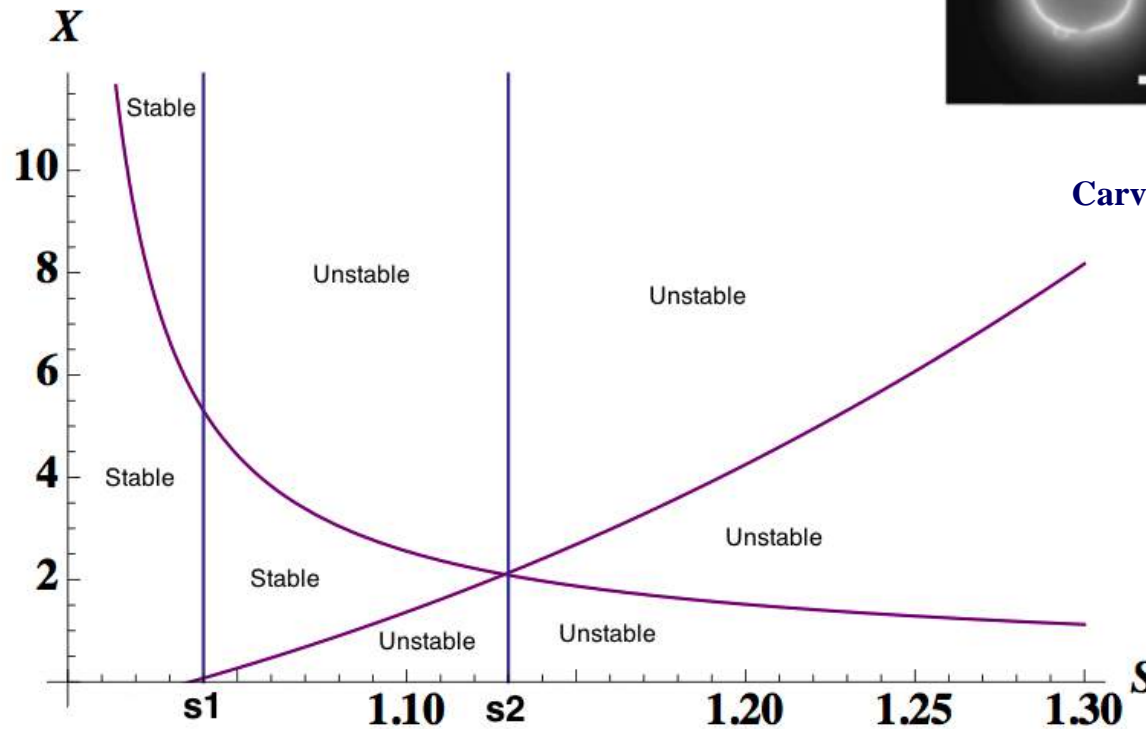
- Unperturbed
- n = 1
- n = 2

Unstable mode n=2

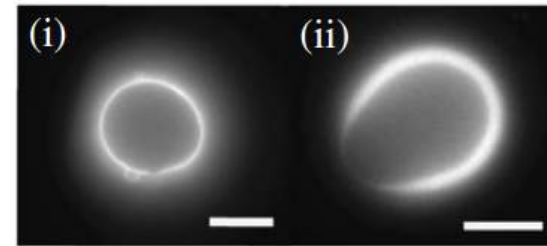
$R = 5 \mu\text{m}$; $h = 0.5 \mu\text{m}$



$$S = \frac{v_p}{v_d^0} \quad X = \frac{\gamma}{\eta v_d^0}$$



Arp2/3, CP



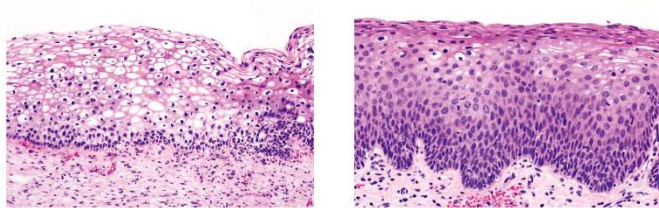
Scale bars: 5 μm

Carvalho *et al.* 2013

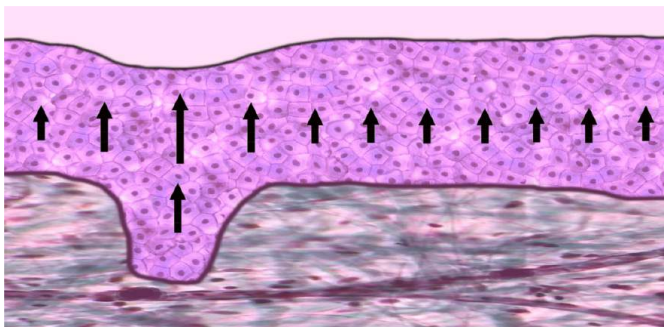
$$s_1 \approx 1.04$$

$$s_2 \approx 1.13$$

Epithelial undulations

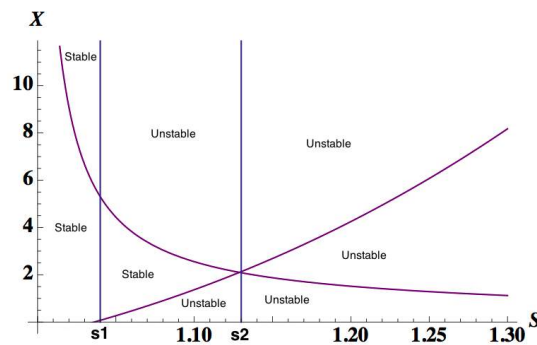
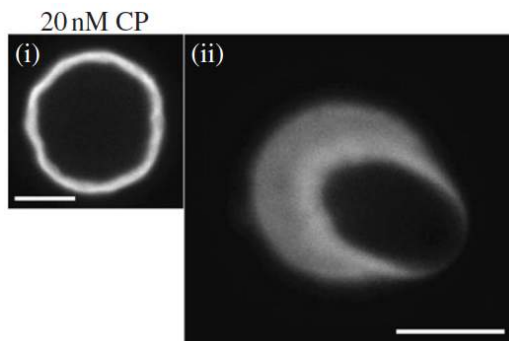


M. Basan
J.-F. Joanny
J. Prost



Basan *et al.*, *PRL* (2011)
Risler and Basan, *New J. Phys.* (2013)

Instability of polymerizing actin gels



P. Loyer

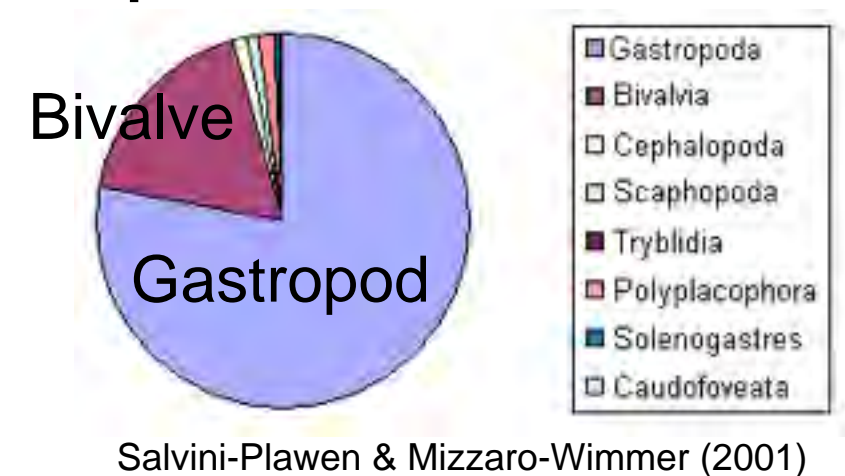
Simulation study of crawling locomotion in gastropod

Daishin Ueyama (Meiji Univ.)
Mayuko Iwamoto (Meiji Univ.)
Ryo Kobayashi (Hiroshima Univ.)

The Advantage of Mucus for Adhesive Locomotion in Gastropods,
Mayuko Iwamoto, Daishin Ueyama, and Ryo Kobayashi,
Journal of Theoretical Biology 353(21)(2014), pp. 133-141.

Gastropods

- belong to Phylum Mollusca, Class Gastropoda.
- are generally called “spiral shell”.
- have the largest number of species among mollusks(軟体動物).
- secrete mucus(粘液) to adjust humidity and salinity.



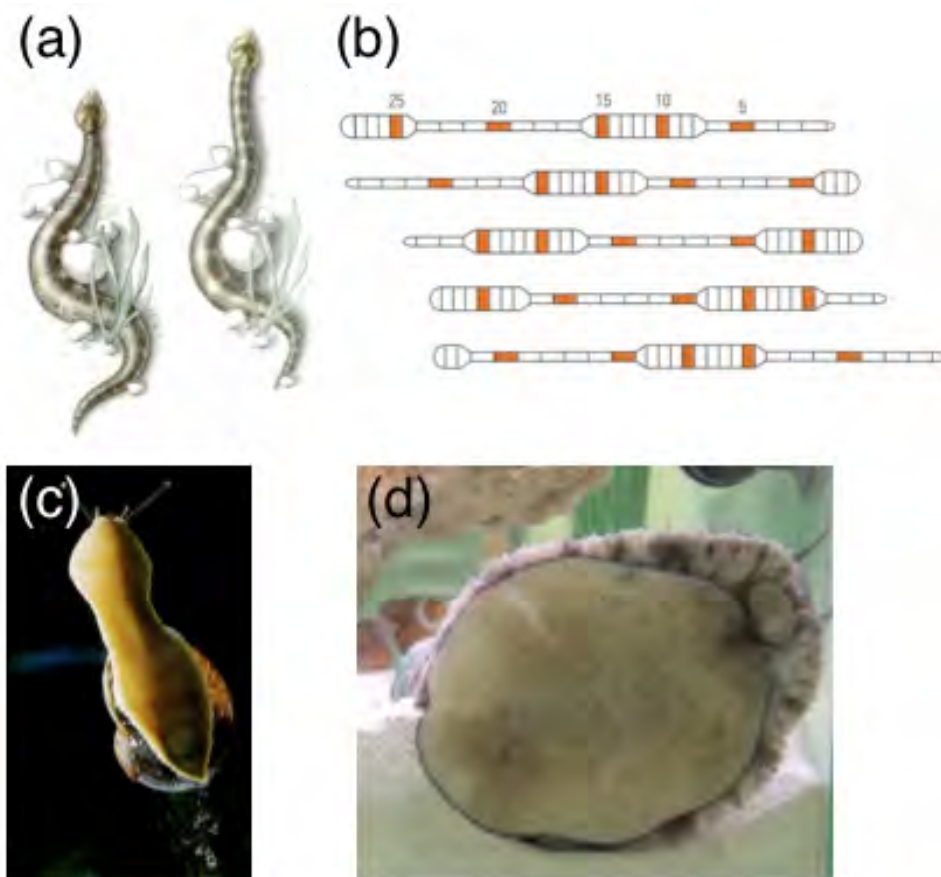
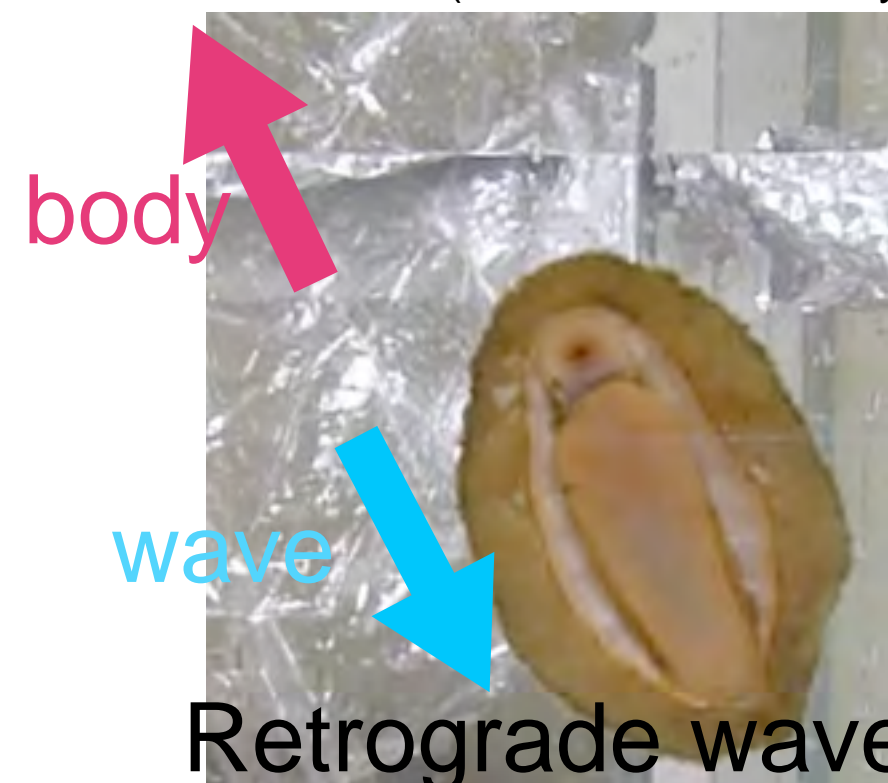
Many gastropods move by adhesive locomotion.

How they walk?

Snail from YouTube
“Gliding Snails On Glass Plate”

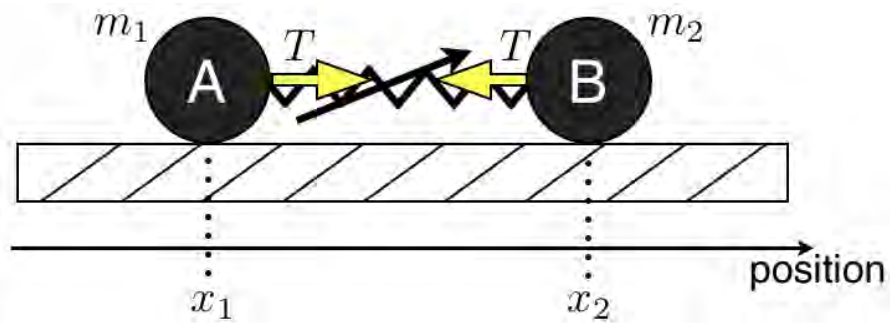


Chiton by Dr. Toshiya Kazama
(Hiroshima University)



Animals that move by crawling, (a) snake, (b) earthworm, and (c) snail [Alexander, 1992b], respectively. (d) Abalone [Iwamoto, 2011].

Importance of Friction Control



Simplest model of spring-mass system.

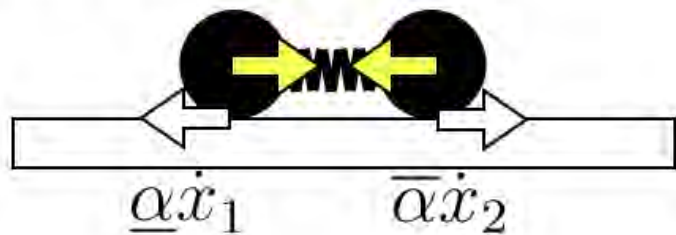
$$m_1 \ddot{x}_1 = T - \alpha_1 \dot{x}_1,$$

$$m_2 \ddot{x}_2 = -T - \alpha_2 \dot{x}_2,$$

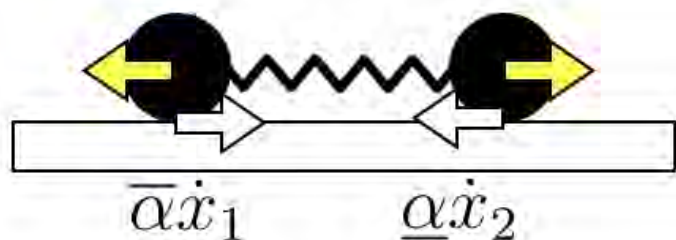
Friction control

$$0 < \underline{\alpha} < \bar{\alpha}$$

(a) Contracting mode

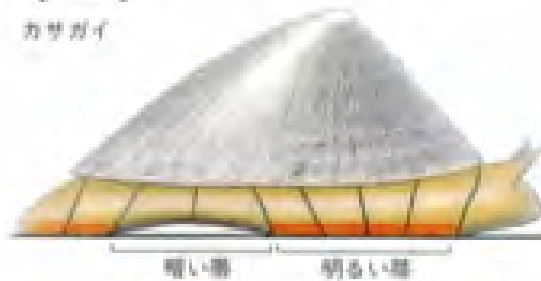


(b) Expanding mode



How to control?

(a)



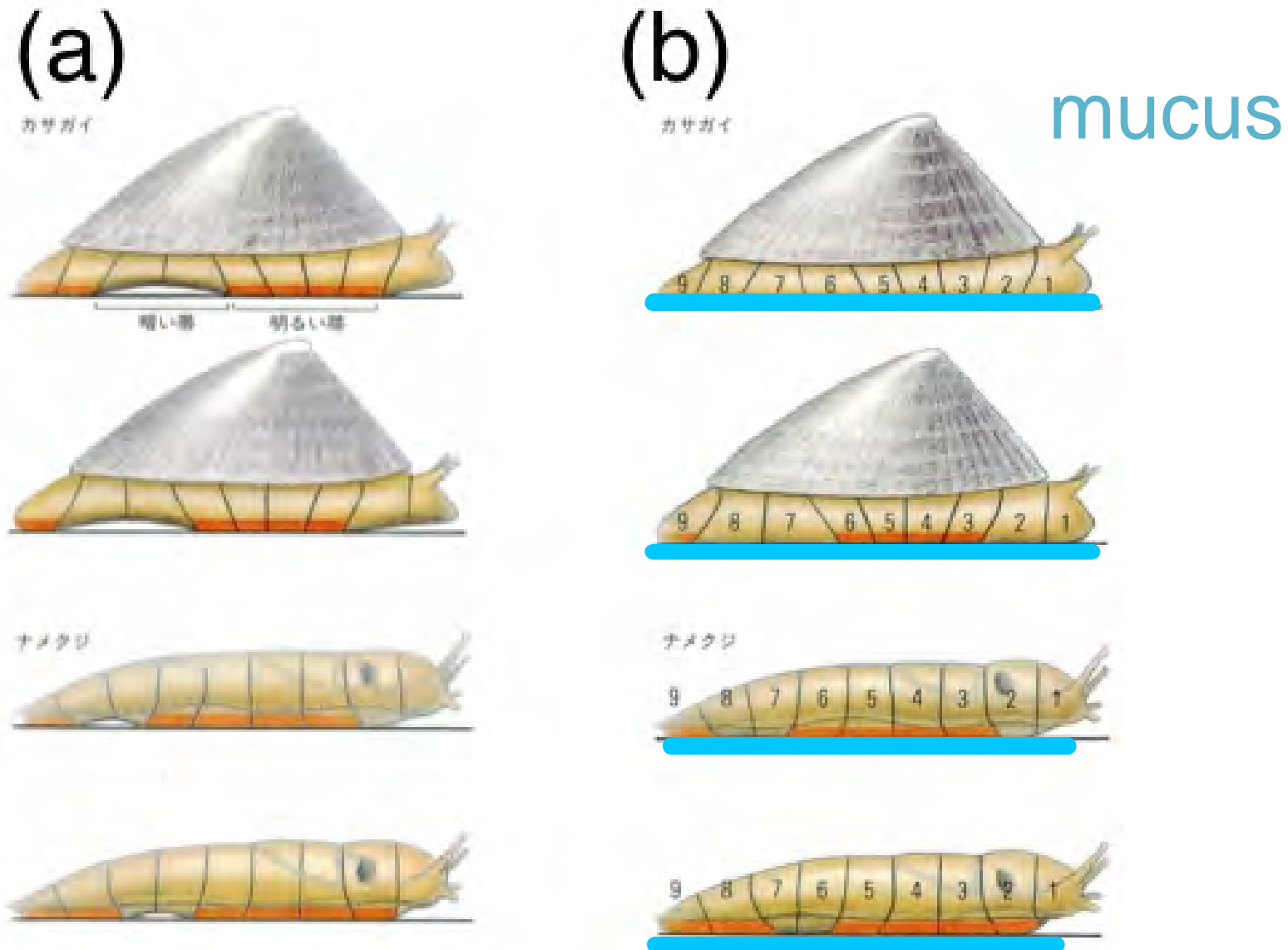
(b)



Images of muscular contraction and elongation, and control of interfacial friction [Alexander, 1992b].

How to generate propulsive force?

How they control friction against the ground?



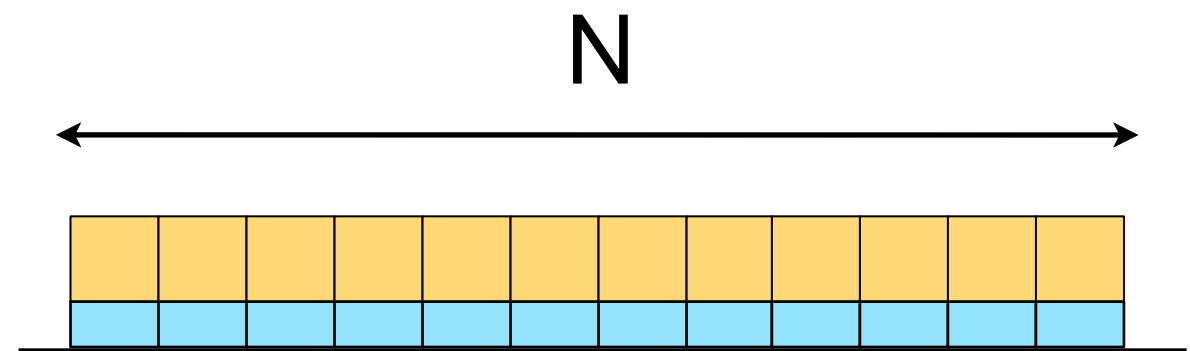
Images of muscular contraction and elongation, and control of interfacial friction [Alexander, 1992b].

Aim:

To investigate the mechanism of adhesive locomotion in gastropods with mucus.

- to verify that the mutual interaction between **propagation of muscular contraction waves** along the pedal foot and **nonlinear property of the mucus** can realize efficient motion.

Method:



1 dimensional mathematical model

Modeling: Muscular Contraction Waves

Real-time Tunable Spring (RTS)

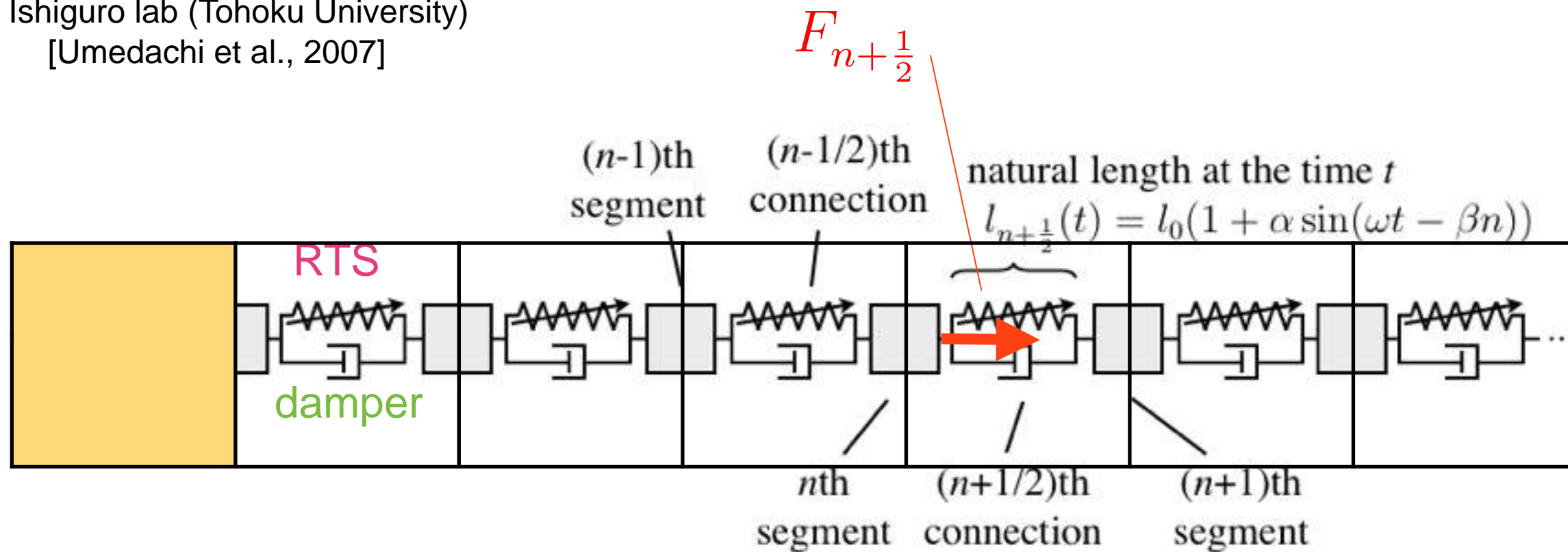


by Ishiguro lab (Tohoku University)
[Umedachi et al., 2007]

$$F_{n+\frac{1}{2}} = \frac{\kappa_{n+\frac{1}{2}}}{l_{n+\frac{1}{2}}} (x_{n+1} - x_n - l_{n+\frac{1}{2}}) + q_{n+\frac{1}{2}} (\dot{x}_{n+1} - \dot{x}_n)$$

x_n : position of n th segment

$\kappa_{n+\frac{1}{2}}$ and $q_{n+\frac{1}{2}}$ are positive.



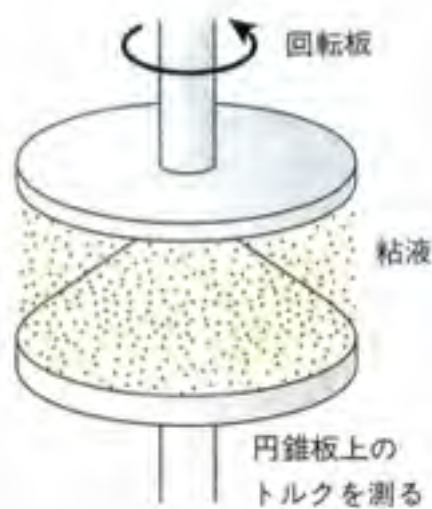
Modeling of the ventral foot of gastropods. Each segment is connected by a Real-time Tunable Spring (RTS) and a damper.

Role of Pedal Mucus

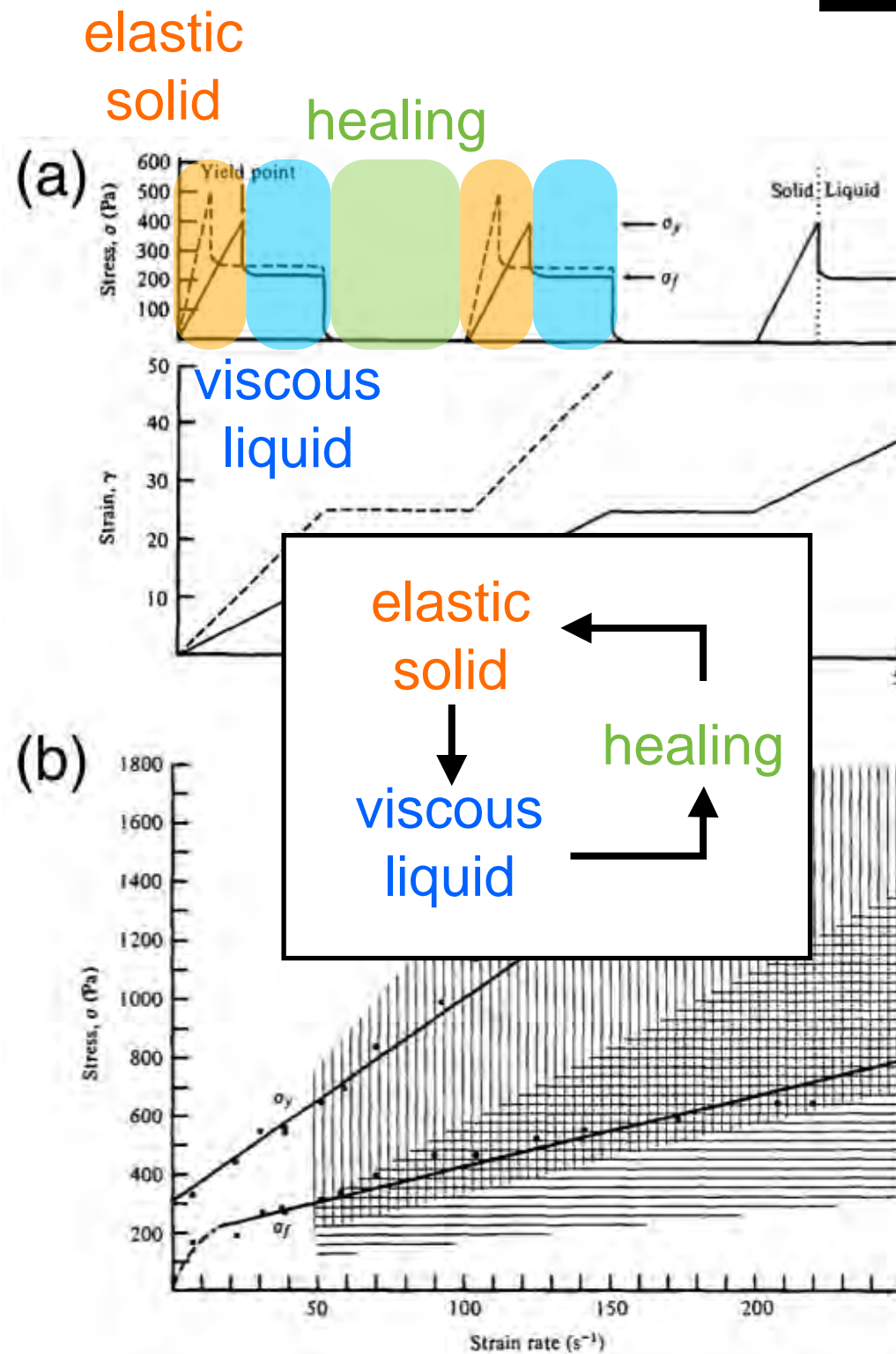
Pacific Banana Slug (*Ariolimax columbianus*)



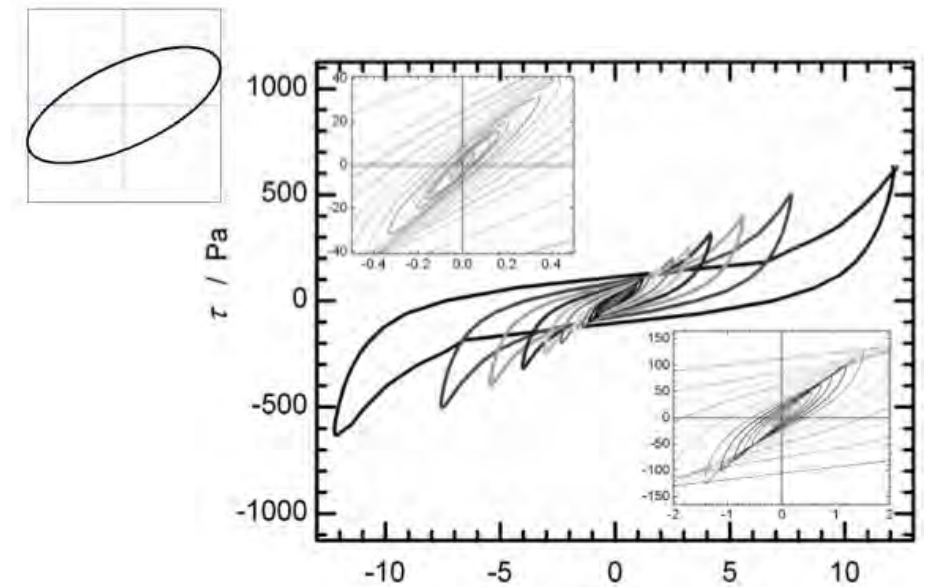
by The New York Times
(Alette Frank)



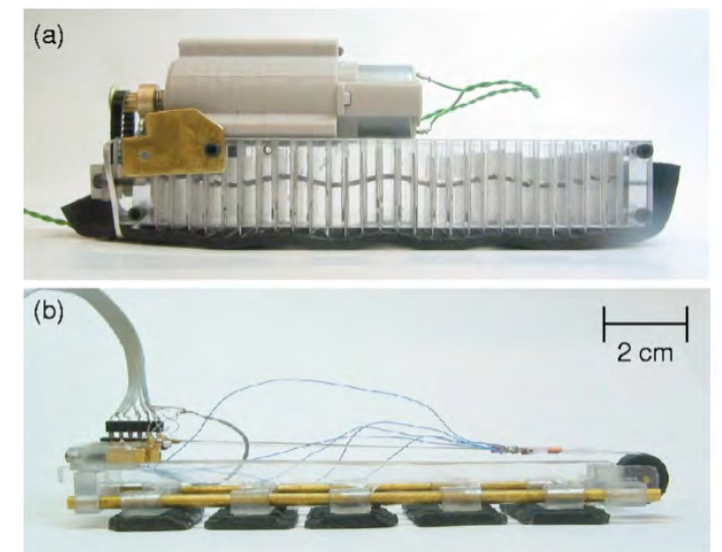
[Alexander, 1992]



The characteristics of *Ariolimax columbianus* pedal mucus [Denny and Gosline, 1980].

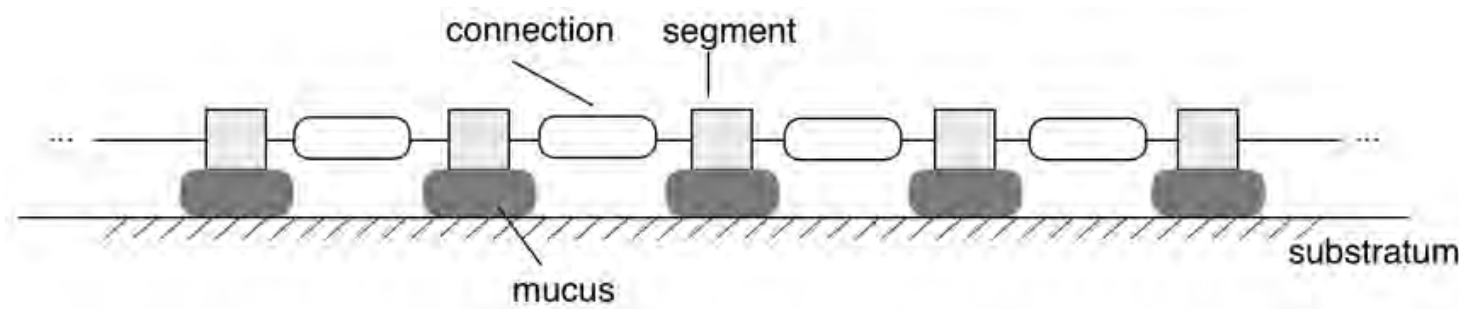


Lissajous curves resulting from LAOS tests using pedal mucus from *Limax maximus* [Ewoldt et al., 2007].



Photographs of two prototype crawler robots, (a) Retrograde crawler and (b) Direct crawler [Chan et al., 2005].

Modeling: Viscoelasticity of Mucus



Pedal mucus under each segment.

σ : switching parameter

Elastic mode

when $\sigma_n = 1$,

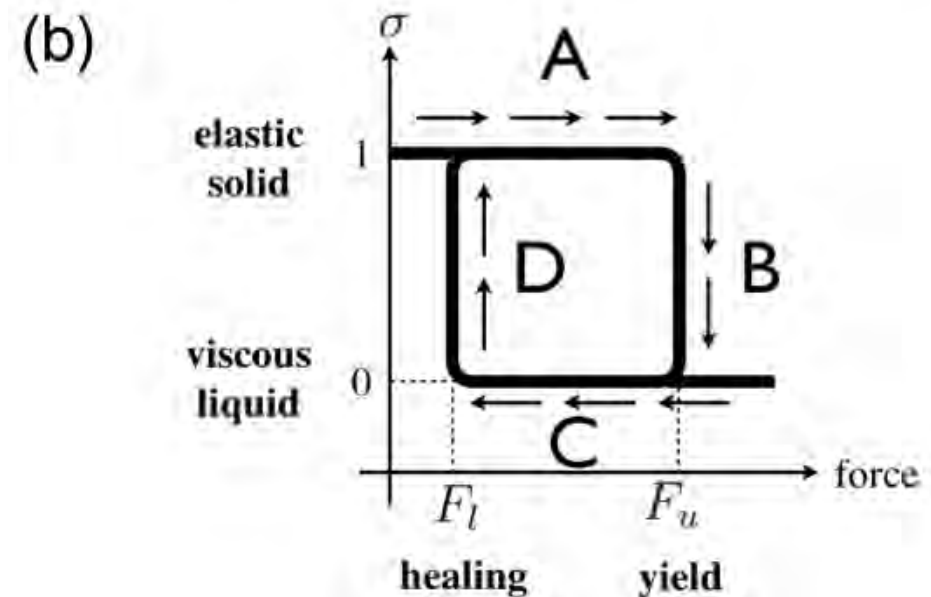
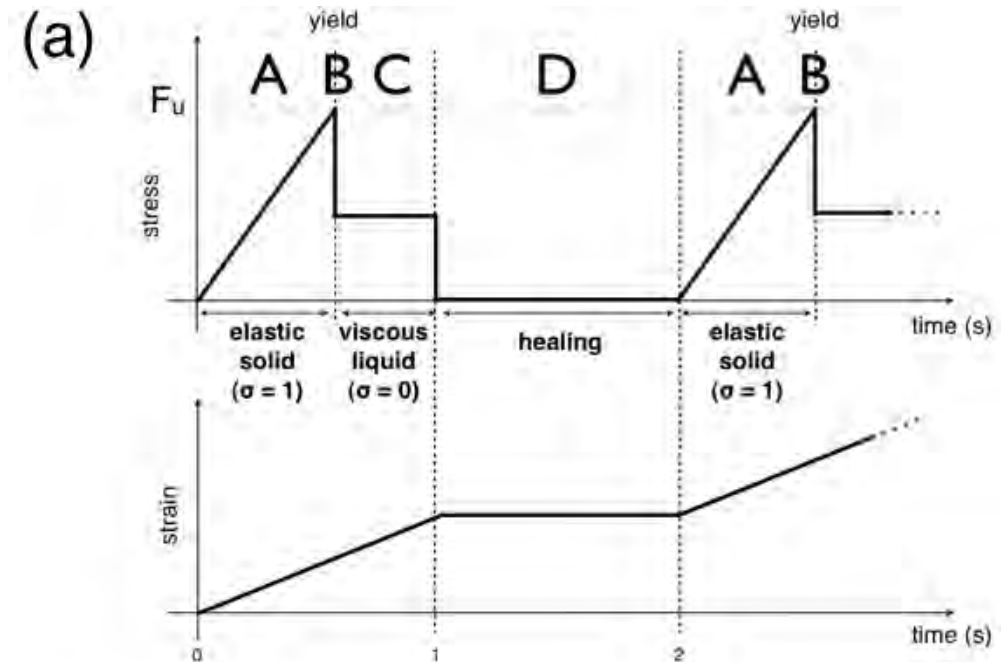
if $|F_{n+\frac{1}{2}} - F_{n-\frac{1}{2}}| > F_u$, then $\sigma_n = 0$,

Viscous mode

when $\sigma_n = 0$,

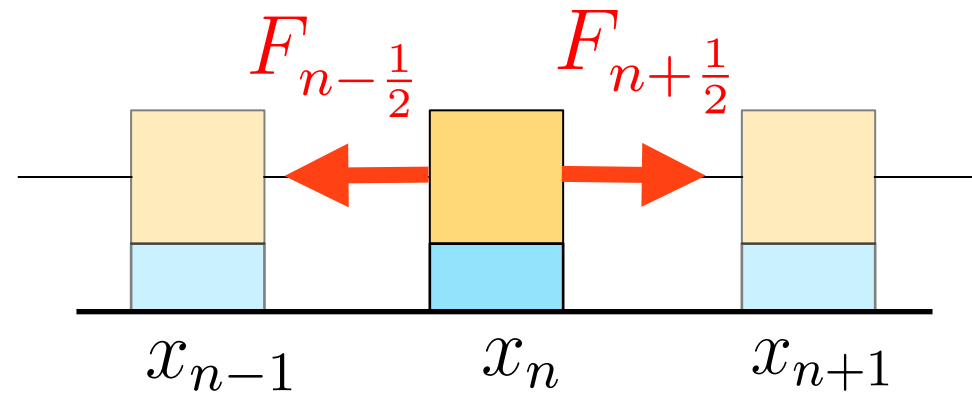
if $|F_{n+\frac{1}{2}} - F_{n-\frac{1}{2}}| < F_l$, then $\sigma_n = 1$

and $\bar{x}_n = x_n$.



Modeling for pedal mucus. (a) Outline of one of the results in Denny's experiments [Denny, 1980b; Denny and Gosline, 1980]. (b) Internal hysteresis loop of pedal mucus.

Modeling: Equation of Motion



$$m\ddot{x}_n = \underbrace{F_{n+\frac{1}{2}} - F_{n-\frac{1}{2}}}_{\text{muscle}} - \underbrace{\left((1 - \sigma_n)\mu\dot{x}_n - \sigma_n\gamma(x_n - \bar{x}_n) \right)}_{\text{mucus}}$$

viscous liquid elastic solid

m : mass of a segment

x_n : position

$F_{n+\frac{1}{2}}$: force by spring and damper

$\sigma_n = \{0, 1\}$: switching parameter

μ : viscous coefficient

γ : elastic coefficient

\bar{x}_n : standard point

Modeling: Dimensionless Equation

The dimensionless equation below is obtained by setting $x_n = LW^{-1}\tilde{x}_n$ and $t = \omega^{-1}\tilde{t}$.

$$\tilde{m}\ddot{\tilde{x}}_n = \tilde{\kappa} \left(\frac{\tilde{x}_{n+1} - \tilde{x}_n}{\tilde{l}_{n+\frac{1}{2}}} - \frac{\tilde{x}_n - \tilde{x}_{n-1}}{\tilde{l}_{n-\frac{1}{2}}} \right) + \tilde{q}(\dot{\tilde{x}}_{n+1} - 2\dot{\tilde{x}}_n + \dot{\tilde{x}}_{n-1}) - (1 - \sigma_n)\tilde{\mu}\dot{\tilde{x}}_n - \sigma_n(\tilde{x}_n - \bar{\tilde{x}}_n),$$

where some coefficients are assumed constant, $\kappa_{n+\frac{1}{2}} = \kappa$ and $q_{n+\frac{1}{2}} = q$, and dimensionless parameters are obtained as

$$\begin{aligned} \tilde{m} &= m\omega^2\gamma^{-1}, & \tilde{l}_{n+\frac{1}{2}} &= 1 + \alpha \sin(\tilde{t} - 2\pi W \frac{n}{N}), \\ \tilde{\kappa} &= \kappa N(\gamma L)^{-1}, & \tilde{q} &= q\omega\gamma^{-1}, & \tilde{\mu} &= \mu\omega\gamma^{-1}, \\ \tilde{F}_l &= F_l W(\gamma L)^{-1}, & \tilde{F}_u &= F_u W(\gamma L)^{-1}. \end{aligned}$$

The order of \tilde{m} is vanishingly small compared with the other dimensionless coefficients, so that means it can be assumed that the inertial force is negligible.

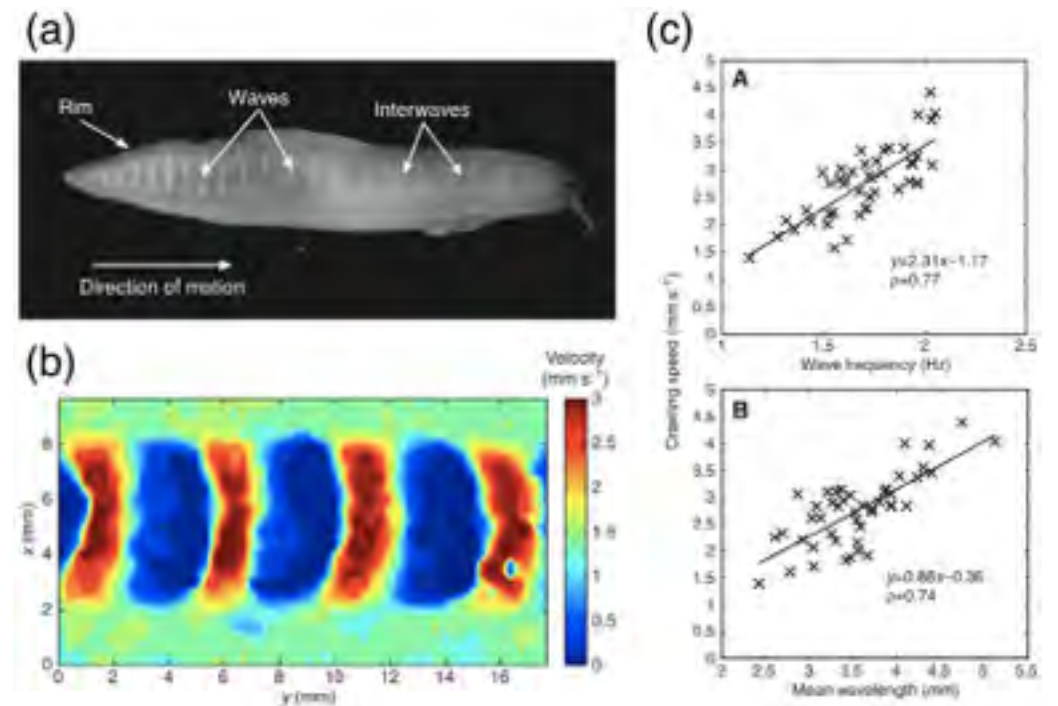
$$(1 - \sigma_n)\mu\dot{x}_n + \sigma_n(x_n - \bar{x}_n) = \kappa \left\{ \frac{x_{n+1} - x_n}{l_{n+\frac{1}{2}}} - \frac{x_n - x_{n-1}}{l_{n-\frac{1}{2}}} \right\} + q(\dot{x}_{n+1} - 2\dot{x}_n + \dot{x}_{n-1})$$

where the tildes are omitted for simplicity.

Modeling: Estimation of Parameters

Data of physical features in animals obtained from [Denny, 1980b; Denny and Gosline, 1980; Lai et al., 2010; Iwamoto, 2011].

	Denny & Gosline (Banana slug)	Lai (Banana slug, garden slug)	Iwamoto (Japanese abalone)
wave frequency [Hz]		1.0-2.5	0.02-0.2
crawling speed [mm/s]		1.0-5.0	0.4-2.84
body length [mm]		7-280	60-90
number of waves		6-23	1.5-2.0
wave speed [mm/s]		1.5-3.28	1.26-15.0
speed ratio (crawling / wave)		0.33-1.0	0.12-0.33
extension rate			0.5-0.85
wave length [mm]		2.5-5.5	30-60
viscosity [Pa s]	3.0-5.0		
stress against strain [Pa]	300 (against 1 Hz)		
thickness of mucus [μm]		70	



Results of detailed experiments [Lai et al., 2010]



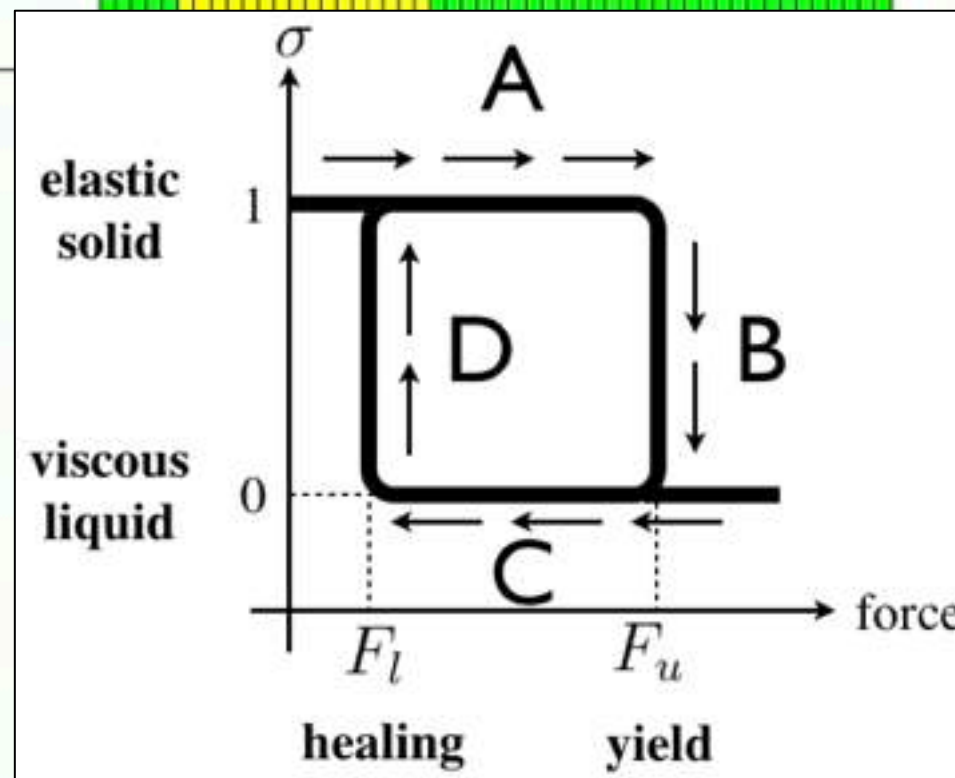
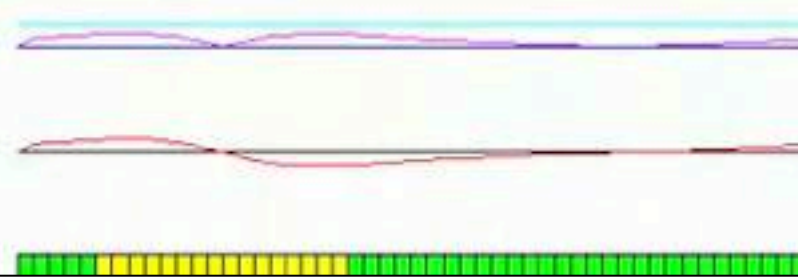
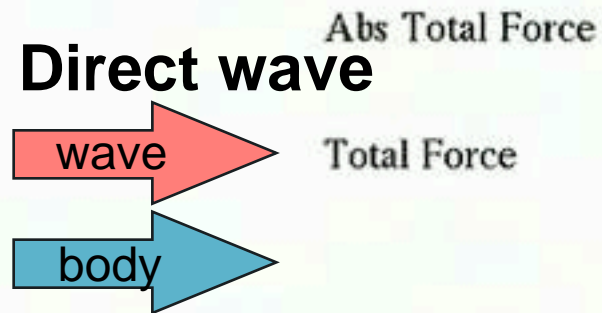
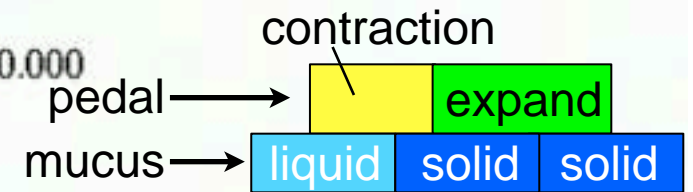
[Iwamoto, 2011]

Numerical Simulations

Calculations were carried out with $\kappa = 1.0$, $q = 0.005$, $\alpha = 0.5$, and $F_l = 0.001 \times 10^{-2}$.

wave velocity = 0.3979
body velocity = -0.000000

moving distance = -0.000



time = 0.0

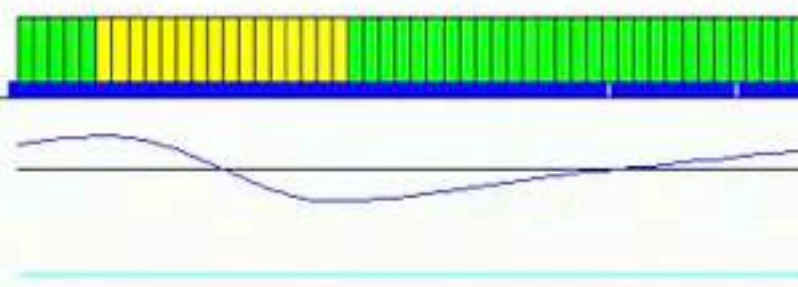
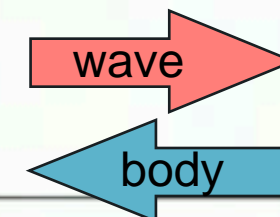
Elastic Force
Viscos Force

moving distance = -0.000

Total Force

Total Force

Retrograde wave



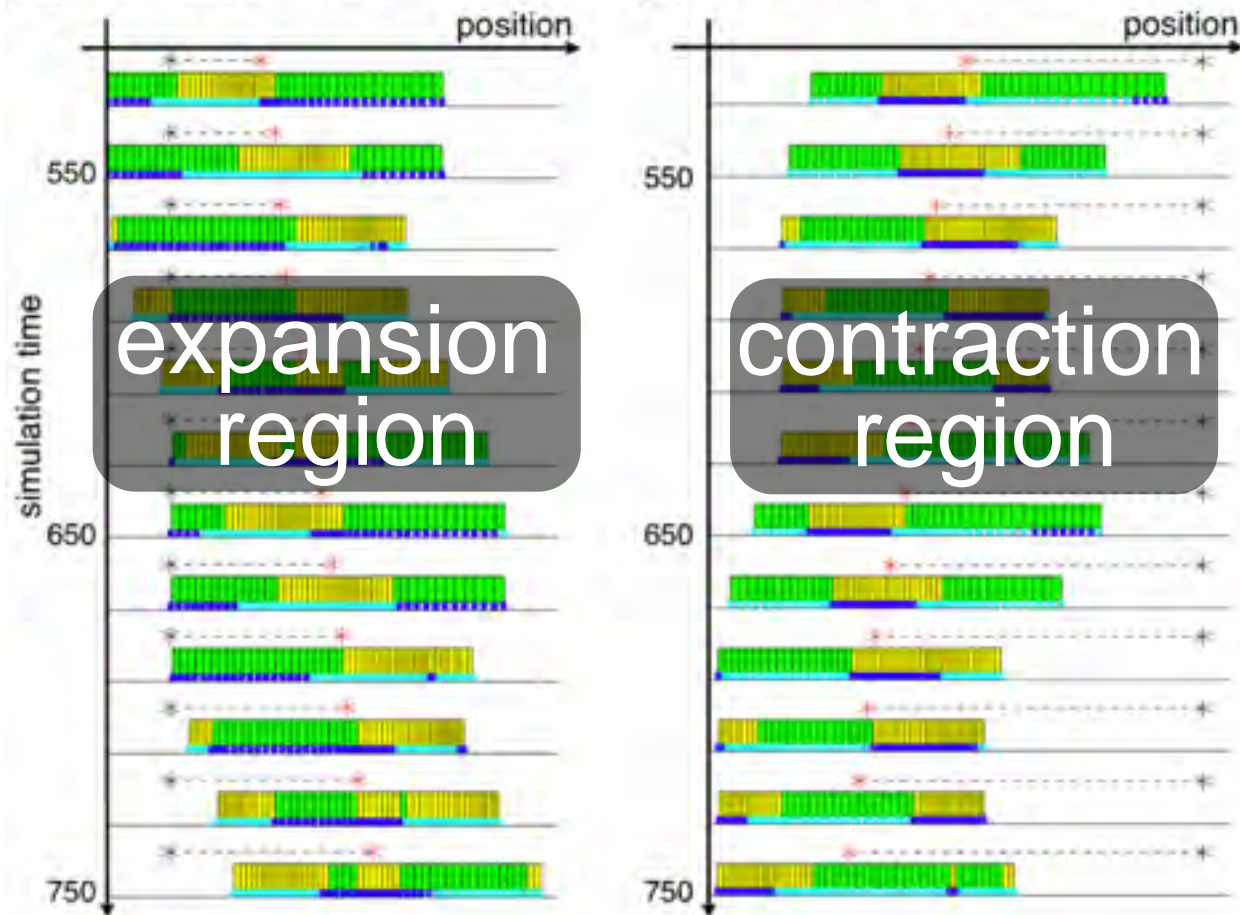
Realization of Locomotion

Direct wave

Retrograde wave

(a) $F_u = 0.35 \times 10^{-2}$

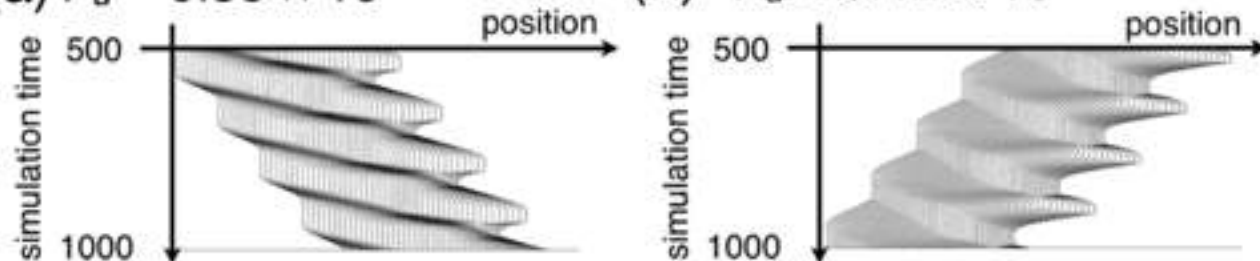
(b) $F_u = 0.42 \times 10^{-2}$



Chronological snapshots of simulations carried out with $F_l = 0.001 \times 10^{-2}$, $\kappa = 1.0$, and $q = 0.005$.

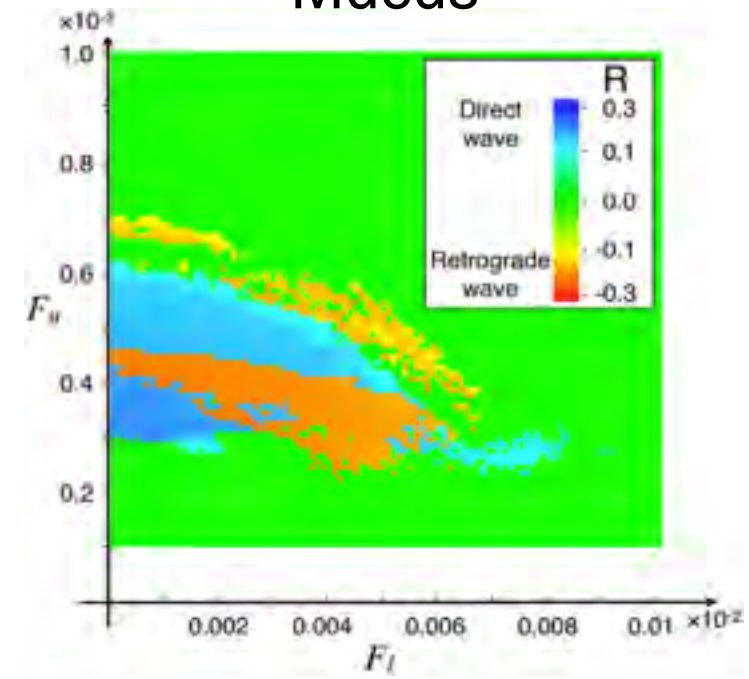
(a) $F_u = 0.35 \times 10^{-2}$

(b) $F_u = 0.42 \times 10^{-2}$



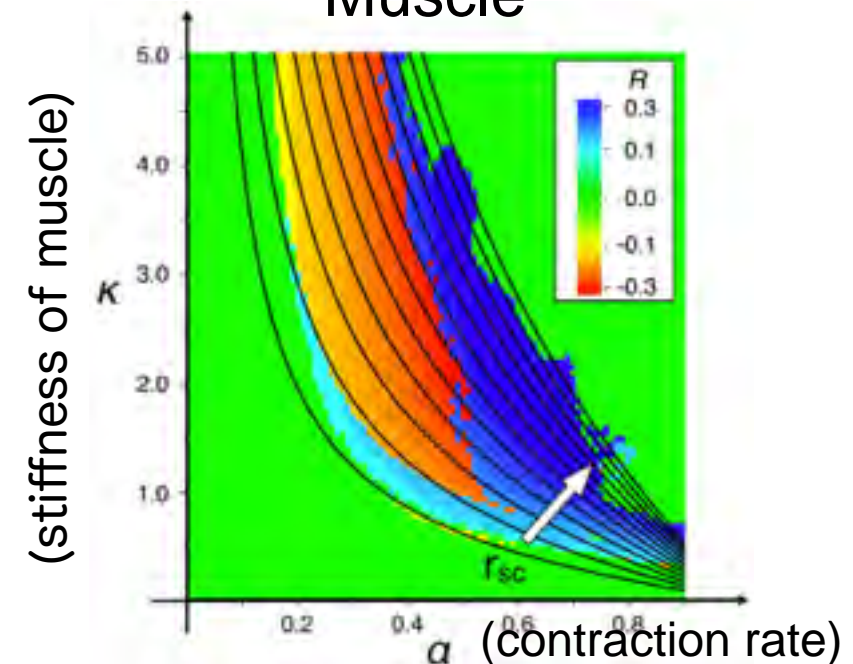
Time series plots of the position of each segment using the same parameters as in Figure 2.17(a) and (b).

Mucus



The effects of properties of mucus on the velocity ratio R for $\kappa = 1.0$, and $q = 0.005$.

Muscle



The effect of muscle features on velocity ratio R .

Direct wave or Retrograde wave

Mucus

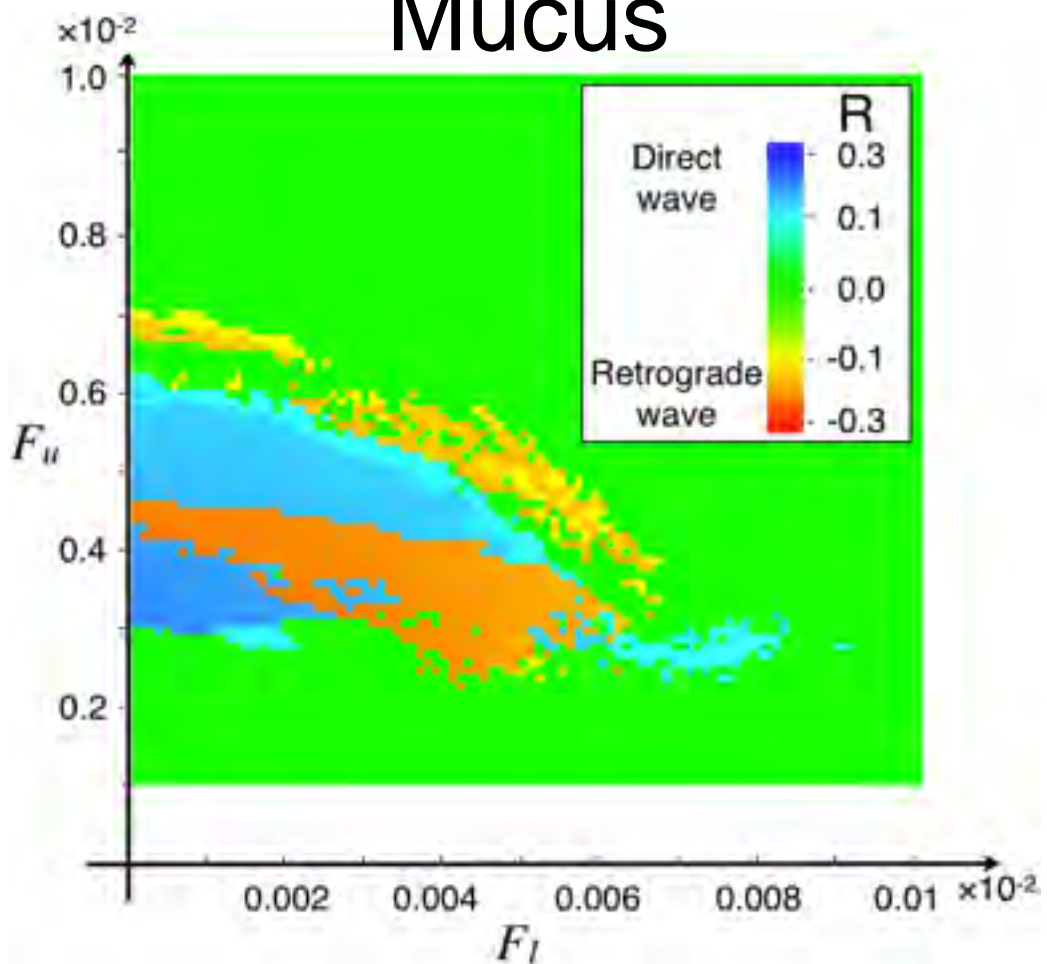


Figure 2.21. The effects of properties of mucus on the velocity ratio R for $\kappa = 1.0$, and $q = 0.005$.

Muscle

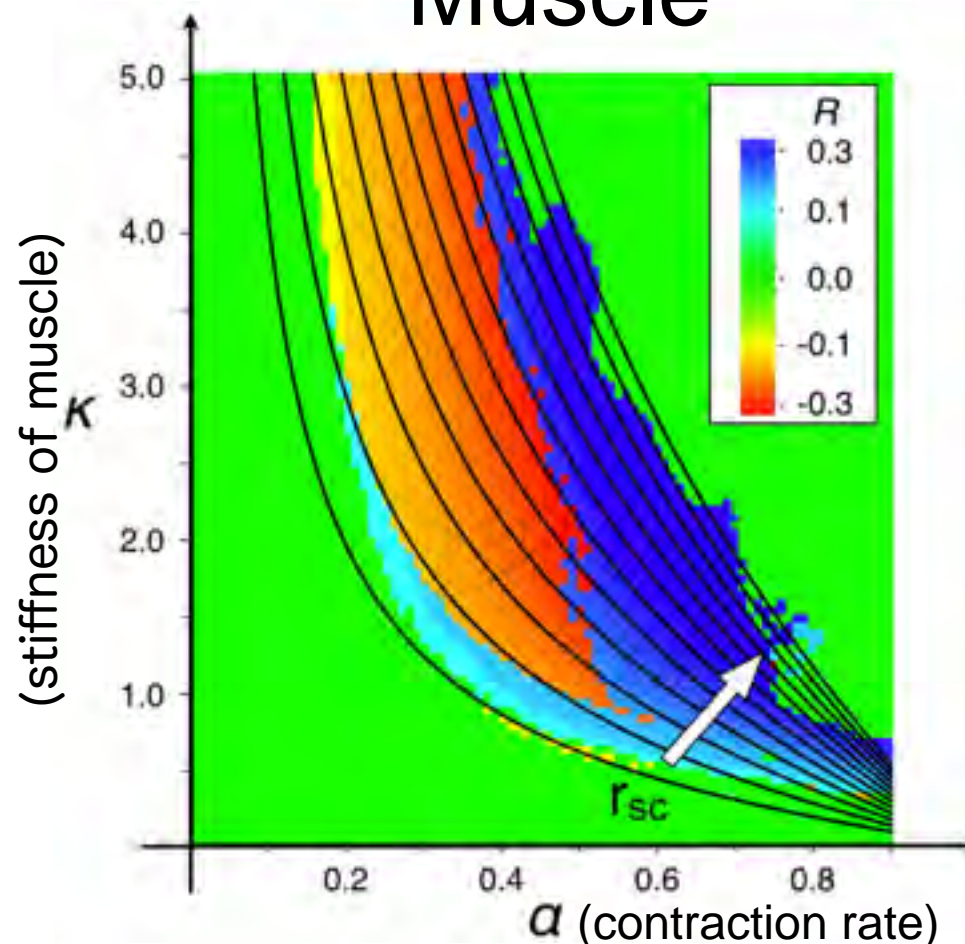


Figure 2.25. The effect of muscle features on velocity ratio R .

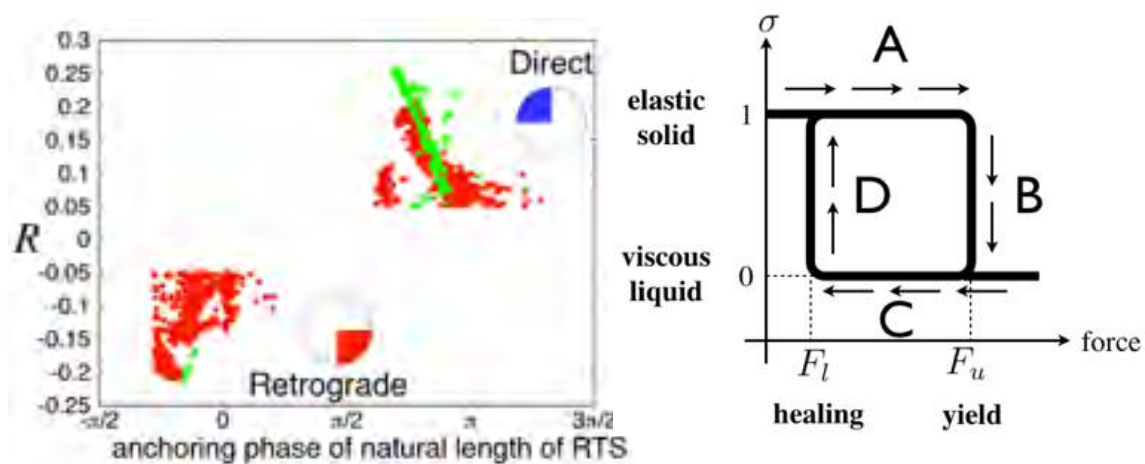


Figure 2.24. The effects of properties of mucus on the velocity ratio R for $\kappa = 1.0$, and $q = 0.005$.

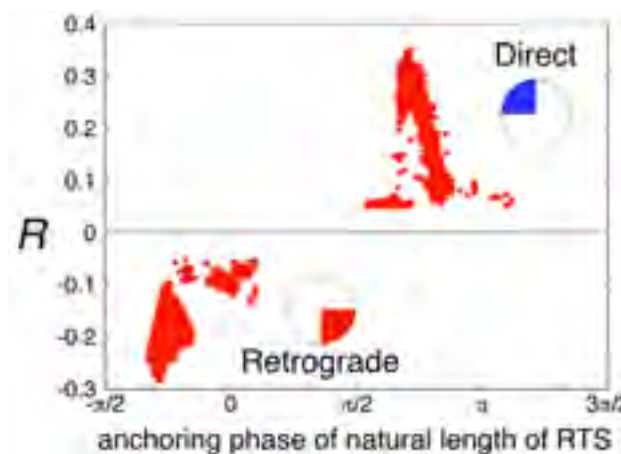


Figure 2.26. The effect of muscle features on velocity ratio R .

Modeling

- To verify the mechanism of adhesive locomotion in gastropods, **1 dimensional mathematical model** has been proposed.

Numerical calculations

- Adequate propulsive force for locomotion could be generated by the interaction between **the propagation of a flexible muscular wave** and **the nonlinear nature of mucus**.
- **Both direct and retrograde waves were realized** by the mechanism.
- The mucus has a role in **controlling the friction** with the ground.
- The features of the mucus and muscle, especially, the yield point of the mucus, stiffness and contraction rate of muscle influence on **determination of locomotion strategy**, direct wave or retrograde wave.

Future works

- A continuous model for **mathematical analysis of the bifurcation**.
- **Detailed experimental research** on the yield point of mucus and the ratio of muscle contraction in various species, and the muscular features.